

Master Thesis



UNIVERSITÄT FÜR BODENKULTUR WIEN
University of Natural Resources
and Life Sciences, Vienna

The influence of continuous light stress on the PHB production in different *Synechocystis* or how to give cyanobacteria a sunburn

submitted by

Ferdinand HUMMEL, BSc

in the framework of the Master programme

Biotechnology

in partial fulfilment of the requirements for the academic degree

Diplom-Ingenieur

Vienna, July 2022

Supervisor:

Ao.Univ.Prof. Dipl.-Ing. Dr.nat.techn. Werner Fuchs

Institute of Environmental Biotechnology

Department of Agrobiotechnology

1 Declaration of authorship

I hereby declare that I am the sole author of this work. No assistance other than that which is permitted has been used. Ideas and quotes taken directly or indirectly from other sources are identified as such. This written work has not yet been submitted in any part.

Vienna, 12. Nov. 2022

A handwritten signature in black ink, appearing to read 'F. Hummel', with a stylized, cursive script.

2 Abstract

The use of plastics has only started about one hundred years ago, but it can already be found all over the world as pollutant. Due to its persistence, it can remain there for hundreds of years. Over time it's broken down into microplastics, that are easily dispersed by wind and water leading to the contamination of soil and sea. They can accumulate in living organisms and are taken up by humans with consumed food. Even though consumers have become more aware of plastic pollution and governments worldwide have started to act against it, the annual production of plastic is still rising. The replacement of conventional petrol-based plastics with an ecological acceptable alternative is urgently needed. Polyhydroxybutyrate (PHB), a microbial produced polymer from the family of polyhydroxyalkanoates (PHA), is a promising alternative as it is biodegradable and biobased. It has comparable properties as conventional plastics and can be produced by photoautotrophic cyanobacteria using sunlight and atmospheric CO₂.

The cyanobacteria strain *Synechocystis salina* is known to produce PHB under nitrogen starvation and many studies have been conducted to understand the nature of PHB synthesis and the underlining biochemical processes. This study tries to further investigate the connection between PHB synthesis and light as external stressor.

Cyanobacteria have adapted to the naturally occurring diurnal rhythm which implies a period of darkness. In this study the effects of continuous illumination on cyanobacterial growth and PHB production was evaluated to understand if the absence of a dark phase can act as stressor on the PHB production. Additionally, the effects of the cultivation at different light intensities were examined by the cultivation at 3000lux, 6000lux and 10000lux.

To investigate the influence of the used *Synechocystis* strain, light intensity and the cultivation at continuous illumination on the polymer quality, PHB was extracted and analysed with a gel permeation chromatography.

The results of this study show, that the cell size of cyanobacteria cultivated at continuous illumination were enlarged, indicating higher growth rates at energy rich conditions compared to the cultivation at a day-night-cycle. The glycogen and PHB content increased continuously at both conditions, but at a higher rate under continuous illumination. Upon entering nitrogen depletion, the glycogen content at both conditions suddenly increased to approximately the same level.

The increase in light intensity and continuous illumination provided cells with excess energy. Cells have to balance their energy and redox levels by consuming ATP and NADPH to maintain homeostasis. This could be achieved by the polymerisation of glycogen and PHB avoiding changes in the osmotic pressure and losses of fixed carbon by secreting fermentation products.

3 Kurzfassung

Die Verwendung von Plastik hat vor ca. 100 Jahren begonnen, aber die Umweltverschmutzung mit Plastik ist bereits weltweit verbreitet. Aufgrund ihrer Langlebigkeit verbleibt es für Hunderte von Jahren in der Natur. Im Laufe der Zeit wird es zu Mikroplastik zersetzt, was die Verbreitung durch Wind und Wasser weiter erleichtert und zur Verschmutzung von Böden und Meeren führt. Mikroplastik kann sich in lebenden Organismen anreichern und wird vom Menschen mit seiner Nahrung aufgenommen. Obwohl Verbrauchern die Plastikverschmutzung bewusster geworden ist und Regierungen beginnen dagegen vorzugehen, nimmt die jährliche Plastikproduktion stetig weiter zu.

Es ist dringend nötig Plastik auf Erdölbasis durch eine ökologisch akzeptable Alternative zu ersetzen. Polyhydroxybutyrate (PHB) ist ein mikrobiell herstellbarer Polymer aus der Familie der Polyhydroxyalkanoate (PHA) und eine vielversprechende Alternative, da es biologisch abbaubar und biobasiert ist. Seine Eigenschaften sind mit herkömmlichem Plastik vergleichbar und kann von photoautotrophen Cyanobakterien mit Sonnenlicht und atmosphärischem CO₂ synthetisiert werden.

Der Cyanobakterienstamm *Synechocystis salina* ist dafür bekannt, dass er bei Stickstoffmangel PHB produziert. Um die PHB-Synthese und ihr zugrunde liegenden biochemischen Prozesse zu verstehen wurden bereits viele Studien durchgeführt. In dieser Studie wird der Zusammenhang zwischen der PHB-Synthese und Licht als externer Stressor weiter untersucht.

Cyanobakterien haben sich an den natürlichen Tagnachtrhythmus und die damit verbundene Dunkelphase angepasst. In dieser Studie wurden die Auswirkungen kontinuierlichen Belichtung auf das Wachstum von Cyanobakterien getestet, um zu verstehen, ob die fehlende Dunkelphase sich auf die PHB-Produktion auswirkt. Zusätzlich wurden die Auswirkungen der Kultivierung bei verschiedenen Lichtintensitäten untersucht, genauer bei 3000lux, 6000lux und 10000lux.

Die Polymerqualität, durch den Polydispersitätsindex (PDI) indiziert, ist entscheidend für die Produktion. Um den Einfluss verschiedener Cyanobakterienstämme, der Lichtintensität und der kontinuierlichen Belichtung auf die Polymerqualität zu untersuchen, wurde PHB extrahiert und mit einer Gel-permeationschromatographie analysiert.

Die Studienergebnisse zeigen eine Vergrößerung der Zellen unter kontinuierlicher Belichtung, was auf das Wachstum unter nicht energielimitierten Bedingungen hindeutet. Der Glykogen- und PHB-Gehalt nahm bei beiden Bedingungen kontinuierlich zu, jedoch schneller unter kontinuierlicher Belichtung. Beim Einsetzen der Stickstofflimitierung stieg der Glykogengehalt unter beiden Bedingungen plötzlich stark an und erreichte das gleiche Level.

Die Zellen wurden durch die kontinuierliche Belichtung und die Steigerung der Lichtintensität mit mehr Energie versorgt, jedoch brauchen Zellen ein ausgeglichenes Energielevel und Redoxpotential, um ihre Homöostase aufrecht zu erhalten. Dies können sie durch den Verbrauch des produzierten ATP und NADPH durch die Polymerisation von Glykogen und PHB erreichen und zugleich eine Veränderung des osmotischen Drucks und Verluste von gebundenem Kohlenstoff durch die Absonderung von Fermentationsprodukten vermeiden.

4 Content

1	Declaration of authorship	2
2	Abstract	3
3	Kurzfassung.....	4
4	Content.....	5
5	Introduction	7
5.1	The overwhelming plastic pollution	7
5.2	Can bioplastic be part of a solution?	10
5.3	Polyhydroxybutyrate (PHB) a polymer with potential.....	11
5.4	Cyanobacteria, the revolutionizing bacteria.....	15
5.5	Stress factors influence the PHB production	21
5.6	The project PHBecol investigates the ecological role of PHB in cyanobacteria	24
5.7	Bioplastic as part of the growing bioeconomy	25
5.8	The need of constant plastic quality for production.....	28
6	Aims	30
7	Material and Methods	30
7.1	Strains	31
7.2	Media.....	31
7.2.1	22O.....	31
7.2.2	BGI	32
7.2.3	Trace elements stock solution, v5	32
7.3	Experimental Setup.....	32
7.3.1	Cultivation at 25°C and room temperature (RT)	32
7.3.2	Cultivation with different light cycles and light intensities.....	33
7.3.3	Production of PHB	36
7.4	Analytical Methods.....	37
7.4.1	Cell Dry Weight (CDW)	37
7.4.2	pH.....	37
7.4.3	Optical Density (OD).....	37
7.4.4	Chlorophyll-a content.....	37

7.4.5	Phycocyanin content.....	38
7.4.6	Nitrate.....	38
7.4.7	Glycogen	38
7.4.8	Polyhydroxybutyrate (PHB).....	39
7.4.9	PHB extraction using an Automated Solvent Extraction System (EDGE)	40
7.4.10	Gel Permeation Chromatography (GPC).....	40
7.4.11	¹ H - Nuclear magnetic resonance spectroscopy (H-NMR).....	42
7.4.12	Microscopy	42
8	Results.....	44
8.1	Influence of elevated temperature on cultivation of two different <i>Synechocystis</i> strains ..	44
8.2	Continuous illumination at 3000lux with S.192 and S.6803 (Exp.1).....	48
8.3	Continuous illumination at 3000lux with 2 different <i>Synechocystis</i> strains (Exp.2)	54
8.4	Continuous illumination at 6000lux with 3 different <i>Synechocystis</i> strains (Exp.3)	60
8.5	Continuous illumination at 10000lux with 3 different <i>Synechocystis</i> strains (Exp.4)	68
8.6	Comparison of three different <i>Synechocystis</i> strains at 3000, 6000 and 10000lux	78
8.6.1	Effects of different light intensities on the strain S.192	79
8.6.2	Effects of different light intensities on the strain S.6803 compared to S.192	81
8.6.3	Effects of different light intensities on the strain IFA compared to S.192 and S.6803.....	83
8.6.4	Influence of different light intensities and illumination regimes on the cell size	85
8.6.5	Influence of different light intensities and illumination regimes on cell density	86
8.6.6	Remaining nitrate levels in the 3k and 10k cultures	87
8.7	Effects of illumination regimes on the cellular structures	87
8.8	PHB extraction and the influence of the cultivation regime on the quality	90
8.8.1	H-NMR	90
8.8.2	PHB analysis with GPC	91
9	Discussion	96
10	Conclusion and Outlook	107
11	Acknowledgements	108
12	References.....	109

5 Introduction

5.1 The overwhelming plastic pollution

Recently the worldwide environmental pollution with plastic and the impacts of microplastic have come to broader public attention. On February 28, 2022, the President of UNEA-5 and Norway's Minister for Climate and the Environment, Espen Barth Eide opened the UN Environment Assembly in Nairobi the words *"Plastic pollution has grown into an epidemic of its own. Paradoxically, plastics are among the most long-lasting products we humans have made – and frequently, we still just throw it away. Plastic is a product that can used again, and then over and over again, if we move it into a circular economy. I am convinced that the time has come for a legally binding treaty to end plastic pollution."* (UN Environment Programme, 2022).

Even though this statement seems promising, it also shows the dilemma of our society. Petrol based plastic finds application in every aspect of our lives and in a very wide range of products. Plastic has many advantages like easy processability, light weight, strength, and stability. But especially the chemical stability is posing a big threat for the world's ecosystems and human health. Plastic that enters the environment persists there (Figure 1) for exceedingly long time periods leading to the entanglement of animals or to their starvation by plastic ingestion. Over time plastic is deuterated by photolytic, mechanical and biological degradation (Napper & Thompson, 2019) into microplastic



Figure 1: Photograph of littered plastic waste accumulating on a beach by © UNEP, Versova Beach, Mumbai, India CC BY-NC-SA 2.0. (Alpizar et al., 2019)

which poses an even greater threat. Microplastics litter into the environment at all steps in the life cycle of plastic products from the producers to waste management. Several studies have reported the ingestion of microplastics by marine organisms (GESAMP, 2016). Microplastic particles were detected in mussels and fish and can adsorb other pollutants on their surface posing a health problem, also for humans at the end of the food web (Bajt, 2021). The amount of microplastics in the ocean is constantly increasing and the amount of plastic is approximately six times greater than the amount of marine planktonic biomass (Moore et al., 2001). Microplastics have been distributed worldwide and can even be found at the most remote places on earth like the deep sea (van Cauwenberghe et al., 2013). Though most is known on the plastic pollution in the marine environment, it is now claimed to be similar across all other ecosystems as well (R. G. Santos et al., 2021). A recent study by Kwon et al. (2022) shows, that microplastic particles can already be found in human brains and leads to changes in the cellular morphology, immune responses, and microglial apoptosis (Kwon et al., 2022).

Since humans live on a planet with finite resources and capacities, the concept of planetary boundaries was introduced by Johan Rockström in 2009, aiming at monitoring our human activities and

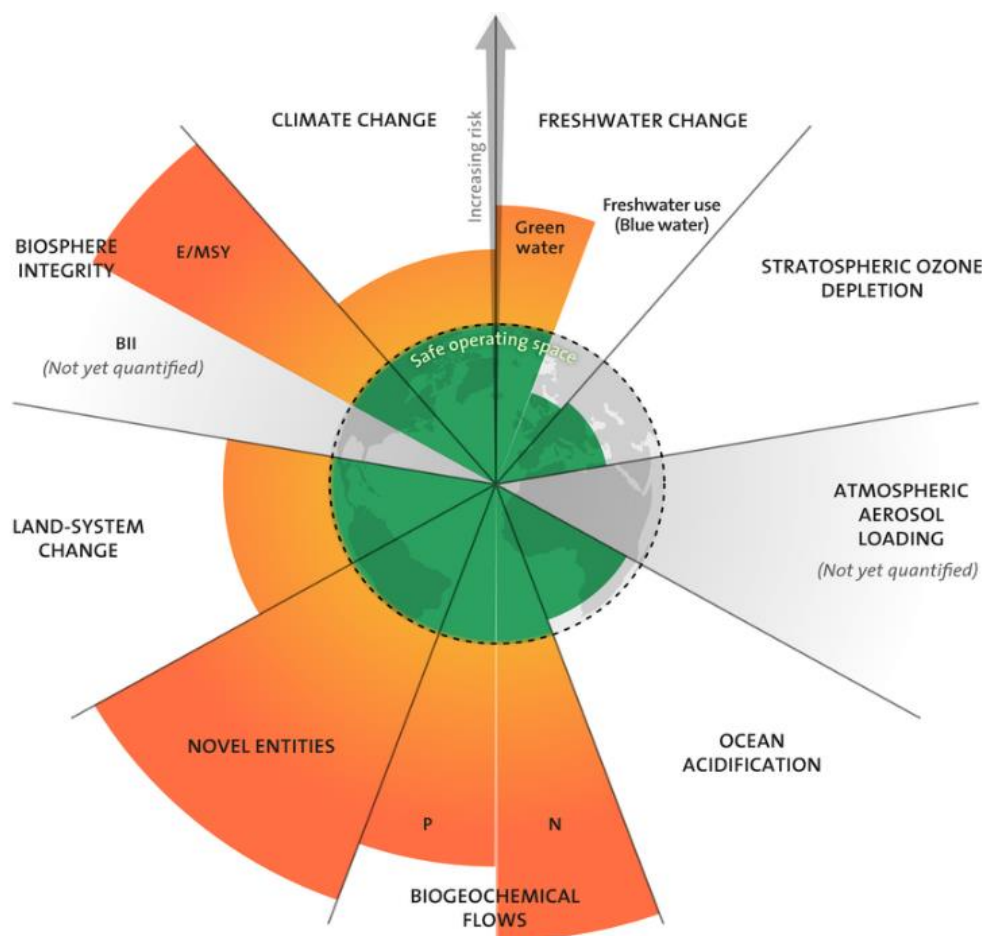


Figure 2: Visualization of the planetary boundaries, with the overstepped boundaries indicate in orange. The boundary titled novel entities is greatly overstepped and including among other plastics. (Wang-Erlandsson et al. 2022)

estimating if we are operating sustainable inside the planetary boundaries. In the new publication by Wang- Erlandsson et al. (2022) it has been stated that humanity is operating outside the planetary boundaries in multiple areas like climate change, biosphere integrity, fresh water change, Land-system change, biogeochemical flows and novel entities (Figure 2), to which plastics and other human produced chemicals count (Wang-Erlandsson et al., 2022).

In a recent publication Persson et al. (2022) evaluated novel entities with regards to the planetary boundaries and concluded, that the boundary is exceeded “since the annual production and releases are increasing at a pace that outstrips the global capacity for assessment and monitoring”. These novel entities refer to entities that are novel in a geological sense, like plastics that are the major contributors within overall production of novel entities (see Figure 3) (Persson et al., 2022). This fact is again highlighting that the plastic pollution is of particular high concern.

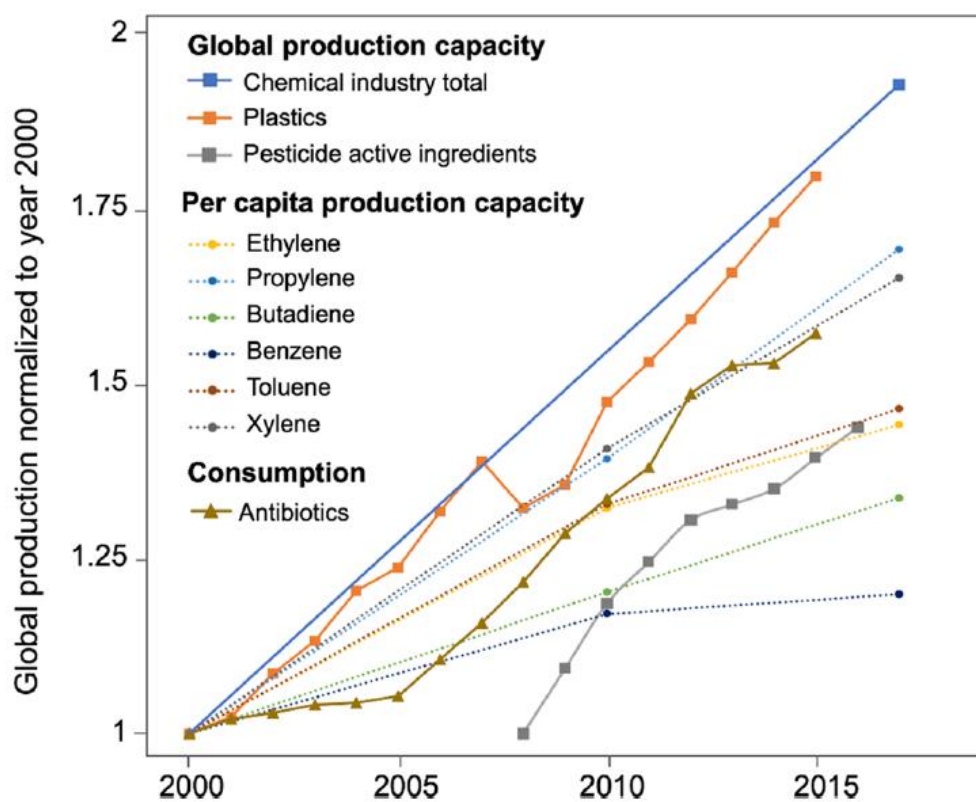


Figure 3: Global trends of currently rising chemical industry production including the rising plastic production indicated in orange being the biggest fraction of the total chemical industry global production capacity until 2020. (Persson et al. 2022)

These findings clearly show that the proposed solutions by the UNEP and other organisations for the plastic pollution cannot be solely the reduction of plastic products and the recycling in a circular economy. Plastic will always end up in nature by littering or by accident in the production, transport, and disposal pathways. By using a dangerous material more efficiently, it will not become less harmful. The only solution ending microplastic pollution is the substitution with an alternative material like bioplastics. Especially considering that the annual production of plastics is

projected to increase from 335 million tonnes in 2016 to approximately 1124 million tonnes by 2050 (Alpizar et al., 2019).

5.2 Can bioplastic be part of a solution?

As a response to plastic pollution the EU commission has introduced the EU's directive on single-use plastics to prevent and reduce their impact on the environment (Directorate-General for Environment [European Commission], 2021; European Union, 2019). The directive and the plans of the EU commission aim at reducing the amounts of plastic littered into the environment and increasing the recycling rate of plastic. The question remains, if these efforts can solve the systematic problem of the persistence of conventional plastic in the environment.

A different approach is the substitution of conventional plastics with bioplastics. These bioplastics are claimed to be an eco-friendly alternative and are therefore frequently used in the industry for campaigning. An example are the bottles made by coca cola (Coca-Cola company) claiming to be eco-friendly, since they are produced from plant-based materials. These bottles are still PET and will not degrade in nature and therefore pose the same danger.

European Bioplastics defines bioplastic (Figure 4) as a material that is either bio-based, biodegradable, or features both properties (European Bioplastics).

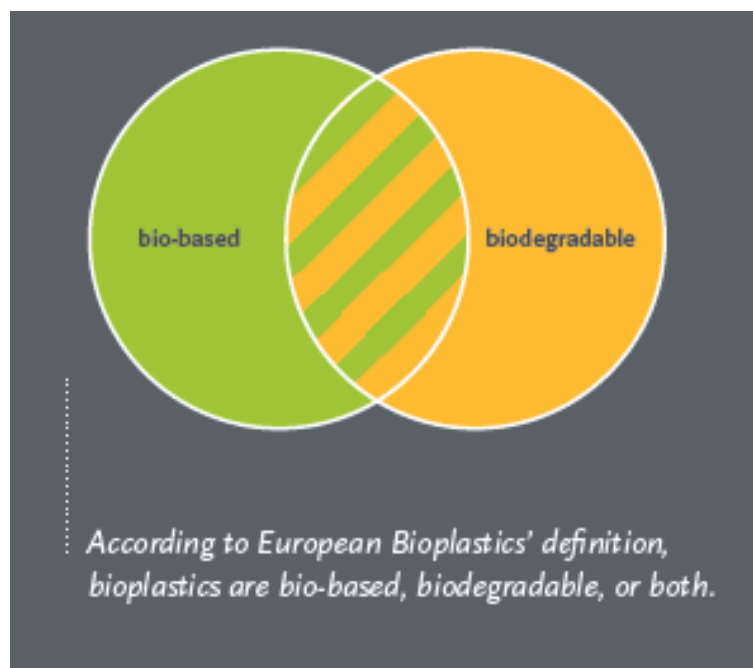


Figure 4: Bioplastic definitions. (European Bioplastics)

A real change can only come from using only both, biobased and biodegradable plastics and at the same time reducing, reusing, and recycling. The currently available bio-based and biodegradable plastics include polylactic acid (PLA), polyhydroxyalkanoates (PHA), polybutylene succinate (PBS), and starch blends. The most promising candidate belonging to the PHA family, is Polyhydroxybutyrate, a natural occurring biobased and biodegradable polymer produced by different bacteria.

5.3 Polyhydroxybutyrate (PHB) a polymer with potential

Among the known biobased and biodegradable plastics especially polyhydroxyalkanoates (PHAs) are suited to substitute the existing petrol-based plastics. PHAs are a family of biodegradable and biocompatible polyesters constituted by different hydroxyalkanoate (HA) monomers, that can be synthesized by various microorganisms (Behera et al., 2022).

They are produced intracellular as an energy and carbon storage under nutrition-deficient conditions (El-Malek et al., 2020) by gram-positive and gram-negative bacteria, as well as fungi, yeast and algae (Anitha & Srivastava, 2021).

The bacterial species accumulating high amounts of PHAs include a wide spectrum of genera including among others *R. eutropha*, *Azotobacter* sp., *Bacillus* sp., *Pseudomonas* sp., *Burkholderia* sp., *Halomonas* sp., and *Haloferax* sp. (M. Kumar et al., 2020).

The biggest advantage is their biodegradability by microbial enzymatical degradation (Mergaert, 1992). Unlike other biopolymers, e.g., PLA, PHAs highly resemble the material properties of synthetic plastics. For instance, PHAs display high melting temperatures and tensile strengths similar to those found in petroleum-based polyesters. These properties vary depending on the synthesizing microorganism and the monomer. So far about 150 different monomers have been identified (Steinbüchel & Fächtenbusch, 1998; Steinbüchel & Valentin, 1995).

Other PHA characteristics valued in plastic production include their biocompatibility, non-toxicity, good processability, and a wide structural diversity (Mokhtarzadeh et al., 2016).

Because of these properties PHAs have been studied extensively, as this family of chemicals includes the most promising biopolymers. The first reported and most common homopolymer among PHAs is poly(3-hydroxybutyrate) (PHB) first described in 1926 by Lemoigne (1926). PHB is a homopolymer classified as short-chain length (SCL) PHA with 3-hydroxybutyrate as monomeric unit (Figure 5) consisting of 4 carbon atoms (Wang et al., 2016).

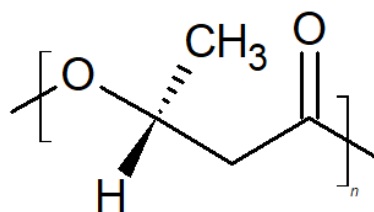


Figure 5: Poly(3-hydroxybutyrate) structure based on Verlinden et al. (2007) sketched with ChemSketch .

Microbial cells accumulate PHAs as a carbon and energy storage for various physiological activities under nutrient-deficient conditions (Koller et al., 2011). By polymerisation the cells become osmotolerant to these substances and can thereby store large quantities of reduced carbons (Anderson &

Dawes, 1990). Thereby the leakage of valuable compounds is prevented and the stored nutrients remain available at low maintenance costs (Peters & Rehm, 2005).

The synthesized polyester compounds range from 0.2 to 0.5 μm in length and are stored in insoluble granules inside the cytoplasm (Figure 6). These granules consist of a hydrophobic polyester core surrounded by an amphiphilic layer containing organizing proteins, called granule-associated proteins (Obruča et al., 2020).

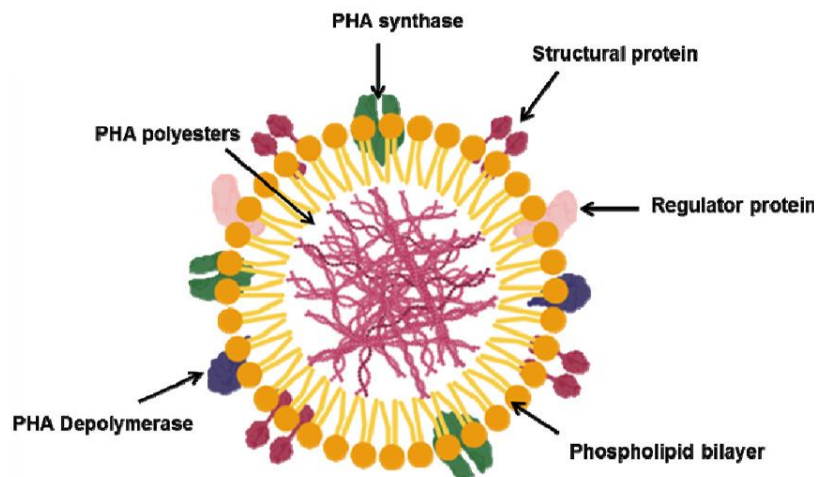


Figure 6: Structure and composition of PHA granules in microorganisms with associated proteins (Behera et al., 2022).

The granules are composed of 97.5% PHAs, proteins and phospholipids. Most of the granule-associated proteins are low molecular weight phasins that show metabolic regulatory functions associated with PHB granule organization which are responsible for the complex subcellular carbonosomes (Jendrossek & Handrick, 2002). They regulate size and number of the PHA granules inside the cells (Pötter & Steinbüchel, 2005).

The most important enzyme for PHA synthesis is PHA synthase which polymerizes hydroxyacyl-coenzyme A (CoA) to PHA and free CoA (Mohapatra et al., 2017). PHA synthases have been classified as separate class of homologous proteins with several PHA synthases from different sources and substrate specific properties (Sudesh et al., 2000).

The PHA Depolymerase (PhaZ) governs the utilization of the PHAs (Anis et al., 2017). The natural degradation of the polymers by various microorganisms results in carbon dioxide and water under aerobic conditions, while the anaerobic degradation results in carbon dioxide and methane (Rudnik, 2013).

There are three biosynthetic pathways for PHA known in microorganisms (Figure 7) with the utilization of sugars (e.g., glucose) being the most common pathway. Glucose is converted to pyruvic acid by the pentose-phosphate pathway and glycolysis. In the next step pyruvate dehydrogenase catalyses the oxidative decarboxylation of pyruvate to acetyl-CoA. Coenzyme A can also be acetylated by the breakdown of fatty acids through β -oxidation. Acetyl-CoA can also be supplied by utilization of CO_2 via the Calvin–Benson–Bassham cycle (CBB) or by the Serine-Pathway utilizing methanol and methane (Behera et al., 2022).

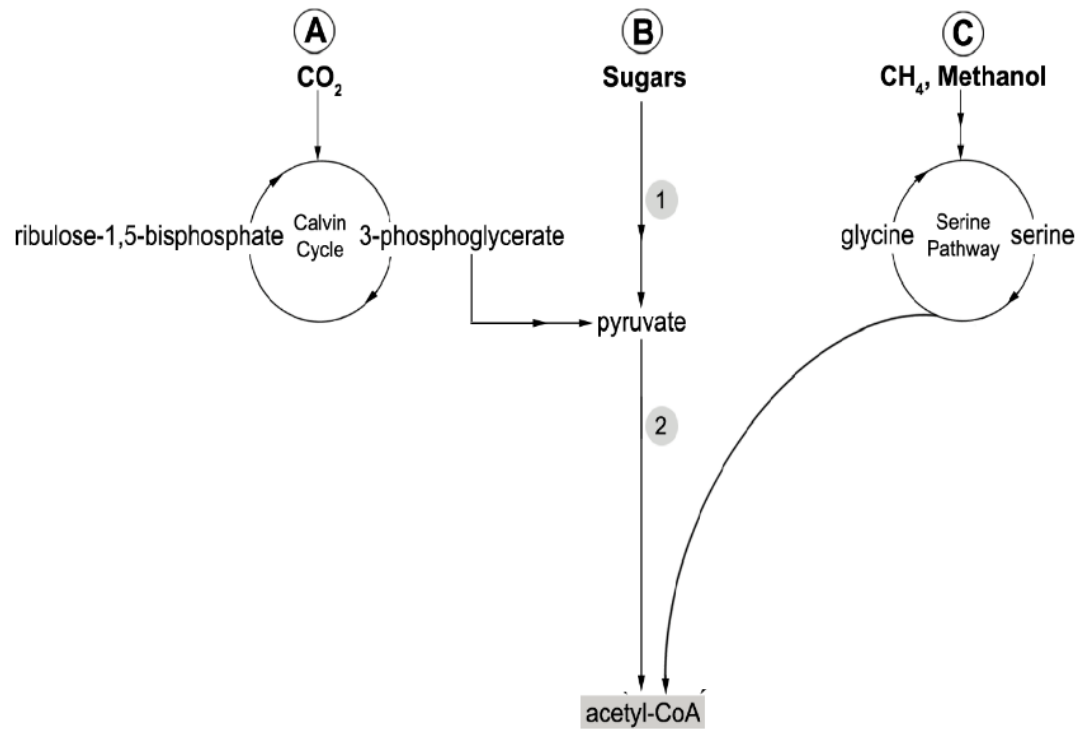


Figure 7: The three main sources for acetyl-CoA supply for PHA synthesis in microorganisms. (Tan et al. 2014)

Instead of entering the tricarboxylic acid cycle (TCA) for further energy production the acetyl-CoA is further converted by mainly three enzymes into PHB (Figure 8). In a first step, acetoacetyl-CoA is formed from two acetyl-CoA by the enzyme β -ketothiolase (PhaA). Acetoacetyl-CoA dehydrogenase enzyme (PhaB) uses NADPH as a cofactor to reduce acetoacetyl-CoA to 3-hydroxybutyryl-CoA. In a last step 3-hydroxybutyryl-CoA is polymerized by P(3HB) polymerase (PhaC) liberating the coenzyme-A (Mohapatra et al., 2017). The NADPH is a critical cofactor and an increase in the ratio of NADPH to NADPH^+ effects the PHA synthesis positively (Alsiyabi et al., 2021).

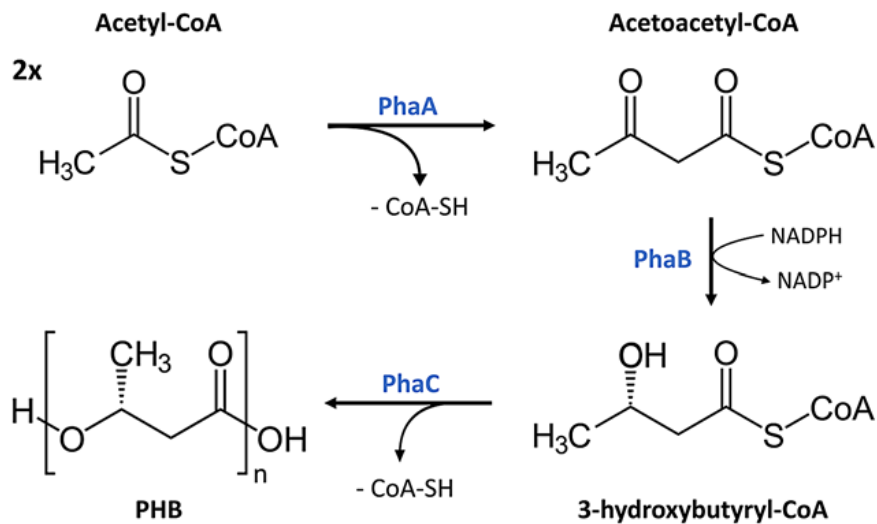


Figure 8: PHB synthesis pathway. Two units of Acetyl-CoA are converted in a three-step enzymatic process into PHB by the enzyme PHB synthase (Koch und Forchhammer 2021).

Due to the PHAs biodegradability and biocompatibility as well as their mechanical properties, PHAs are suitable alternative for a wide range of applications in various sectors (Figure 9) such as packaging, material coating or as polymeric films (Akaraonye et al., 2010) and also as animal feed (Masood et al., 2015). They are very well suited for the biomedical sector in applications such as bone-crafting, tissue-engineering and drug-delivery systems, as they do not induce any negative immune response from the receiving organism (Williams, 2008). For example the monomeric compound of PHB, 3-Hydroxybutyric acid, is found as normal metabolite in human blood (Mierziak et al., 2021) and therefore these biomaterials do not induce any antigenic response or pose any risk for thrombosis even after long-term contact (Grigore et al., 2019). By coating with PHA biofouling of hulls can be prevented and they can be additionally used as antimicrobial agents (Kavitha et al., 2018).

There are various challenges for the large-scale microbial production of these biopolymers. Especially the cost for the carbon source to be metabolized by heterotrophic microbes to PHAs and the high energy demands for the fermentation process are major drawbacks (Fradinho et al., 2013). Even though there have been approaches to use waste as substrate, like domestic wastewater or from olive oil mill effluents, sugarcane molasses and food waste, the process is still very expensive and only feasible for high value products used in medical applications (Koller et al., 2011; Verlinden et al., 2007).

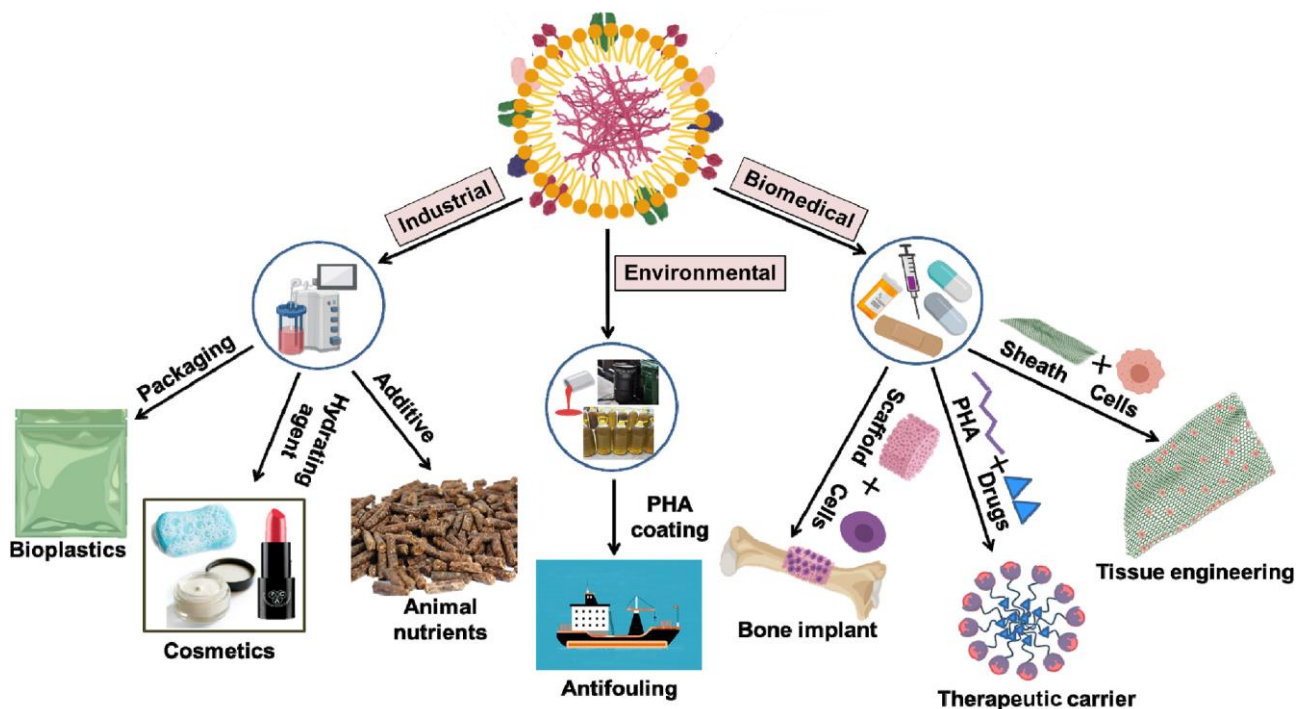


Figure 9: Overview of PHA products and applications in industrial, environmental and biomedical sectors. (Behera et al., 2022)

In contrast, photoautotrophic microalgae only require inorganic nutrients for their growth like CO_2 , nitrogen, phosphorus etc. (Markou & Nerantzis, 2013). Therefore, cyanobacteria are a potential low-cost alternative additionally fixing CO_2 from the atmosphere, posing as a carbon sink and demonstrating a combined strategy for fighting human induced climate change by reducing greenhouse gases as well as mitigating plastic pollution by substituting petrol-based plastics with biobased and biodegradable polymers.

5.4 Cyanobacteria, the revolutionizing bacteria.

The gram-negative cyanobacteria are autotrophs living on oxygenic photosynthesis. They constitute one of the largest sub-groups of gram-negative prokaryotes and the most diverse monophyletic group (Stanier et al., 1979). They are very heterogenous in their morphologies, including unicellular, multicellular, colonial, filamentous, and branched filamentous forms and also their cell size can vary over two orders of magnitude, which makes them more diverse than any other prokaryotic group (Sharma, 2014).

Their origin dates back more than 2450 million years ago, therefore they constitute to the oldest life forms on earth (Schopf, 2011). During the Great Oxidation Event, they have shaped this planet by enrichment of the atmosphere with oxygen (Holland, 2002). Thereby they have induced the first mass extinction on the planet making the atmosphere unliveable for strict anaerobic live forms, but

also enabling multicellular live forms by providing the oxygen required for aerobic respiration yielding higher energy.

Thereby they have not only left their mark on the planet but also on the evolution of all plants. The endosymbiont theory states that cyanobacteria are the origin of all chloroplasts of eukaryotic plant cells. Cyanobacterial ancestor cells were taken up through endosymbiosis by a eukaryotic host cell, that later evolved into plants (Delwiche & Palmer, 1997).

Even though they lack sexual reproduction and solely multiply by asexual cell division, they managed to adapt to a great span of conditions including life in extreme environments. This makes them one of the most successful organisms on the planet with a global distribution spanning from cold arctic lakes to hot springs. They can be found in fresh water as well as marine and terrestrial habitats. They adapted to tolerate high temperature, UV radiation, desiccation, water and salt stress making them capable to survive hot deserts with combined drought and high temperature stress, while others tolerate high pH and high salinity (A. K. Srivastava et al., 2013; Whitton & Potts, 2002).

They also exist in many symbiotic relationships including cyano-lichens which is one of the best-studied terrestrial symbioses (Calcott et al., 2018).

As a significant contributor to the marine carbon dioxide fixation and as a major primary producer, they contribute to the annual global biomass an estimated of $3 \cdot 10^{14}$ g C or a thousand million metric tons (10^{15} g) of wet biomass (Garcia-Pichel et al., 2003). Cyanobacteria therefore play an important role in the global carbon cycle and food web (Flombaum et al., 2013). Quantitatively they are the world's most significant organisms (Whitton, 2012).

Because of the ability of many cyanobacteria species to fixate atmospheric nitrogen they can be described as carbon and nitrogen autotrophs (Herrero & Flores, 2008). This ability makes them to an essential player in the global biogeochemical cycles of nitrogen, carbon, and oxygen (Sharma, 2014; Shih et al., 2013).

Most unicellular cyanobacterial cell consist of three different membrane systems (Figure 10). The outer membrane, rich in lipopolysaccharide, is separated from the inner plasma membrane by the periplasmic space, which is divided by a peptidoglycan layer. The third membrane system are the thylakoid membranes enclosing the so-called thylakoid lumen. The thylakoid membrane accommodates the protein complexes for the photosynthesis and respiration, making it the primary energy-transducing membrane system. The thylakoid membrane is structured into stacked arrays of parallel sheets converging in certain areas neighbouring the plasma membrane attached at so called thylakoid centres (van de Meene et al., 2006).

Cyanobacteria can also be surrounded by slime coats, capsules and mucoid sheaths formed by released extracellular polysaccharides. These biofilms play a protective role against extreme environmental conditions and are necessary for gliding movement (Sciuto & Moro, 2015).

In the cytoplasm the genetic material is present in the form of the nucleoid, which is organized in most cyanobacteria as circular chromosome with different ploidy levels. For example *Synechocystis* sp. PCC 6803 can contain up to 218 chromosome copies per cell (Noreña-Caro & Benton, 2018). Also other important cell organelles like ribosomes, lipid-droplets, vacuoles, Cyanophycin granules and carboxysomes are present in the cytoplasm. The carboxysomes have a special role and engage in the carbon concentration mechanism. They do so by forming a protein envelope around the RuBisCO enzyme which is involved in carbon dioxide fixation (Dai et al., 2018; Ducat et al., 2011).

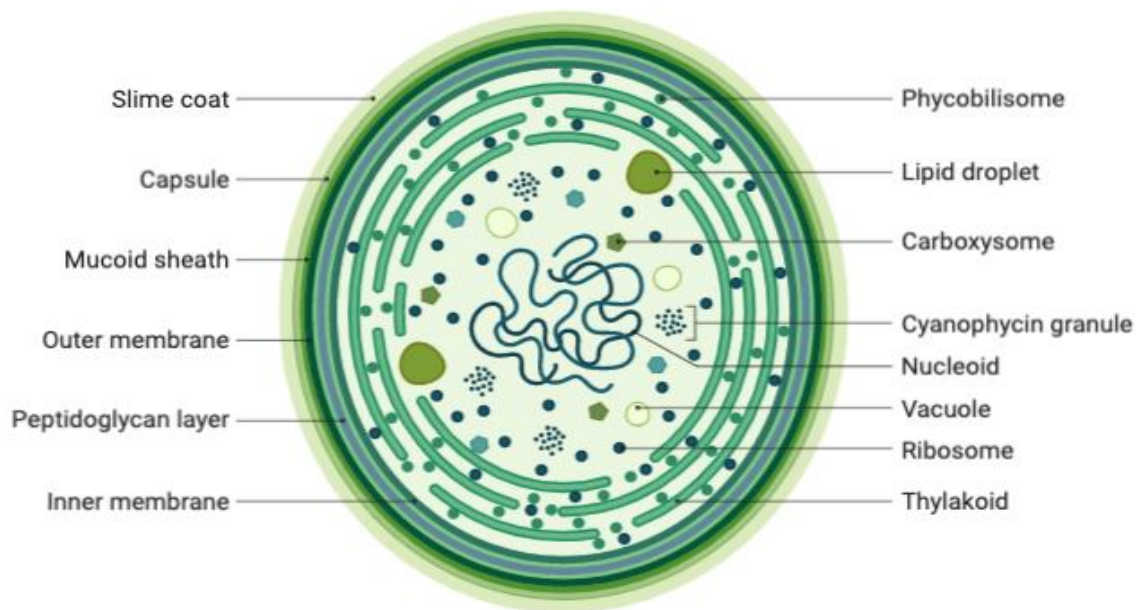


Figure 10: Cyanobacteria Structure (BioRender, 2020). (Retrieved from <https://app.biorender.com/biorender-templates/t-5ffdfec7a0005e00aa69816e-cyanobacteria-structure>)

Besides unicellular cyanobacteria also multicellular cyanobacteria species are known, with the ability to differentiate vegetative cells to specialized cells. These so called heterocyst have the ability to fix nitrogen (K. Kumar et al., 2010).

For their autotrophic lifestyle cyanobacteria depend on structures for harvesting the solar energy. These very organized light-harvesting complexes include chlorophylls, carotenoids, and phycobiliproteins.

The best-known photosynthetic pigment found in higher plants, algae and cyanobacteria is chlorophyll-a, which can absorb light in the red and blue spectrum of the visible light and therefore emits the complementary green light. Chlorophyll-a is also the pigment found in the reaction centres of photosystem I and II, involved in the photon harvesting, but some cyanobacteria species contain the alternative chlorophyll-b, -d and -f in their photosystems (Prashant Kumar Singh et al., 2020;

Sharma, 2014; Trampe & Kühl, 2016). Carotenoids additionally support light absorption and protects the cells from light damage (Sharma, 2014).

The phycobiliproteins are a family of accessory pigments exclusive to cyanobacteria, red algae and cryptomonads. They are large water-soluble supramolecular protein aggregates classified depending on their spectral properties as phycoerythrin, phycocyanin, and allophycocyanin. They are involved in the light harvesting as so called phycobilisomes. The phycobilisome structure can change depending on the light quality, light quantity, and nutrient availability of e.g., nitrogen, sulphur. Furthermore, stress conditions can impact the composition and function of phycobiliproteins in cyanobacteria (Chakdar & Pabbi, 2016).

Cyanobacteria can therefore have different colours depending on their pigment type and concentration e.g., green, blue-green, brown, purple, red and even completely black (Oren, 2014).

This diversity of pigments allows cyanobacteria to utilize the available visible light ranging from 400 nm to 700 nm most efficiently. The cyanobacterial chlorophylls absorb blue ($400 < \lambda < 500 \text{ nm}$) and red light ($600 < \lambda < 700 \text{ nm}$), aided by carotenoids for harvesting the blue and blue-green light. The otherwise by chlorophyll emitted yellow-green, yellow and orange spectra are absorbed by phycobillin ($480 < \lambda < 600 \text{ nm}$) (Noreña-Caro & Benton, 2018; Oren, 2014; Shevela et al., 2013).

Phycobilisomes are light harvesting complexes located on the cytoplasmic side of the thylakoids connected to the internal antenna subunits of Photosystem II. These multidimensional extraneous antennae are larger in size than the photosystems consisting of a horizontal cylindrical protein structure as a core from which peripheral rods stick out (Figure 11). This rods are formed by stacked disc-shaped proteins constituted by phycobiliproteins attached via thioester bonds (Noreña-Caro & Benton, 2018; Shevela et al., 2013).

The phycobiliproteins are classified as phycocyanin, phycoerythrin, and allophycocyanin (Bermejo, 2014), depending on their composition and content of chromophores that are again in term

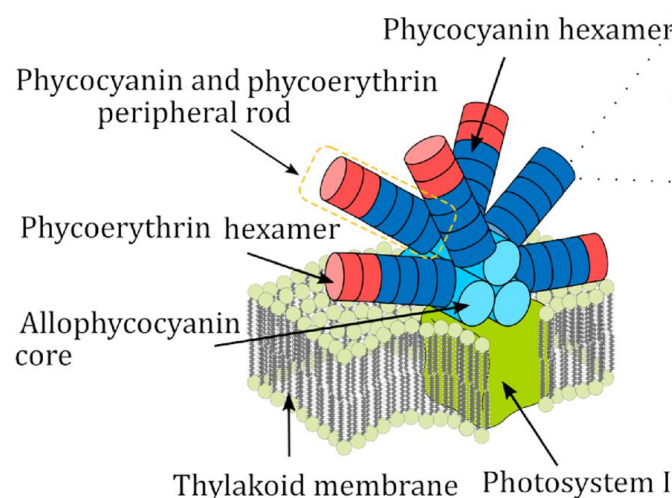


Figure 11: General structure of a phycocyanin rich phycobilisome attached to photosystem II. (Noreña-Caro & Benton, 2018)

constituted by phycocyanobilin, phycoerythrobilin, phycourobilin, and phycoviolobilin, which are blue, red, yellow, and purple, respectively (Chakdar & Pabbi, 2016).

With the ability of cyanobacteria to change the size of the phycobilisomes and thereby control the energy flow, they can adapt to varying light conditions. The phycocyanin and phycoerythrin at the periphery adsorb more energetic radiation, while the allophycocyanin located at the core absorbs the less energetic radiation. At low light intensity the peripheral rods grow by adding more phycocyanin and phycoerythrin, whereas they shrink with increasing light intensity even leaving only allophycocyanin under extreme illumination (Shevela et al., 2013).

The harvested light is used to produce oxygen and carbohydrates from carbon dioxide and water in a process called photosynthesis, converting electromagnetic energy into chemical energy by an electron transport process.

The Photosynthesis reactions are divided into two phases, the light and the dark phase. The first big difference of the two phases is their location. While the light phase reactions occur in the thylakoids, the dark phase reactions take place in the cytoplasm (Shevela et al., 2013).

The second major difference is their function. The purpose of the light reactions is to capture photons, oxidize water and reduce NADP to NADPH. During the process also molecular oxygen and ATP are formed. The NADPH and ATP function as chemical energy transporters that can be used in the light independent dark phase to power energy dependent biochemical reactions producing organic compounds like sugars from carbon dioxide (Noreña-Caro & Benton, 2018).

The ATP needed to power the primary metabolism of the cell is produced in cyanobacteria either by photosynthesis or cellular respiration, both located in the thylakoids. The light reaction and carbon fixation are the initial processes in all photoautotrophic organisms for sugar synthesis.

The bottleneck process is the carbon fixation by the enzyme ribulose-1,5-biphosphate carboxylase (RuBisCO) (Durall & Lindblad, 2015). Cyanobacteria have evolved a so-called carbon concentration mechanism, which enables them to convert up to 10% of the sun light into biomass. This is ten times more efficient than the maximum photosynthetic conversion of terrestrial plants and twice as high as in algae (Noreña-Caro & Benton, 2018).

This can be achieved because of special organelles called carboxysomes. They are proteinaceous polyhedral bodies covered by a protein shell (Nogia et al., 2016). Their structure and various inorganic carbon transporters are able to concentrate the CO₂ in close proximity to RuBisCO, present at high concentrations in the carboxysomes (Price, 2011).

The carbon fixation takes place in the Calvin–Benson–Bassham cycle (CBB) or pentose phosphate cycle connecting the light reactions with the following metabolic pathways (Durall & Lindblad, 2015). High energy compounds of less stability are converted by the biochemical reactions in the CBB cycle

into more stable molecules used for building and storage. Glucose can be produced from the triose phosphate pool filled by the CBB cycle, after carbon fixation (Blankenship, 2002).

The carbon storage of cyanobacteria differs from plants and algae that use the glucose for building their cellulose cell walls and to form starch as storage. Cyanobacteria's main glucose storage is glycogen and they also use carbohydrates for building their EPS layer (Hays & Ducat, 2015).

Glycogen is a branched polymer consisting of glucose subunits linked by α -1,4-glycosidic bonds (~90%) and α -1,6-glucosidic bonds (~10%) (Iglesias & Preiss, 1992).

Another storage substance produced by cyanobacteria is the former mentioned PHB directly from sunlight and CO₂ using the oxygenic photosynthesis.

The responsible genes are regulated by a common promoter. The genes *phaC*, *phaA* and *phaB* translate into the necessary enzymes for the biosynthesis of PHB in cyanobacteria. The synthesis starts, as shown in in Figure 12, with the acetylation and reduction of acetyl-Co-A by the enzyme β -ketothiolase (PhaA) and acetoacetyl Co-A reductase (PhaB). The PHA synthase (PhaC) is responsible for the final polymerization of the hydroxyacyl-CoA thioesters (Behera et al., 2022).

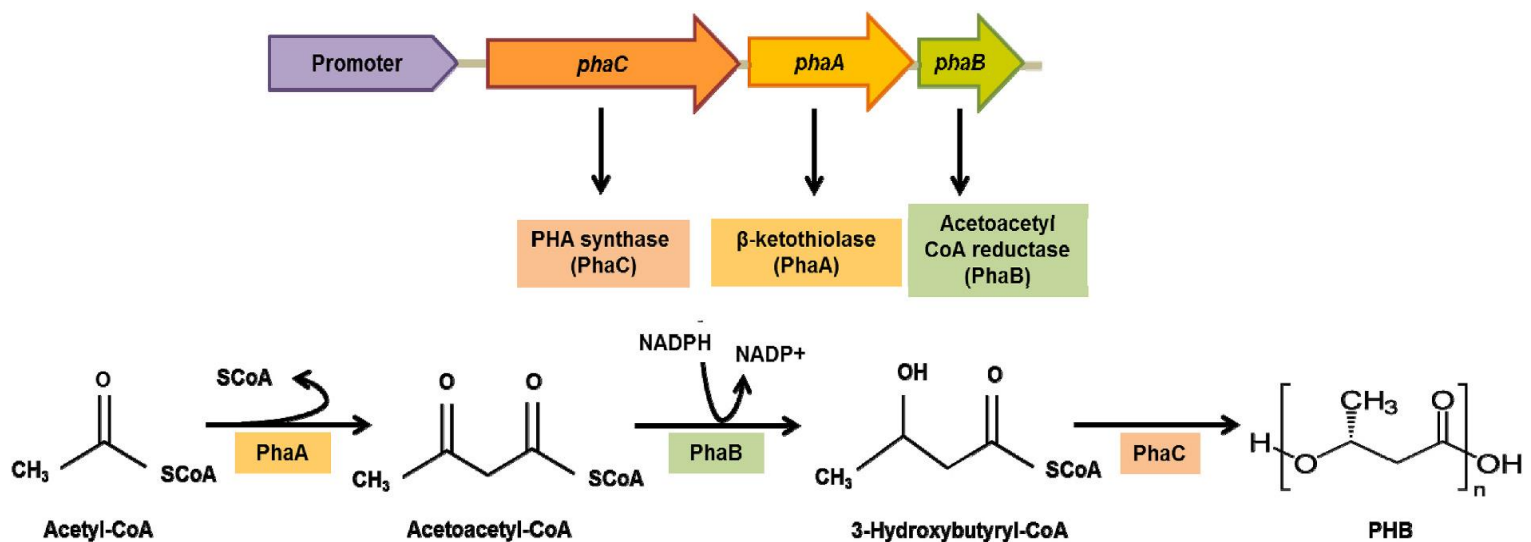


Figure 12: Operon structure of the genes involved in the PHB synthesis (phaC, pha A and phaB) (Behera et al., 2022).

The glucose accumulated during illumination is used in the catabolism in the glycolysis and the oxidative pentose phosphate pathway (OPP). Glycolysis produces ATP and pyruvate from the stored glucose, while the OPP pathway is used during aerobic dark respiration and is divided in an oxidative and a nonoxidative part which consists of the reverse CBB cycle. The TCA cycle as the first cellular respiration stage provides precursor metabolites and reductive power in form of NADH and FADH₂ by oxidising carbon fuels like carbohydrates, fatty acids, and amino acids. To enter the TCA cycle molecules must be transformed into acetyl-CoA. The pyruvate, resulting from glucose undergone glycolysis, is decarboxylated and fused with coenzyme A by the pyruvate dehydrogenase complex. The TCA cycle initiates the oxidative phosphorylation pathway as the final cellular respiration stage. The NADH and FADH₂, as well as succinate are oxidized by the ubiquinone-oxidoreductase

complex-I and complex-II, respectively. The electrons are further transferred to cytochrome-c by the cytochrome-c-oxidoreductase complex-III. In the final step cytochrome-c is oxidised by the cytochrome-c oxidase (COX) reducing one O_2 to H_2O . For the reduction of oxygen four protons are used and at the same time four protons are translocated from the cytoplasm across the thylakoid membrane. The resulting increase of hydrogen ions inside the thylakoid lumen result in an increase in the proton motive force used by the ATP synthase to produce ATP (Noreña-Caro & Benton, 2018).

From all cyanobacteria the genus *Synechocystis* is best suited for the PHB production in a photobioreactor, since they fail to produce aggregates which distinguishes them from other genera (Sauvageau, 1892). They are unsheathed, spherical and monocellular, with cells only occurring singly or in pairs. They divide by binary fission in two planes at right angles to one another (Stanier et al., 1979).

The PHB production is used by *Synechocystis* for buffering excess acetyl-CoA and NADH during darkness and under stress conditions. It is especially synthesized during nitrogen and phosphate depletion. After glycogen, PHB is degraded for energy production in the TCA cycle (Drosg et al., 2015).

5.5 Stress factors influence the PHB production

The extraordinary metabolic flexibility of cyanobacteria implies high complexity in the regulation of their PHB synthesis and could be influenced by different biotic and abiotic factors. Recently it has been shown by Obruča et al. (2020) that unfavourable environmental conditions stimulated the PHB production in cyanobacteria. Additionally Nitrogen and phosphorous starvation with a simultaneous energy and carbon surplus has been shown to induce the PHB production (Obruča et al., 2020; Panda et al., 2005).

This ability is owed to the adaptation to their natural habitat in microbial mats characterized by fluctuations in the nutrient and carbon availability. The most important carbon source in the mats are the organic carbons produced by photosynthesis. The ability to store excess organic compounds produced by photosynthesis during the day as PHB and glycogen to consume them during the night has advantages for the bacteria (Koller et al., 2011).

When the cyanobacteria *Synechocystis* enter nitrogen limitation a survival process is induced called chlorosis (Forchhammer & Schwarz, 2019). In this state they can survive prolonged periods of nitrogen starvation and the process is characterized by degradation of the photosynthetic machinery and most thylakoid membranes, which leads to a change in the cells coloration from green to yellow. The cell cycle is arrested and the metabolism is shut down (Doello, Burkhardt, & Forchhammer, 2021). Additionally large amounts of glycogen and PHB are accumulated inside the cells (Figure 13). The glycogen serves as sink for newly fixed CO_2 , however prolonged starvation leads in the same time to lower glycogen metabolism (Gründel et al., 2012).

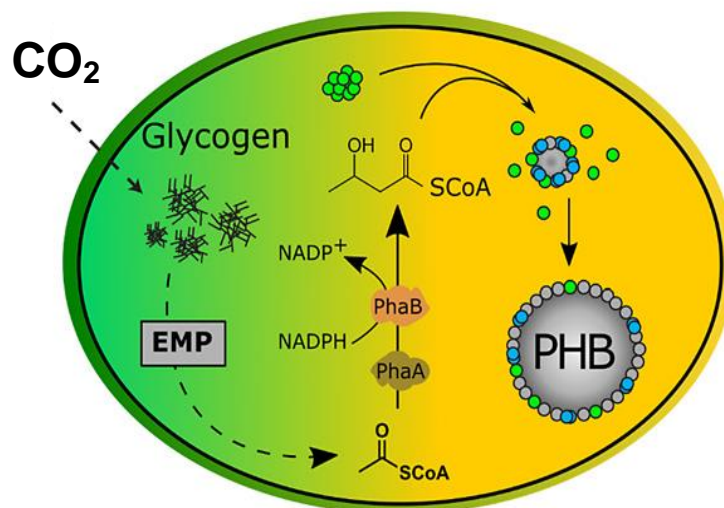


Figure 13: Illustration of the PHB metabolism in chlorotic cells. Carbon dioxide is fixed as glycogen which is degraded by the EMP cycle to ac-

These metabolic and morphological changes induced by nitrogen starvation result in the cells entering a dormant state, which allows them to survive for an extended period of time under such unfavourable conditions (Schwarz & Forchhammer, 2005).

Even though the exact functions of PHB is still under investigation, it is known to be accumulated by chlorotic and of nitrogen starving cyanobacteria. Therefore, it is assumed to play a major role in their strategy to overcome environmental stress. Isotope labelling experiments by Dutt and Srivastava (2018) showed that the majority of the PHB carbon originates from intracellular metabolites. Koch et al. (2019) provided evidence that the carbon for the PHB synthesis during nitrogen starvation comes indeed from the intracellular glycogen pool.

When the chlorotic cells enter the dormancy state, they still need a residual metabolism to ensure repairs of essential biomolecules such as proteins and DNA. Therefore, even non-growing starving cells need a constant supply of ATP, reduction equivalents and cellular building blocks. The PHB production is mainly powered through the Embden–Meyerhof–Parnas (EMP) pathway, which has the highest ATP yield among the three main carbon catalytic pathways (Koch et al., 2019).

The limitation of nutrients indirectly increases the acetyl-CoA concentration which is used for the PHA synthesis (Costa et al., 2019). Though the limitation in nitrogen has been shown to result in the accumulation of a higher percentage of PHA (30.7%) compared to the limitation of phosphorous (14.1%). Additionally the nitrogen limitation can also increase the carbon reserve inside the cell via the degradation of various macromolecules (Behera et al., 2022; Costa Coelho et al., 2015). Phosphorus limitation directly influences the synthesis of nitrogen containing molecules such as nucleotides, ATP and phospholipids (Samantaray & Mallick, 2015). Thus, nitrogen limitation is crucial for PHA accumulation in microalgal cells.

Once the nitrogen limitation has been overcome the glycogen catabolism supports the reawakening and re-greening of the cells (Doello et al., 2018). As soon as nitrogen becomes available again, the dormant cells immediately initiate a resurrection program. First, they metabolise the glycogen for energy and intermediates to rebuild the degraded cell components. The cells switch back to photosynthesis once the machinery has been restored. For the initial anabolic reactions after nitrogen addition, energy is quickly required and therefore the ATP content rapidly increases to 50% of that of a vegetative cell. This ATP is initially not produced by glycogen catabolism, but by sodium gradient dependent ATP synthases (Doello, Burkhardt, & Forchhammer, 2021).

Cyanobacteria sustain their cell growth by performing oxygenic photosynthesis and they synthesize glycogen towards the end of the day to fix the excess fixed carbon as storage to survive the night (Welkie et al., 2019). Like the glycogen, PHB serves as an additional carbon and energy storage helping the cell to survive periods of shortages. Still, the true functions are under investigation, but the PHB could also serve as an electron sink eliminating a surplus of reducing equivalents (Batista et al., 2018).

Also bacteria convert glycogen to PHB, however under anaerobic conditions in the dark metabolism (van Gemerden, 1968) which allows the cells to keep the carbons compared to secreting fermentation products (Hauf et al., 2013).

Also, the limitation of gas exchange can boost the PHB production as the cyanobacteria have adapted to natural day-night rhythm. They produce oxygen through photosynthesis and are therefore oxygen-oversaturated during the day, while they consume oxygen during night. This results in transient periods of limited oxygen availability. Cultivation under limited gas exchange led to an overall lower PHB production, while shaking cultivation with continuous oxygen availability led to higher PHB yields. It has also been reported, that the cultivation under a day-night rhythm resulted in an increased content of PHB per cell-dry-weight compared to continuous illumination (Koch, Berendzen, & Forchhammer, 2020).

Artificial light can act additionally as stressor as it can deviate from the natural light in its availability (e.g., continuous illumination), light composition, and light intensity. Especially excess light can harm the cells and can damage the photosynthetic apparatus, therefore the light-harvesting complexes perform photoprotective quenching functions to prevent the formation of harmful chemical species such as triplet chlorophyll and singlet oxygen (Magdaong & Blankenship, 2018).

Under dark or low light conditions, the metabolism has to rely on the oxidative phosphorylation generating ATP from NADPH. And only a negligible flux was detected through the EDP pathway under heterotrophic conditions (Wan et al., 2017).

The main carbon flux for the PHB synthesis comes from the light-driven CO₂-capturing through the CBB cycle. The polymers supply carbon and energy during imbalanced nutrient conditions and are

accumulated during limited growth, because of nitrogen and phosphorus (Shang et al., 2003) or oxygen depletion and the presence of an excess amount of carbon sources (Verlinden et al., 2007).

The presence of PHA granules in prokaryotic cells enhances their stress resistance and robustness beyond that as results of Obruča et al. (2020) showed. The authors found that PHA-rich cells have higher survival rates under stress conditions and can better withstand environmental stress factors such as high or low temperature, freezing, oxidative, and osmotic pressure. Concluding that the protective properties PHA granules are associated with are due to their unique architecture and biophysical properties as well as their fundamental interconnected metabolism

Additionally, PHA granules also protect cells against UV radiation by efficiently scattering it. Thereby the intracellular level of reactive oxygen species in UV-challenged cells is decreased and they present much higher resistance to UV exposition (Slaninova et al., 2018).

These protective properties are even more enhanced by PHB granules specifically binding to DNA which provides shield-like protection for the very UV-sensitive DNA molecules (Obruča et al., 2020).

5.6 The project PHBecol investigates the ecological role of PHB in cyanobacteria

The project PHBecol aims at elucidating the ecological role of PHB in cyanobacteria. This project is funded by the FWF as an international project (I 4082-B25) facilitating the collaboration of the University of Natural Resources and Life Science Vienna (BOKU), the Brno University of Technology (FCH BUT) and the Czech Academy of Science Institute of Scientific Instruments.

The projects goals are subdivided into five work packages (Figure 14), with the work package 2 focusing on the connection between PHB accumulation and the stress resistance of cyanobacteria. There have been several studies concerning the functions and interactions of PHA's in heterotrophic bacteria, but still little is known about their role in photoautotrophic cyanobacteria. This project aims at better understanding the biological and ecological role of PHB's in cyanobacteria by conducting highly specialised methods for measurements of chemical, physical, morphological, and molecular parameters of cyanobacteria cells exposed to favourable and unfavourable environmental conditions. With the collected data the insights into the stress response and it's connection to PHB accumulation can be used for future process optimisation to overcome the current limitations in biotechnological mass production (Fritz, 2019).

By improving such processes this project contributes to the ongoing venture of our society toward a circular and sustainable society, which is independent of fossil fuels. By producing polymers with cyanobacteria fixing carbon from the atmosphere this technology could impact the growing bioeconomy.

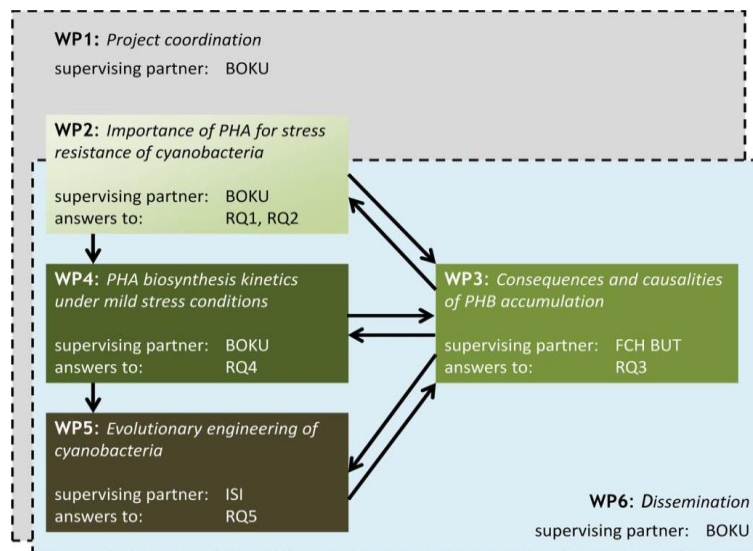


Figure 14: Excerpt of the Joint Project Proposal representing the working package structure from the Project PHBecol and their main tasks and the relations and dependencies between the topics. RQ1-RQ5 are references to the project core questions and are not shown.

5.7 Bioplastic as part of the growing bioeconomy

Bioeconomy is often referred to as ‘biobased economy’, as such it encompasses the production and conversion of biobased resources into food, feed, bioenergy, and biobased materials. Biobased value chains include the primary production of the used bioresource, the conversion into higher-value goods and their commercialization. This transdisciplinary approach supports the bioeconomy in its aim to overcome the most relevant societal challenges and the switch from a fossil-based economy to a new biobased sustainable economy. By exploiting new resources and building on renewable biomass the use of limited fossil resources can be reduced or substituted and thereby contributing to climate change mitigation and the transition can be made towards a sustainable society (Lewandowski et al., 2018, pp. 5–15).

Biobased plastics as derivatives from biomass are therefore part of the bioeconomy, but this doesn’t make them automatically sustainable. They also have to be biological degradable to ensure no further accumulation of macro- and subsequently microplastics in the environment. Since the recycling of conventional plastics is difficult and prone to downcycling by thermal degradation of some degree, the enzymatic recycling or use as nutrient source for the microbial production of bioplastics represents a system of a much higher degree in circularity.

Even though the regrowing biobased resources form a large and theoretically unlimited resource, with an annual increment of 300,000 billion tons of biomass (Lewandowski et al., 2018, p. 10), an often-discussed problem in biomass based production is the need of mainly land, soil and plant nutrients. This often leads to the discussion ‘fuel versus food’ or in the case of bioplastics ‘materials vs. food’, when talking about PLA (polylactic acid), that is derived from bacteria fermented sugars, mainly produced from sugar beets or corn. This is not the case for the production with photoautotrophic cyanobacteria since there is no competition of their production with any agricultural food production. The cultivation of phototrophic microorganisms does not provoke such conflicts but is a relatively new research segment and far less optimised compared with agriculture. The major challenge in photoautotrophic cultivation is the provision of sufficient sunlight for the culture. Different reactor systems have been developed with unique advantageous and disadvantageous, that are selected according to the desired product and the requirements of the cultivated species. Open ponds, tubular reactors, and flat-panel reactors (Figure 15) are the most common systems applied today. The aim of reactor systems is to control and regulate various process parameters to optimize the biomass yield. In this context, the nutrient and the light supply are of the most importance for microalgae growth (Schließmann et al., 2018).

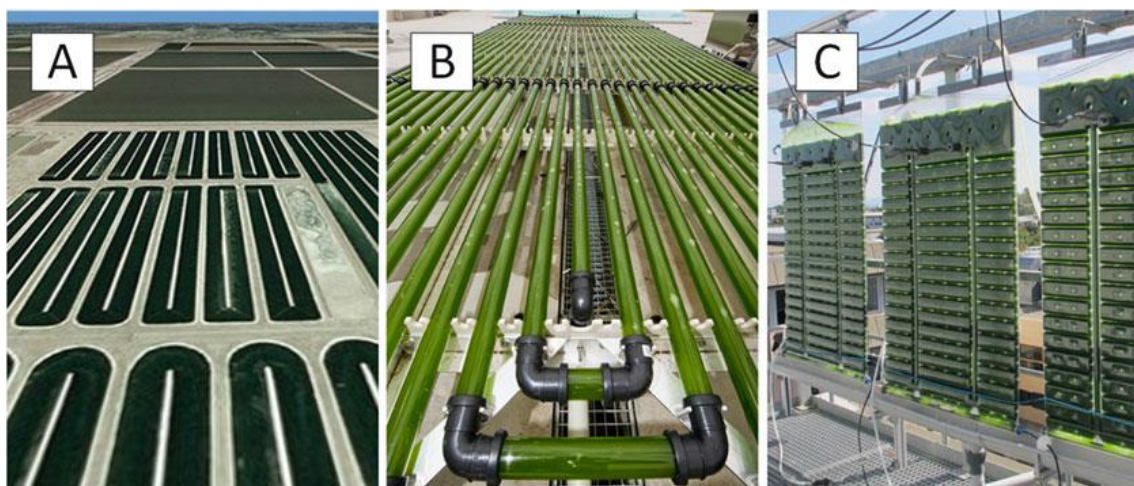


Figure 15: Different bioreactor systems used for microalgae cultivation: (A) race-way ponds in southern California (White 2011, AlgaeIndustryMagazine.com), (B) tubular reactors (AlgaePARC, Wageningen University, Netherlands) and (C) flat-panel-airlift bioreactors (Fraunhofer IGB, Stuttgart, Germany). (Schließmann et al., 2018)

In general, the open pond cultivation reflects the natural algae environment and are natural or artificial lakes. Their main disadvantage is the inability to avoid contaminations, low process control and a rather large area needed accompanied by a corresponding high-water evaporation. An improvement are raceway ponds, which require less space and are equipped with a paddle wheel to generate a higher flow velocity. The big advantage of such systems is the low investment needed and their simple operation. Due to the insufficient light supply and inadequate mixing the biomass productivity in these systems is low. Tubular reactors on the other hand are closed systems, in which the biomass

is pumped through transparent tubes. Thereby the evaporation and contamination risk can be avoided, and the process parameters are more easily controlled. But since the flow is usually not turbulent, CO₂ and oxygen gradients can arise along the tubes. The most important parameter for the cultivation remains the light and therefore reactors with a high surface-to-volume ratio called Flatpanel reactors exhibit the highest productivity. These are vertical systems only a few centimetres thick and aerated and mixed by bubbling gas from the bottom (Schließmann et al., 2018).

Even though there are already examples for cyanobacteria biorefinery concepts for the production of PHB (Meixner et al., 2018; Troschl et al., 2018) this process still needs a lot of further development to become competitive with conventional plastic production and the production of other bioplastics based on fermentation rather than photosynthesis.

One of the biggest obstacles for the economic feasibility remains the low PHB accumulation inside the cells (Singh et al., 2017). Most cyanobacteria only produce less than 20% PHB of their cell dry mass naturally, while chemotrophic bacteria (e.g., *Cupriavidus necator*) produce more than 80% (Drosg et al., 2015). Additionally, the growth rate and the culture density of cyanobacteria is too low to compete with chemotrophic bacteria. There have been some attempts to increase the yield also by genetic modification, but the success was so far limited by a lack of knowledge about the details of the cells' metabolism (Koch et al., 2019).

Another advantage could be the successive use of the cyanobacterial biomass, since microalgae are known to produce many other additional valuable biomolecules like different carbohydrates that could be used as renewable energy source (e.g., bioethanol, biodiesel, palm oil substitute), proteins as supplements for food and feed applications (e.g., animal feed in aquacultures or fish oil), pigments, phytosterols and triacyl glycerides. By the employment of a combination of multiple extraction steps in a cascaded extraction procedure a multiple of products could be potentially extracted from the microalgae biomass instead of only the biopolymer (Schließmann et al., 2018, 154–160).

Synthetic biology could allow engineering cyanobacteria to become solar biofactories for sustainable conversion of CO₂ emissions, sunlight, and water into valuable products. Such cyanobacterial biofactories could bring great benefits for the post-petrochemical era (Noreña-Caro & Benton, 2018).

Concluding, bioplastics can be considered an essential part of the bioeconomy. As they have the advantage over conventional plastics to reduce the dependency on limited fossil resources and to reduce greenhouse gas emissions by replacing the fossil content in plastics with plant-based content. Life cycle analysis show significant lower CO₂ emissions compared to conventional plastics, depending on the feedstock, the product and the application. The resource efficiency can be increased through a closed resource cycle and cascades use, since the enzymatic recycling is feasible

more easily or the use as substrate is possible, additionally residues can be used for energy recovery such as biogas digester.

According to the European Bioplastic association, the bioplastic industry is fast-growing and innovative with the potential to reduce negative environmental impacts by replacing fossil feedstock with bio-based feedstock, while continuing to harness the benefits of plastics. They state that the market for innovative biopolymers such as PHAs is increasing, and their production capacities are set to more than triple in the next five years. The bioplastic industry accounts for around 23,000 jobs in Europe and this number could increase more than tenfold by 2030. According to European Bioplastic up to 300,000 high skilled jobs could be created, if the right framework conditions and legislations came in place, but therefore an integrated political and economic framework is still needed (European Bioplastics).

5.8 The need of constant plastic quality for production

To make PHB as a biobased and biodegradable plastics competitive with petroleum-derived plastics besides their price and economically feasibility especially their quality is of most importance.

PHAs are in general semi-crystalline polyesters, which differ in their properties according to their chemical structure. The PHB homopolymer is highly crystalline (Padermshoke et al., 2005) and a stiff, but brittle material. It displays a hard-elastic behaviour when spun into fibres (Antipov et al., 2006). The crystalline PHB homopolymer has a helical structure, which seems to be similar in its various copolymers (Padermshoke et al., 2004).

PHB is a strong, but also brittle material and therefore not shock resistant. The relatively high T_m of around 170°C is close to its decomposition temperature, limiting the processability of the homopolymer. When using copolymers, the mechanical and thermal properties of the PHB homopolymer can be improved significantly. Some copolymers are less stiff and brittle improving the mechanical properties even further, resulting in polymers comparable to conventional plastics such as polypropylene (PP), polystyrene (PS) and polyethylene terephthalate (PET). A range of properties is feasible from the hard and brittle homopolymer by using copolymers to balance stiffness and toughness to soft and still tough. Copolymers can also be used to tune the hydrophilicity, hydrolytic stability of the polymer and additionally the degradation can be controlled (Muhammadi et al., 2015).

For the characterisation of the polymer processability certain material properties have to be determined to predict their behaviour during processing as well as of the final product. Therefore the most conducive parameters are the thermal and rheological properties additionally to the molecular mass distribution and structure (Kovalcik et al., 2017).

Since polymers consist of long chains of repeating monomeric subunits bound by chemical bonds, knowledge of the polymer length is required to understand the physical properties of the polymer. The chain length is commonly expressed as molecular weight of the polymer chain, because this directly relates to the relative molecular mass of the monomer and the number of monomers in the chain. But all polymers are polydisperse, which means that they are containing polymer chains of different length and therefore the molecular weight is also not a single value. The polymers are rather present as a distribution of chain lengths and molecular weights. The polymer molecular weight is therefore described as average molecular weight calculated from the molecular weight of all chains. The commonly used molecular weight averages (M_n) are mostly determined by gel permeation chromatography (GPC) or size exclusion chromatography (SEC). Another parameter is the number average molecular weight (M_w), which is the statistical average molecular weight of all the polymer chains in the sample. M_w additionally considers the molecular weight of a chain compared to M_n . By determining the contributions to the molecular weight average, M_w expresses that more massive chains contribute more to the final value. The fraction of M_w over M_n expresses the broadness of a molecular weight distribution of a polymer and is called polydispersity index (PDI). The broader distributed the molecular weight the larger the PDI becomes. If all chains have the same length, for example in a pure protein fraction, the PDI is equal to 1 and called a monodisperse polymer. But it has to be mentioned, that two polymer samples could have the same PDI and at the same time their standard deviations could be completely different (Rane & Choi, 2005).

The PDI is often used to evaluate if a polymer sample is suitable for production. The more homogenic the polymer chains are in length and weight, the lower the PDI and the more consistent is the final product in its quality. Products from high PDI polymer samples have fewer constant properties and cannot meet the material requirements. Therefore, the molecule length and the size distribution of a polymer fraction is decisive for its application.

The PHB polymers derived from *S. salina* displayed average M_w up to about 8MDa, but generally it can vary greatly depending on the origin, different kind of producing bacteria, growth conditions and polymer extraction procedure (Kovalcik et al., 2017).

6 Aims

The project PHBecol investigated the physiological role of PHB production in cyanobacteria. With the contributed knowledge the replacement of petrol-derived polymers with PHB as bio-based and biodegradable alternative should be further promoted.

In a previous master thesis conducted by Antonia Zerobin it was shown, that continuous illumination increased PHB accumulation compared to the cultivation with a day-night cycle (16/8h) (Zerobin, 2021). Since this finding opposes the general view of a higher intracellular PHB accumulation under alternating day-night rhythm, this work tries to elucidate the reasons for this observation.

Therefore, the work focused on investigating the effects of continuous illumination on the growth of three different cyanobacteria strains and their PHB production. To evaluate if light can be used as stressor boosting PHB production, the light intensity was increased in three consecutive experiments. Additionally, the morphology of the cells is checked throughout all experiments to find out the cause of the increased cell size reported by Zerobin.

Since consistent quality is important for the manufacturing process and the practical use of PHB, the impact of the used illumination conditions on the PHB quality given as the dispersive index (PDI) was examined by PHB extraction and analysis with gel permeation chromatography (GPC).

With this work the connection between illumination conditions and PHB production is further elucidated to improve PHB production conditions in the future and overcome current obstacles using cyanobacteria.

7 Material and Methods

7.1 Strains

Three different Cyanobacteria strains were used in the experiments of this study. *Synechocystis* sp. PCC6803 (S.6803) was obtained from the Pasteur culture collection (FRA), *Synechocystis* cf. *salina* CCALA192 (S.192) was obtained from the culture collection of autotrophic organisms (CZE) and the wild-type *Synechocystis* strain called IFA-3, was isolated from a pond in Lower Austria and identified by sequencing the 16S-rDNA (Meixner et al., 2022). The cultures used in the experiments were not axenic and were cultivated with their accompanying flora of unidentified heterotrophic bacteria.

7.2 Media

The cyanobacteria were cultivated in BGI medium, a mineral medium based on BG-11 (Stanier et al., 1979). For the experiments the medium was adapted to the 22O medium with a lower nitrogen content to expose cells faster to nitrogen depletion.

7.2.1 22O

Table 1: Composition of 22O medium

Component	Concentration [g/L]	Element	Concentration [mM]
NaNO ₃	0.450	N	5.48
Fe(NO ₃)•9H ₂ O	0.025	P	0.46
MgSO ₄ •7H ₂ O	0.100	K	0.92
CaCl ₂ •2H ₂ O	0.600	Ca	5.38
Trace element solution, v5	1.5 mL	Mg	0.41
Na ₂ CO ₃	0.200	Na	10
K ₂ HPO ₄	0.080	C	2.38

Final N:P ratio corresponds to 11.9.

Two different solutions were prepared and mixed, to prevent precipitation of components because of interactions. Therefore, the first five components were weight separately and added to half of the end volume of reverse osmosis water (RO-water) while stirring. The last two components were weighted in separately and added to a third of the end volume while stirring. The two separate solutions were mixed thoroughly and filled up to the final volume.

7.2.2 BGI

Table 2: Composition of BGI medium

Component	Concentration [g/L]	Element	Concentration [mM]
NaNO ₃	1.2	N	14.19
Fe(NO ₃)•9H ₂ O	0.010	P	0.23
MgSO ₄ •7H ₂ O	0.075	K	0.46
CaCl ₂ •2H ₂ O	0.036	Ca	0.32
Trace element solution, v5	1.0 mL	Mg	0.30
Na ₂ CO ₃	0.020	Na	14.60
K ₂ HPO ₄	0.040	C	0.24

FFinal N:P ratio corresponds to 61.8.

The medium was prepared in the same manner as the 22O medium.

7.2.3 Trace elements stock solution, v5

Table 3: Composition of the Trace elements solution, v5

Component	Actual amount [g/L]	Desired amount [g/L]
H ₃ BO ₃	0.512	0.509
CuSO ₄ •5H ₂ O	0.149	0.150
KI	0.182	0.181
FeCl ₃ •6H ₂ O	0.291	0.293
MnSO ₄ •H ₂ O	0.294	0.296
Na ₂ MoO ₄ •2H ₂ O	0.084	0.082
NiSO ₄ •6H ₂ O	0.275	0.275
Co(NO ₃) ₂ •6H ₂ O	0.101	0.100
ZnSO ₄ •7H ₂ O	0.492	0.490
KAl(SO ₄) ₂ •12H ₂ O	0.395	0.395
KCr(SO ₄) ₂ •12H ₂ O	0.472	0.470

7.3 Experimental Setup

7.3.1 Cultivation at 25°C and room temperature (RT)

To investigate the influence of temperature on the PHB production of cyanobacteria, the strains S.192 and S.6803 were cultivated at 25°C and at a room temperature of 20°C (RT). For illumination a halogen-metal vapor lamp (Phillips, MASTER, HPI-T Plus, 250W/645) with a light intensity of

1464.3±258.7lux was placed above a regular shaker, on the left side, and a temperature-controlled shaker (Heideolph Titramax 1000), on the right side (Figure 16). The temperature [°C] and light intensity [lux] were continuously measured inside the Titramax 10000 with a data logger (ONSET, HOBO Pendant® MX2202).



Figure 16: Setup temperature experiment. Left: regular shaker at RT (left side) and Titramax 1000 at 25°C (right side); Right: setup with halogen-metal vapor lamp.

20x100mL Erlenmeyer flasks with 40mL sterile 22O medium were inoculated with 4mL of preculture and 10 flasks were placed on each shaker, at RT and at 25°C. For the inoculation 10 flasks were inoculated with S.192 and 10 flasks with S.6803 under sterile conditions in a lamina flow. 5 of each strain were placed on each shaker at the two different temperatures respectively. The initial optical density (OD) was set between 0.3 and 0.4.

The cultures were cultivated for a total of 40 days with an illumination cycle of 16 hours light and 8 hours dark phase and continuous shaking. During cultivation an aliquot of each culture was taken for analysis.

At day 5, 14, 21, 28, 35 and 38 the evaporated water was first replaced with sterile ddH₂O. After, a mixed sample was taken by combining 200µL of all 5 flasks with the same strain at the same condition. The OD and the pH of the mixed sample was measured, and photos of the flasks were taken. At day 7, 12, 18, 25, 33 and 40 the evaporated water was replaced and 50mL (10mL each) of mixed sample was taken, in the same manner as before, for the analysis of the OD, pH and additionally the chlorophyll, phycocyanin, PHB and Glycogen content.

7.3.2 Cultivation with different light cycles and light intensities

To investigate the influence of continuous illumination and the effects of different light intensities three experiments were conducted. The first experiment at about 3000lux, the second at about 6000lux and the last experiment at about 10000lux. The measured light intensity (lux) depended on the measuring device and measuring place, see table 4 and 5.

In two wooden boxes, to screen the cultures from ambient light, the cultures were placed on a shaker and illuminated from above by 6500K LEDs (Paulmann, SimpLED, 78976: 6500K, 12V, 450LED, 7.5m). The LEDs were placed equally distributed over the whole lid surface to ensure even light distribution (Figure 17). The number of LEDs was adapted to the required light intensity of about 3000, 6000 and 10000lux, respectively. The boxes were lined with aluminium foil to minimize losses in light intensity. To ensure constant temperature inside the boxes, commercial computer ventilators (60x60x25 mm, 24 V dc, 1.2 W, 22.1 m³/h) were added (Zerobin, 2021, p. 22).

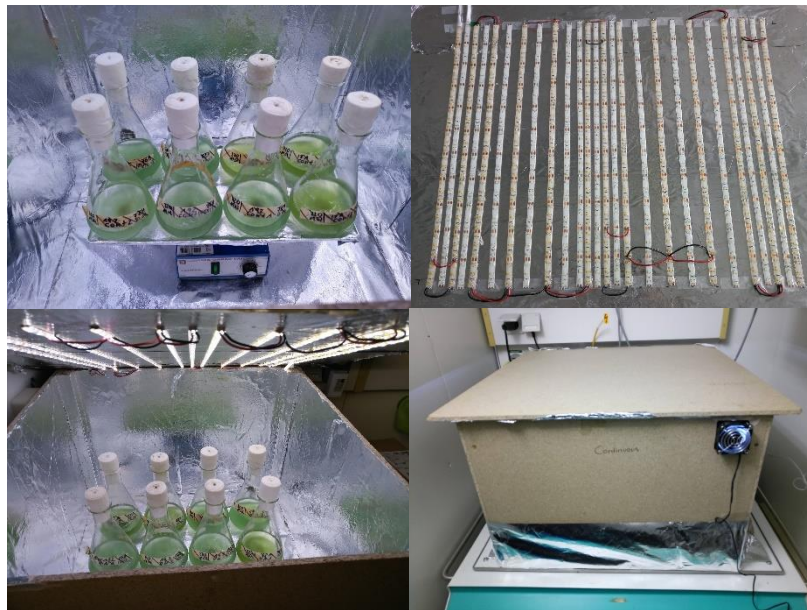


Figure 17: Setup of the continuous illumination experiments. Upper Left: Cultures in 500mL flasks placed on the shaker. Upper Right: LEDs placed on the lids inside. Lower Left: Box with opened lid and LEDs. Lower Right: Closed box with ventilation.

This setup was the same for all illumination experiments. One box was continuously illuminated with 24 hours light, while the other box had an illumination cycle of 16 hours light and 8 hours dark phase. The cultures in both set-ups were continuously stirred.

16x500mL Erlenmeyer flasks with 200mL sterile 220 medium were inoculated with 12-14mL of preculture under lamina flow to achieve a starting OD between 0.2 and 0.7. The strains used for inoculation varied between the three experiments. 8 flasks were placed on each shaker and cultivated for 40 days. During cultivation aliquots were taken for analysis. The days of sampling varied slightly between the three experiments due to weekends and holidays. The standard sampling scheme was the following.

At day 5, 14, 21, 28, 35 and 38 the evaporated water was first replaced with sterile ddH₂O and then 1mL aliquot was taken from each flask. The OD and the pH of the sample was measured, and photos of the flasks were taken.

At day 7, 12, 18, 25, 33 and 40 the evaporated water was replaced and 50mL of aliquot was taken from each flask for the analysis of the OD, pH and additionally the chlorophyll, phycocyanin, PHB and Glycogen content. Additionally, the cultures were examined with a light microscope and microscopic images were taken. On the last day (40) samples were taken for the examination with the confocal scanning microscope the next day (41) and were stored in the fridge overnight.

The light was measured with a luxmeter (Voltcraft, LX-10), a light spectrometer (LI-COR, LI-180) and a lightmeter (WALZ, ULM-500). Additionally, the temperature [°C] and the light intensity [lux] were continuously measured over the whole time of the experiment with a data logger (HOBO, Pendant, MX Temp/Light). For the measurements the devices were placed on the shaker, where the cultures were later placed, while the data logger had to be placed on the ground beside the shaker during the experiment. Thus, the light intensity measurements of the data logger were lower and were only for monitoring the stability of the set up.

Table 4: Light source measurements continuous illumination setup.

Continuous	Voltcraft, LX-10 [lux]	LI-COR, LI-180 [lux]	WALZ, ULM-500 [μ]	Data logger HOBO [lux]	Temperature [°C]
1. (3000lux)	2900	1972	86.4	2277±120	23.3±0.6
2.				2217±262	23.6±2.0
3. (6000lux)	6168	3692	228.2	3237±757	23.8±0.4
4. (10000lux)	10180	5304	349.2	5203±240	24.9±0.22

Table 5: Light source measurements day-night-cycle illumination setup.

day-night-cycle	Voltcraft, LX-10 [lux]	LI-COR, LI-180 [lux]	WALZ, ULM-500 [μ]	Data logger HOBO [lux]	Temperature [°C]
1. (3000lux)	3100	2301	99.5	2158±169	24.1±0.3
2.				2109±122	23.0±0.5
3. (6000lux)	5648	4453	206.2	3154±637	23.1±0.8
4. (10000lux)	10800	5390	382.3	5303±403	23.7±1.0

The emission profile of the LEDs was additionally recorded with the light spectrometer (LI-COR, LI-180) displayed in the following Figure 18.

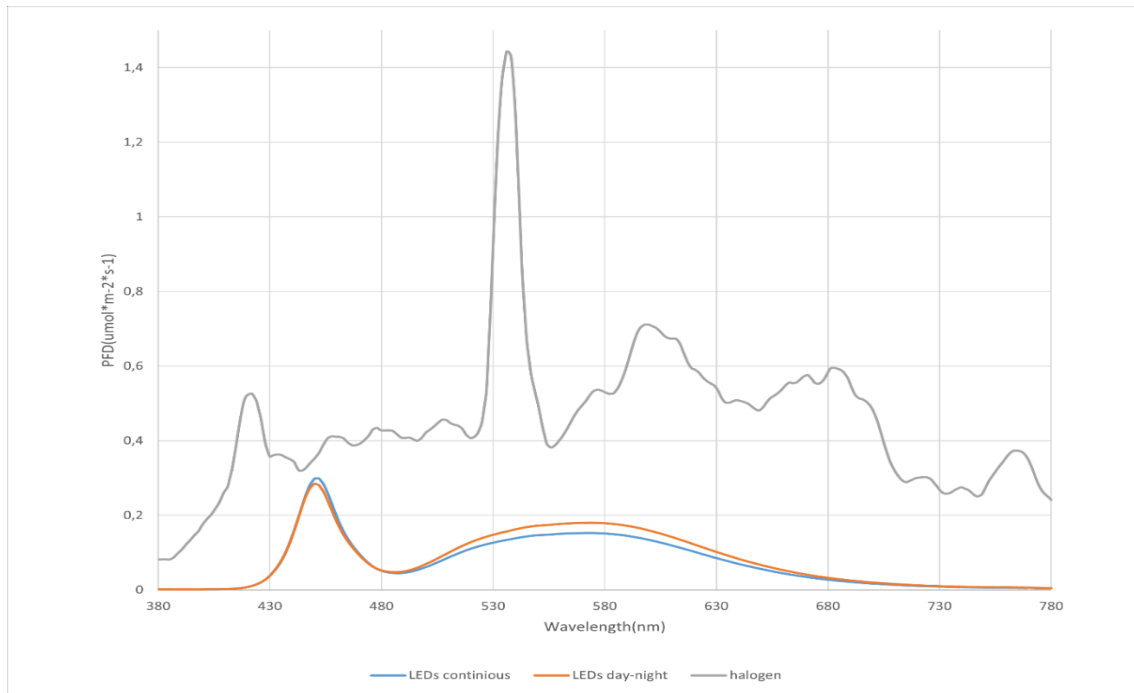


Figure 18: Emitted spectra of the used LEDs in the 3000lux setting and of the halogen bulb used for the temperature and PHB cultivation experiment (grey).

The maximum of the LEDs was at ~450nm overlapping with the chlorophyll a absorption peak with a maximum at 428nm (Barragán Campos et al., 2018).

7.3.3 Production of PHB

To investigate differences in the length and size distribution of the PHB polymers, some cultures were cultivated solely for harvest and no aliquots for analysis were taken.

To compare the polymer quality of the three strains, S.6803, S.192 and IFA3, they were cultivated in 2000mL Erlenmeyer flasks, at a day-night cycle (16/8h) illuminated with a halogen-metal vapor lamp (Phillips, MASTER, HPI-T Plus, 250W/645), see Figure 19.



Figure 19: Setup for PHB production under day-night-cycle conditions.

To compare the influence of different lux and cycle condition, 2*200mL flasks with the strain S.192 were cultivated only for PHB production in the previous described 3 illumination experiments at 3000lux, 6000lux and 10000lux at day-night-cycle and continuous illumination.

7.4 Analytical Methods

7.4.1 Cell Dry Weight (CDW)

For determination of the cell dry mass of the bacteria culture 10 mL aliquot of the culture was taken and centrifuged at 3500rpm for 30 min (Eppendorf, 5810) in a glass cuvette. The supernatant was discarded after centrifugation, and the pellet was washed with 5mL ddH₂O. The obtained pellet was dried over night at 105°C, left to cool in a desiccator and weighted out. The cell dry mass was calculated by the following equation 1.

$$\text{Cell Dry Mass} \left[\frac{g}{L} \right] = \frac{(\text{total weight} - \text{net weight})g}{10mL} * 1000$$

Equation 1: Cell Dry Mass

7.4.2 pH

The pH of an aliquot of the bacteria culture was measured with a pH meter (Mettler Toledo, FiveEasy Plus) by inserting the probe into the sample, measuring until a stable pH was reached. The pH meter was calibrated weekly.

7.4.3 Optical Density (OD)

To monitor the growth of the bacteria cultures the OD was measured at 435nm and 750nm with a UV-Spectrophotometer (Shimadzu, UV-1800). The samples were diluted to reach a result in the range of 0.3-0.8 OD. As reference reverse osmosis water (RO-H₂O) was used. At 428nm the maximal absorbance of chlorophyll-a occurs, while at 750nm most organic substances absorb, thus the combination of both can give a rough estimate of the growth of the culture. The ratio OD₄₃₅/OD₇₅₀ is an estimate of the proportion of the accompanying heterotrophic bacterial flora to the cyanobacteria.

7.4.4 Chlorophyll-a content

For the determination of the chlorophyll content 1.2mL aliquot of bacteria culture was taken and centrifuged at 8000rpm for 5min (Eppendorf, 5430). The supernatant was discarded and 1.2mL absolute ethanol was added. The chlorophyll a was extracted by ethanol over two days at 4°C.

For analysis the solution was centrifuged at 12400rpm for 10min and the concentration of chlorophyll-a in the supernatant was measured with the UV-Spectrophotometer (Shimadzu, UV-1800) at 470nm, 665nm and 720nm. Pure ethanol was used as blank, and the concentration was calculated by the following formula from Ritchie (2008):

$$\text{Chlorophyll } a \left[\frac{mg}{L} \right] = 13,2969 * A(665nm)$$

Equation 2: Formula for chlorophyll a concentration (Ritchie, 2008).

7.4.5 Phycocyanin content

The phycocyanin extraction and analysis method was adapted from (Bennett & Bogorad, 1973). 2.5mL aliquot of bacteria culture was transferred to a 15mL falcon tube and 50µL of a 50mg/mL lysozyme solution (from hen egg, Fluka, 81551 U/mg) was added. The mixture was incubated for 5h at room temperature and put subsequently at -20°C. Two freeze and thaw cycles were performed. Afterwards, the mixture was put at 4°C for 3days. The mixture was centrifuged at 3000rpm for 10min, and the pigment concentration measured right after with the UV-Spectrophotometer (Shimadzu, UV-1800) in glass cuvettes at 652nm, 615nm, 280nm, 620nm and 562nm. RO-H₂O was used as blank and the concentration was calculated by following formula after Bennet & Bogorad (1973):

$$\text{Phycocyanin} \left[\frac{mg}{L} \right] = \frac{A_{615} - 0.474 * A_{652}}{5.34 * 1000}$$

Equation 2: Phycocyanin concentration formula (Bennett & Bogorad, 1973).

7.4.6 Nitrate

For determination of the nitrate content in the bacteria culture broth a kit was used from HACH (LCK339, HACH®) with automated barcode detection and analysis in a Photometer (HACH, Dr2800).

After centrifugation of bacteria culture at 3500rpm for 30min (Eppendorf, 5810) 1mL of the supernatant was taken and pipetted into the kits test-tube. 0.2mL of reactant A was added and the tube was mixed by inverting it 3 times. After 15min incubation at room temperature the test tube was inserted into the Photometer for detection. The HACH Photometer calculated the nitrate concentration with the stored calibration.

7.4.7 Glycogen

The glycogen content was determined by an adapted method from (Koch et al., 2019). Therefore, 2mL aliquot of bacteria culture was harvested (at higher cell densities 1mL) and centrifuged at 8000rpm for 5min. The pellet was washed twice with 1mL of double-distilled water (ddH₂O) and resuspended in 400µL 30%w/v KOH solution. The mixture was incubated for 2h at 95°C and 4500rpm on a thermomixer (Eppendorf, Thermomixer comfort). For the glycogen precipitation 1200µL ice cold absolute ethanol was added and the solution was incubated at -20°C for 2-24h. The solution was centrifuged at 4°C at 10000g for 10min (Eppendorf, 5417R) and the pellet was washed

once with 700µL of 4°C pre-cooled 70% ethanol and once with absolute ethanol. The pellet was dried at 60°C until the entire ethanol was evaporated.

The pellet was resuspended in 1mL of 100mM sodium acetate, pH4.5, and 10µL amyloglucosidase solution (from *Aspergillus niger*, SIGMA-ALDRICH, 57 U/mg) was added. For the enzymatic degradation of the glycogen the solution was incubated at 55°C and 500rpm for 2h on a thermomixer.

The enzymatic reaction was stopped by carrez precipitation, and the solution was centrifuged at 12500rpm for 20min. The supernatant was transferred to HPLC vials with a syringe via a 0.45µm polyamide filter (Machery-Nagel, CHROMAFIL Xtra PA-45/25).

The glucose content was measured with an Ion Exclusion High Performance Liquid Chromatography and a Refractive Index Detector (HPLC-RID), the instrument from Agilent 1260 Infinity II series was used with an ion-exclusion column (Concrise Coregel ION 300 SS 7.8mmIDx300mm, part no. CON-ICE-99-9850) and a mobile phase of 0.01 N H₂SO₄. The actual concentration was calculated from the mean recovery rate, determined from standards (≥ 85% glycogen from oyster, Fluka). In the formula below, the dilution and the stoichiometric multiplication factor of 0.9 were considered.

$$Glycogen \left[\frac{mg}{L} \right] = \frac{glucose \left[\frac{mg}{L} \right] * 0.9}{dilution\ factor * recovery\ rate}$$

Equation 3: Glycogen concentration formula

7.4.8 Polyhydroxybutyrate (PHB)

For determination of the PHB content the cell dry mass was used. Therefore, the dried pellet of 10mL and 5mL bacteria culture were used. For the pellet of 10mL bacteria culture the twofold volumes of the following reagents were used.

100µL concentrated H₂SO₄ (97%) was pipetted directly onto the pellet in a glass test tube preventing any acid lost by unused droplets on the walls. The test tubes were closed with cork stoppers and put in an ultrasonic bath for 5 min. Afterwards the test tubes were incubated for 30min at 90°C in a water bath. After cooling to room temperature, 4.9mL Milli-Q® water (MQ-H₂O) was added to the dissolved pellet and homogenized thoroughly with a syringe. A HPLC vial was filled with the solution over a 0.45µm polyamide filter (Machery-Nagel, CHROMAFIL Xtra PA-45/25) for analysis.

The procedure was done in duplicates, once with 10mL and once with 5mL of bacteria culture. At high cell densities (A₄₃₅ > 5) only 3mL instead of 5mL was used, because the H₂SO₄ amount was not sufficient to completely convert the PHB to crotonic acid.

The HPLC analysis of the solution was carried out with an Agilent 1100 system, equipped with an ion-exclusion column (CARBOsep Coregel 87H, part no. CHO-99-9861, 0.01 N H₂SO₄) measuring the crotonic acid content, the degradation product of the PHB. The PHB content was calculated with the following formulas from the crotonic acid content, and the recovery rate determined from PHB standards.

$$PHB \left[\frac{mg}{L} \right] = crotonic\ acid \left[\frac{mg}{L} \right] * recovery\ rate$$

Equation 4: PHB concentration equation.

7.4.9 PHB extraction using an Automated Solvent Extraction System (EDGE)

The bacteria cultures cultivated in 250mL Erlenmeyer flasks at continuous and day/night cycle conditions for PHB production were harvested by transferring part of the bacteria culture to glass test tubes and centrifugating the bacteria culture at 3500rpm for 30min (Eppendorf, 5810). The supernatant was discarded, and additional bacteria culture was transferred into the test tube containing the pellet and again centrifuged. This step was repeated until the whole bacteria culture was combined in one test tube as one pellet. The pellet was dried at 105°C and the CDW was weighted. For pigment removal, absolute ethanol was added to the dried pellet and mixed. The solution was left for 2-24h at room temperature. The solution was centrifuged at 3500rpm for 30min, and the supernatant was discarded. Acetone was added to the pellet, mixed and incubated for 2-24h at room temperature. Then the solution was centrifuged at 3500rpm for 30min, the supernatant was discarded, and the pellet was dried at room temperature.

The dried pellet was transferred into EDGE® aluminium cartridges with a filter (Q-Dic™, CEM) on the bottom. The cartridges were set into the EDGE® (CEM) and the program PHB CHCl₃ was started (2 cycles, 5mL chloroform, T=100°C, P=35). The PHB was dissolved in chloroform under elevated temperature and pressure resulting in 15mL of PHB extract.

The chloroform volume was restricted by evaporation under a fume hood over night to approximately 5mL. 50mL of ice-cold absolute ethanol was put into a beaker and the extract was slowly poured into the ethanol under continuous stirring. The mixture was put at -20°C for more than 10min and transferred into glass test tubes afterwards for centrifugation at 3500rpm for 30min. The supernatant was discarded carefully. The resulting PHB pellet was dried under the fume hood at room temperature and weighted once completely dry. The isolated PHB was further analysed with GPC and H-NMR.

7.4.10 Gel Permeation Chromatography (GPC)

For the analysis of the PHB molecule length distribution a GPC was used. The PHB was dissolved in chloroform to a concentration of about 5mg/mL. Additionally, a PHB standard (poly-β-hydroxybutyric acid from *Algaligenes* sp., SIGMA-ALDRICH, approx. mol wt 535,000) was analysed as reference. About 10mg of standard was dissolved in 2mL chloroform. In case the PHB did not dissolve entirely in the chloroform, 5 drops of Trifluoroacetic acid (SIGMA-ALDRICH) were added,. The dissolved polymere was filterd through cotton wool packed pasteur pipettes into HPLC vials.

The samples were analysed with an GPC setup on an HPLC system composed of an Agilent Technologies HPLC system (1260 Infinity) connected to a 17 369 6.0 mm ID x 40 mm L HHR-H, 5µm

guard column and a 18 055 7.8mm ID x 300 mm L GMHHR-N, 5µm TSK gel liquid chromatography column (Tosho Bioscience, Tessenderlo, Belgium) at 30°C. The eluent was Chloroform at an isocratic flow rate of 1mL/min. The detection device was a refractive index detector (Agilent Technologies G1362A).

Three polystyrene standards (ReadyCal-Kit Poly(styrene), Mp 370-2520000Da, Lot No: pskitr1sa-11, PSS Polymer Standards Service GmbH) with 1mg/mL were used for a standard calibration curve, used to calculate the polyester length of the samples.

With the GPC-Agilent Software the standard calibration was performed and used for the integration of the measured peaks with a 3rd order polynomial function. With the software the number average molecular weight (Mn) and the weight average molecular weight (Mw) was calculated. From these values the dispersive Index (PD) was calculated with the formula:

$$PDI = \frac{Mw}{Mn}$$

Equation 5: Formula for the calculation of the Polydispersity Index (PDI) (Rane & Choi, 2005).

Since the results with this method did not yield the expected molecular weight given by the producer of the PHB standards, the PHB samples were send to the project partners Stanislav Obruča and Adriana Kovalčík at the faculty of chemistry at the Brno University of Technology for further analysis with the methods described in 7.4.10.1 and 7.4.10.2 conducted by Michal Kalina.

7.4.10.1 Samples measured by SEC-MALS:

Molecular weight (Mn and Mw) and polydispersity (PDI) of analysed PHBs were measured at 25 °C by the size exclusion chromatography (SEC, Infinity 1260 system with size separation by PL gel MIXED-C column, Agilent Technologies, USA) coupled with a multiangle light scattering (MALS, Dawn Heleos II, Wyatt Technology, USA) and differential refractometer (dRI, Optilab T-rEX, Wyatt Technology, USA). The individual PHB samples were dissolved in chloroform (concentration 1.5 mg/mL) and filtered (0.45µm syringe filter with nylon membrane) before the analysis. For the analysis chloroform was used as eluent at a flow rate of 0.6 mL/min, the injection volume was 100µL. The obtained molecular weights were calculated using the value of refractive index increment of PHB (dn/dc) 0.0336 mL/g (Kovalcik et al., 2018). Data acquisition and evaluation were performed using Astra 7.3.2 software (Wyatt Technology, USA).

7.4.10.2 Samples measured with AF4-MALS

Molecular weight (Mn and Mw) and polydispersity (PDI) of analysed PHBs were measured at 25 °C by the asymmetric flow field-flow fractionation (AF4 Eclipse system, Agilent Technologies, USA) coupled with a multiangle light scattering (MALS, Dawn Heleos II, Wyatt Technology, USA) and differential refractometer (dRI, Optilab T-rEX, Wyatt Technology, USA). The individual PHB samples

were dissolved in chloroform (concentration 1.5 mg/mL) and filtered (0.45µm syringe filter with nylon membrane) before the analysis. The size fractionation of individual samples was performed by the AF4 Eclipse short channel with an installed 350 mm spacer by using the regenerated cellulose membrane (lowest molecular weight cut-off 10kDa). For the analysis chloroform was used as eluent at a detector flow rate 1.0 mL/min and the used cross flow was 3 mL/min. The used injection volume was between 100 and 200µL. The obtained molecular weights were calculated using the value of refractive index increment of PHB (dn/dc) 0.0336 mL/g (Kovalcik et al., 2018). Data acquisition and evaluation were performed using Astra 7.3.2 software (Wyatt Technology, USA).

7.4.11 ¹H - Nuclear magnetic resonance spectroscopy (H-NMR)

For the confirmation of PHB in the extract, it was analysed with a H-NMR system. The dried specimen was dissolved in deuterated chloroform and analysed by the BOKU core facility using a Bruker Avance III HD 400 spectrometer (resonance frequency of ¹H of 400.13 MHz, and ¹³C of 100.61 MHz, respectively), equipped with a 4 mm dual broadband CP-MAS probe.

7.4.12 Microscopy

7.4.12.1 Light Microscope

The bacteria cultures were visually monitored with a light microscope (Olympus, BX43F) with 40x magnification and using a phase contrast (40x/0.65Ph2, PlanC N, Olympus). Images were taken from every culture at every condition every week with a camera (Canon, EOS 1300D) connected to the microscope (Olympus, U-TV1X-2). The cell number was counted at the last day of each experiment with a counting chamber (Neubauer, MARIENFELD, depth 0.01mm, 0.0025mm²).

7.4.12.2 Confocal Scanning Microscope

For visualization of the PHB granules inside the cells, the PHB was colourized with Nile-red solution. Therefore, 11µL of Nile-red solution (50µg/mL in 98%ethanol) was added to 89µL cell suspension. 20µL of the mixture was pipetted onto a microscope slide and distributed with the tip over the whole surface. The glass slides were air dried in a laminar flow cabinet and afterwards the cells were heat fixated by moving the slide two times through a flame very rapidly.

The samples were analysed with a confocal scanning microscope (Leica Microsystems, TCS II SP5, Mannheim, Germany) at The BOKU Core Facility Multiscale Imaging. The used objective was a HCX PL APO CS 63x1.20 water immersion objective. A drop of water was added to the heat fixed sample on the glass slide and covered with a glass cover slip. Before lowering the objective onto the sample, a drop of water was put on the glass cover slip for the water immersion.

The sample was irradiated with an argon laser at 488nm and detected with the photomultiplier tube PMT3 with the Leica/EGFP setting at an emission bandwidth of 548nm - 596nm. Multiple images were taken of each strain at each condition for later analysis.

The computer software LAS X (Leica Application Suite X, Leica Microsystems) was used for image processing and determination of the cell size. For the average cell size one image was selected of each strain and condition. The image was split into quarters and about the same number of cells was measured from each part to ensure an equal distribution (Figure 20). 50 cells in total were measured per image with the software and the average value was calculated.

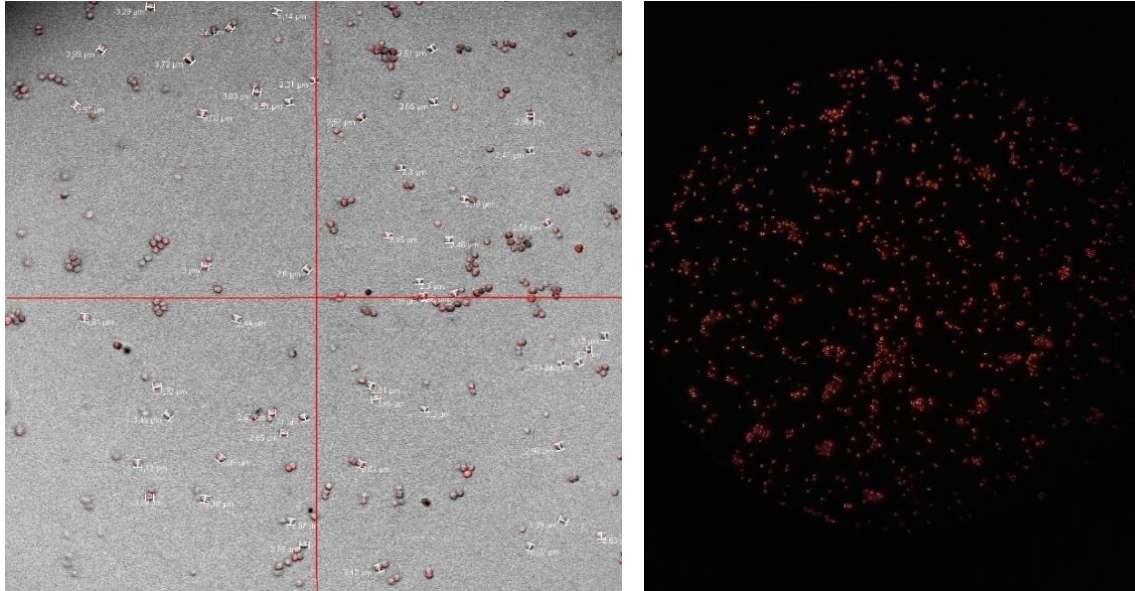


Figure 20: Left: Cell size measurement of S.IFA at continuous illumination with LAS X; Right: Emission of the Nile-red stained PHB granules.

7.4.12.3 Transmission electron microscopy (TEM)

The cells cultivated at CONT and DNC illumination regimes were analysed by the project partner from the Bruno university of technology, with transmission electron microscopy (TEM) and Scanning electron microscopy (SAM) (results not shown) to see the effects of the treatment on the cellular structures of the cell.

8 Results

8.1 Influence of elevated temperature on cultivation of two different *Synechocystis* strains

In a first experiment the *Synechocystis* strains S.192 and S.6803 were cultivated at two different temperatures to investigate the influence of elevated temperatures on the cultures, since a higher temperature was expected under continuous illumination. Therefore, quintuplicates of both cultures were cultivated at a set room temperature of 20°C and at a set temperature of 25°C with a day-night-cycle (16/8) and the same illumination conditions of about 1500lux (Table 6).

Table 6: Cultivation conditions in experiment 1.

Condition	Temperature [°C]	Light intensity [lux]
Room Temperature (RT)	20,0 (Set temperature)	1464±260
Elevated Temperature (25°C)	24,124±0,288	1464±260

Over the whole course of the experiment the temperature and the light intensity of the 25°C cultures were measured with a data logger (Figure 21). The temperature fluctuated because of the day-night-cycle (DNC) between approx. 25.5 °C during illumination and 23.5°C during darkness. The mean temperature of the experiment was 24,1±0,3°C.

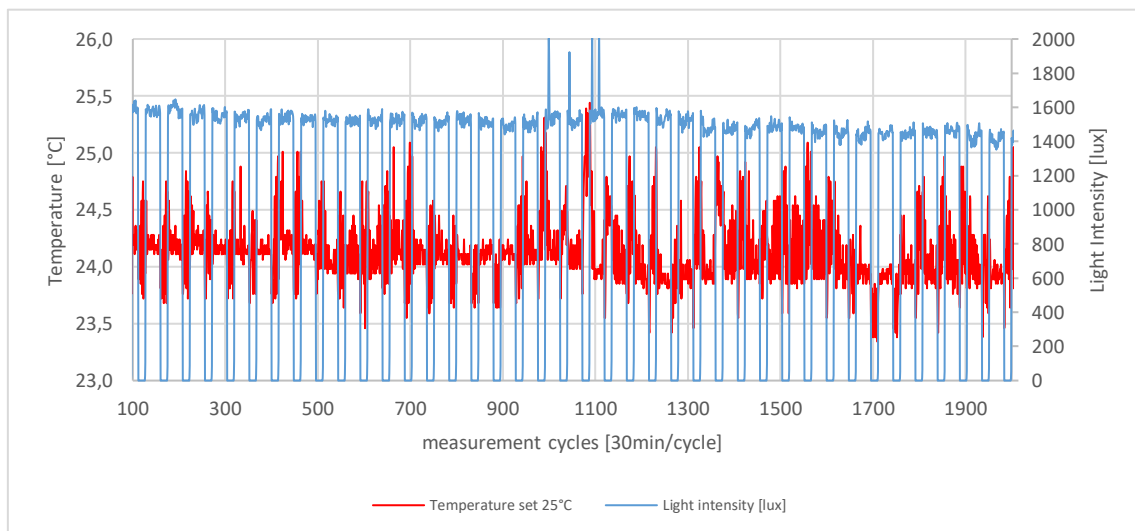


Figure 21: Temperature of the 25°C culture and illumination profile of experiment 1 over 40 days.

The cultures appearance was monitored, and photos were taken to visualize the proceeding chlorosis due to nitrogen starvation (Figure 22). There was no observable difference between the two different temperature conditions in the strain S.6803. At 25°C and at RT the culture displayed discoloration as a sign of chlorophyll degradation which started on day 25, while in the strain S.192 the

discolouration at 25°C started on day 33. There was no significant difference in the appearance between the cultures at 25°C and RT.

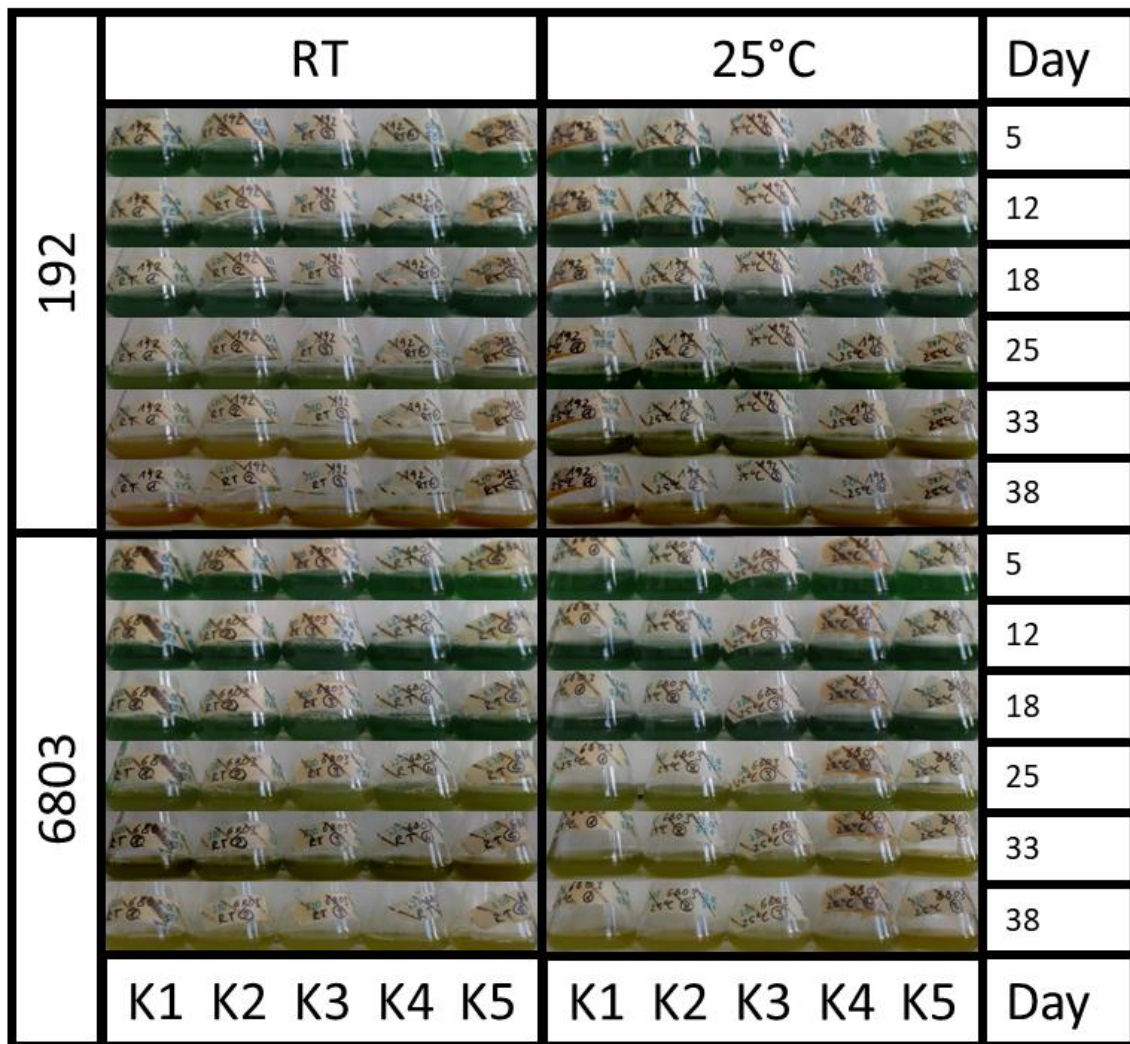


Figure 22: Visual appearance of S.192 and S.6803 at RT and 25°C.

Additionally, the physiological state of the cultures was analytically monitored. The obtained data is visualized in Figure 23 as an overview over all measured parameters, starting with the optical density (OD) measured at 435nm, pH, cell dry weight (CDW), chlorophyll and phycocyanin content as well as the PHB and Glycogen content of the cells. On the left side the results of the strain S.192 and on the right side the results of the S.6803 strain are shown.

The OD at 435nm represents the chlorophyll absorption spectrum as a proxy for the culture density. After an initial drop in the beginning, the OD_{435nm} increased linearly until day 25, which corresponds with the start of the chlorosis. The RT cultures had an overall lower OD, but the difference was minor. On the other hand, the S.192 strain reached an OD of 15, while the S.6803 only reached a maximal OD of 10 at day 25 and afterwards the values dropped again.

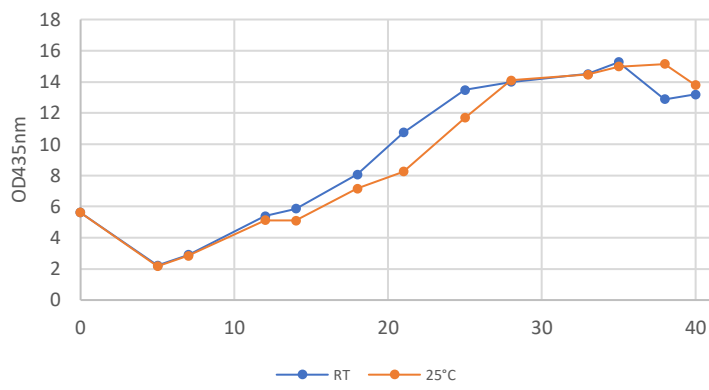
The same trend was seen in the CDW, with a maximum of 2 g/L was reached by S.192 and only a maximum of 1.5 g/L by S.6803 on day 25. Afterwards the S.6803 CDW declined again. But other than the OD, the CDW of the RT cultures was slightly higher than at 25°C, but again the differences were small.

The pH of all cultures started slightly above 10, because of high carbon sequestration the carbonic acid was assimilated from the medium leading to a basic pH. In all cultures the pH started to drop constantly on day 18 until day 40 down to a slightly basic pH of 8. This could be explained with the cultures nutrient shortage which resulted in a reduction of their metabolic activity and carbon sequestration. There was no consistent difference visible between the two strains or the two conditions. At the same time the PHB content in all cultures increased starting with day 18. At the same time the glycogen levels were dropping significantly in all cultures until day 25 after which they increased again until day 40. The strain S.6803 accumulated approx. 45% of its CDW in glycogen with slightly lower levels (4% less) in the 25°C culture. In the S.192 the difference between 25°C and RT was about 10% with the cells at 25°C reaching almost 41% and the cells at RT only 30.5% glycogen.

The phycocyanin in the S.192 strain behaved similar in the RT and 25°C cultures. First the phycocyanin content dropped from ~7%CDW in the RT culture and ~4% in the 25°C culture on day 7 down to below 1% on day 12 at both conditions. Thereafter the phycocyanin content increased again reaching ~4.5% on day 25 in the 25°C culture and ~3.5% in the RT culture. In the S.6803 the phycocyanin behaved similar, but the starting levels at both conditions were below 1% on day 7 and decreased from there (with only a small increase on day 12) to almost 0 on day 25. After day 25 there was a sudden increase on day 33 with ~3.3% (25°C) and ~1.5% (RT) followed by a sudden decrease to again about 0 on day 40. The chlorophyll content was more or less the same at both conditions and in both strains. It started at about 1.25%CDW chlorophyll and decreased to almost 0 on day 25 and thereafter slightly increased again until day 40 never reaching 1%CDW chlorophyll. Due to the fluctuations of the pigment content no trends or differences between strains and conditions could be noticed, the data was therefore inconclusive. Only a minimum in the chlorophyll measurement on day 25 was observed, corresponding with the starting chlorosis and the drop in glycogen content.

Since pooled samples were taken from all five cultures of each strain at both conditions for the analytics no standard deviation could be calculated. This approach was chosen, because the temperature-controlled shaker for the 25°C cultivation only allowed 5 small flasks of each strain, but for the analysis sufficient amount of sample could only be obtained by pooling. This error is neglectable when looking at the finding that an elevated temperature of about 4°C only had a minor influence on the growth and PHB accumulation of the two *Synechocystis* species S.192 and S.6803. Therefore, this error did not affect further investigations since this preliminary experiment could rule out any significant influence of an elevated temperature up to 4°C on the growth or PHB content.

S.192



S.6803

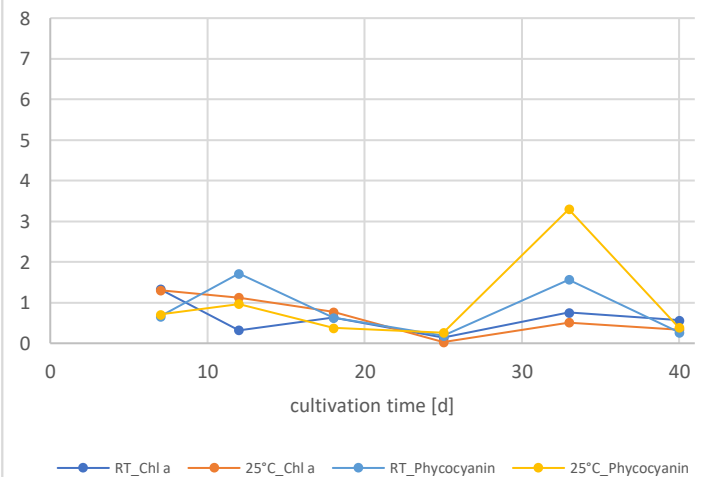
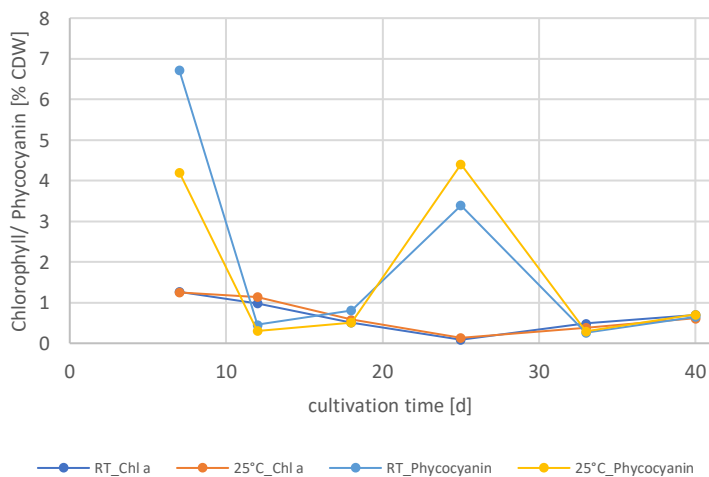
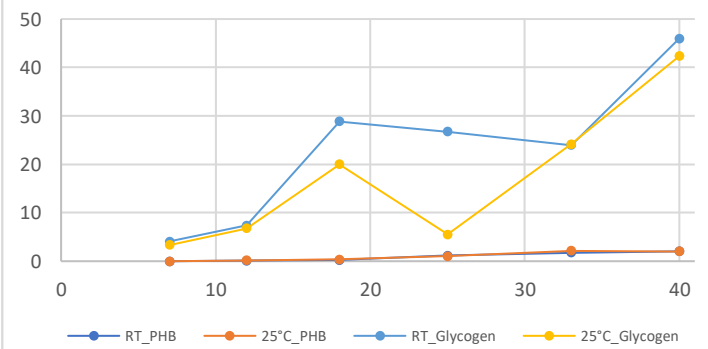
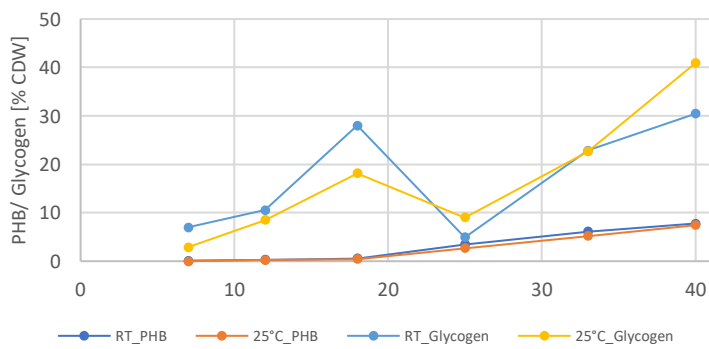
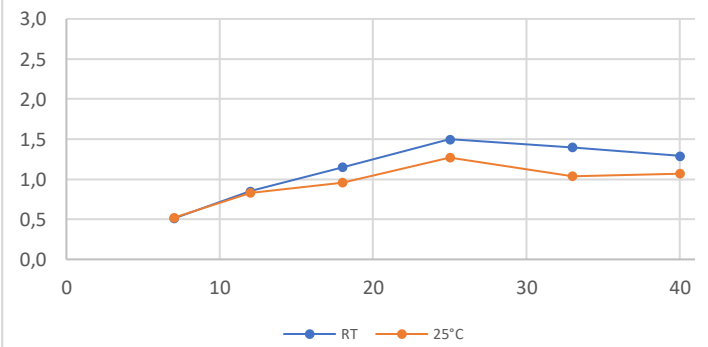
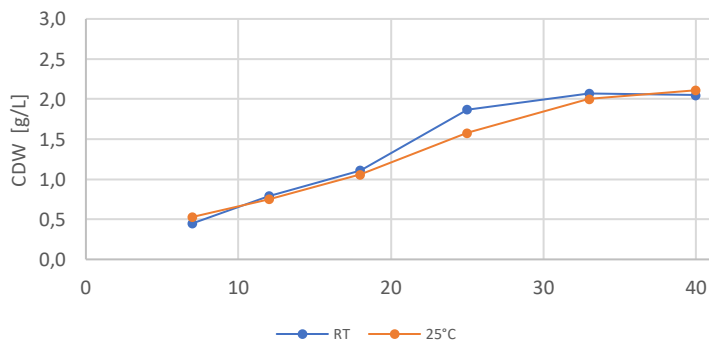
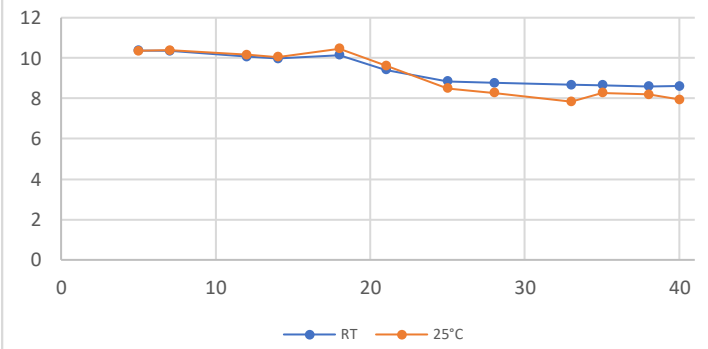
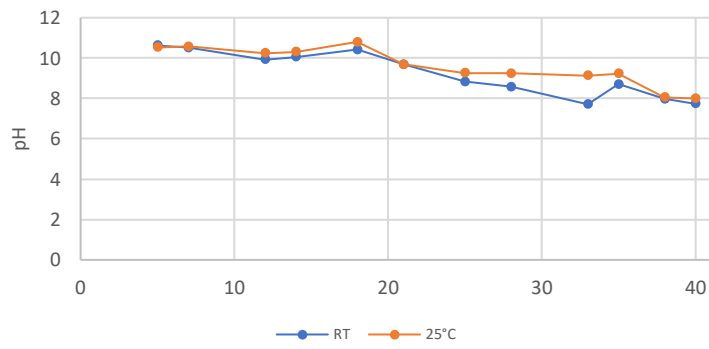
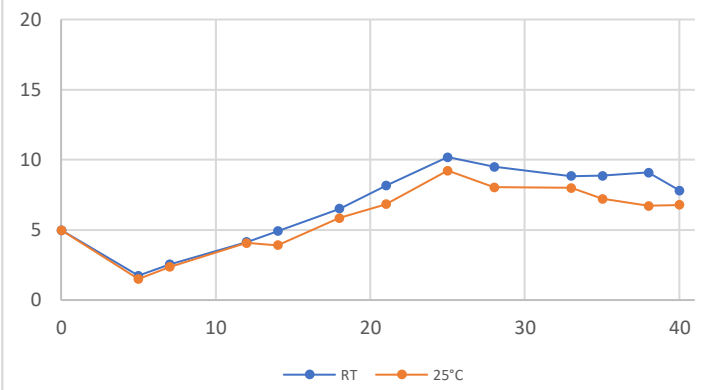


Figure 23: Analytical data representing the physiological state of the cultures cultivated at 25°C and RT. On the left S.192, on the right S.6803. In blue cultures at RT and in orange/yellow cultures at 25°C.

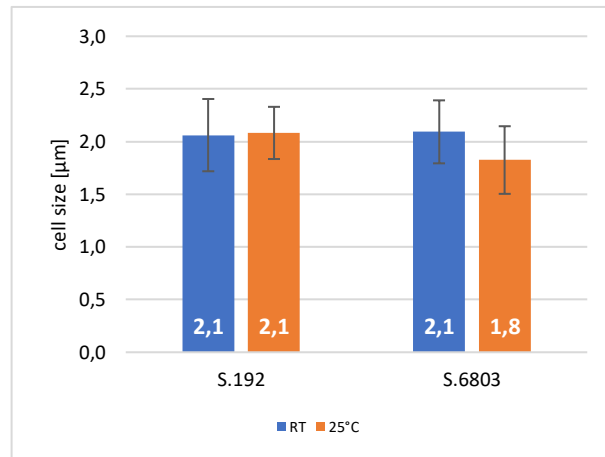


Figure 24: Measured cell size of S.192 and S.6803 cultivated at 25°C and RT.

The cells were examined on day 40 using a confocal scanning microscope and images were taken. The cell size was measured with the software LAS X (Figure 24). The PHB granules inside the cells were clearly visible with the confocal scanning microscope after Nile-red staining. The cell size of both strains at both conditions was about 2μm on average with only S.6803 at 25°C deviating with an average of 1.8μm.

8.2 Continuous illumination at 3000lux with S.192 and S.6803 (Exp.1)

In the illumination experiment 1, triplicates of the S.192 and S.6803 strains were cultivated und day-night-cycle (DNC) and continuous illumination (CONT). The temperature and light intensity were monitored with a data logger and the mean values were calculated (Table 7). The monitored light intensity was consistent over the whole duration of the experiment, but the mean value was lower than the real value, since the data logger was placed beside and not on the shaker resulting in a further distance to the light source and therefore lower values for the light intensity then on the shaker, see table 4 and 5. The temperature of the continuous illuminated set-up was slightly higher compared to the DNC.

Table 7: Cultivation conditions in experiment 1 monitored with a HOBO data logger

Condition	Temperature [°C]	HOBO data logger Light intensity [lux]	Voltcraft Light intensity [lux]
DNC	23,29±0,62	2290±145	3100
CONT	23,57±0,53	2184±170	2900

Photos of the cultures were taken every time before sampling, see Figure 25. There were several optical differences visible between the two strains and between the two illumination regimes.

The S.192 culture at DNC displayed the darkest green coloration and entered chlorosis on day 38 at the end of the experiment. The culture at CONT never reached the same dark green colour and had a brown tint to it, but at the end of the experiment they displayed a comparable green tone. The difference in the S.6803 strain between the two illumination regimes was better visible. At DNC the culture appeared to become slowly brown from day 18 on and clearly reached full chlorosis on day 38. The CONT culture behaved differently as it appeared more blue from day 18 on and also became chlorotic on day 38, but never displayed the same clear yellow chlorotic colour as the DNC culture.























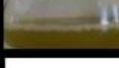
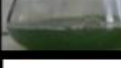
	DNC			CONT			Day
192							5
							12
							18
							25
							33
							38
6803							5
							12
							18
							25
							33
							38
	K1	K2	K3	K1	K2	K3	Day

Figure 25: Visual appearance of S.192 and S.6803 at 3000lux. Left cultivated with a day-night-cycle and on the right cultivated under continuous illumination.

The phenotypic appearance substantially differed between the cultures at the two different illumination regimes.

Additionally, to the visual monitoring analytical measurements were conducted to represent the physiological state of the cultures, see Figure 26. For the S.192 strain the OD_{435nm} of the DNC was always higher and reached an OD of 10 on day 40. The CONT culture only reached a maximal OD of 8.35 on day 38. For the OD_{750nm} the trend was vice versa with slightly higher values displayed by the

CONT culture. The OD at both 435nm and 750nm increased linearly over time, but from day 38 to 40 a slight decrease occurred, which corresponded to the observation of chlorosis on day 38 (Figure 25). The behaviour of the S.6803 strain differed from that, since its OD_{435nm} was more or less the same at both conditions with a maximum OD of 9. The strain also displayed a decrease of the OD at DNC and a plateau at CONT from day 38 to 40. The OD_{750nm} of the S.6803 behaved the same as in the S.192, since the OD_{750nm} of the DNC culture was lower than the CONT values and the S.6803 also reached similar values.

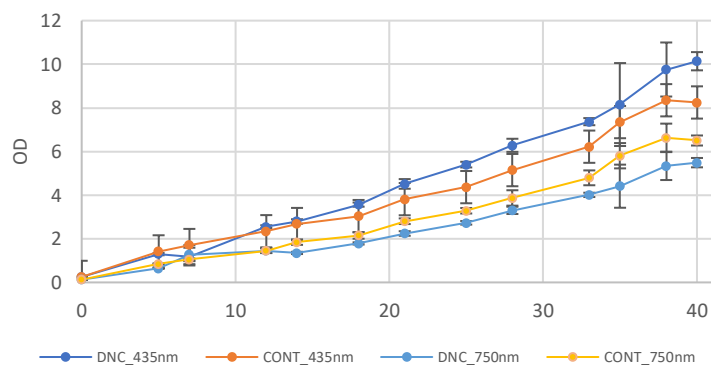
The pH of all cultures was around 10, only the pH of the S.6803 culture at DNC displayed a rapid pH drop that started on day 35 from pH10.5 down to pH8 on day 40. This was also the only culture displaying a clear yellow chlorotic colour on day 38.

The pigment content displayed no clear trend, only the chlorophyll content dropped on day 25. The chlorophyll content had overall low values of below 1% of CDW in S.192 and around 1% in S.6803. The chlorophyll values of the CONT cultures were consistently lower by a factor of about 0.75 compared to the DNC. The phycocyanin content in %CDW was overall higher in the S.192 strain. Furthermore, the DNC cultures displayed 2 to 3-fold of the CONT cultures phycocyanin, even though the cell dry weight was higher for the CONT cultures in both strains. The CDW increased linearly in both cultures the same way and reached a maximum of 1.65g/L for the S.192 CONT culture and 1.7g/L for the S.6803.

The biggest difference between the two conditions was the PHB content. The PHB increased linearly in both cultures from the start until the end of the experiment, but the PHB content of the CONT cultures increased at a higher rate. The difference was more pronounced in the S.192 strain. On day 12 the S.192 CONT culture contained 37 times as much PHB as the DNC culture and on the last day the maximum PHB content of 12.3% was reached which was still 6 times the amount of the DNC culture. The S.6803 strain only reached a maximum of 3.2% in the CONT culture, which was still double the amount found in the DNC culture.

The glycogen content on the other hand increased linear at first but grew from day 25 on exponentially. In the S.192 strain the glycogen content of the DNC was significantly lower compared to the CONT culture, but at the end of the experiment they both reached a similar high glycogen content of about 40%. The glycogen content in the S.6803 strain was overall lower compared to the S.192 and there was no significant difference between the DNC and CONT culture. Only on day 40 the S.6803 cultures bypassed the S.192 cultures reaching a maximum glycogen content of 47% of the cell dry weight at both conditions.

S.192



S.6803

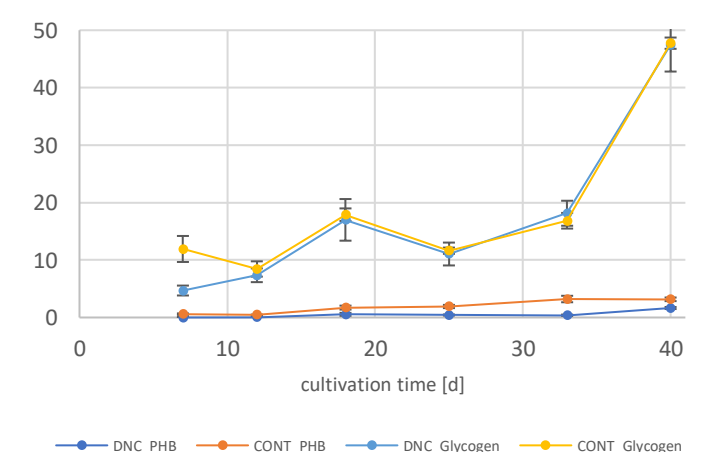
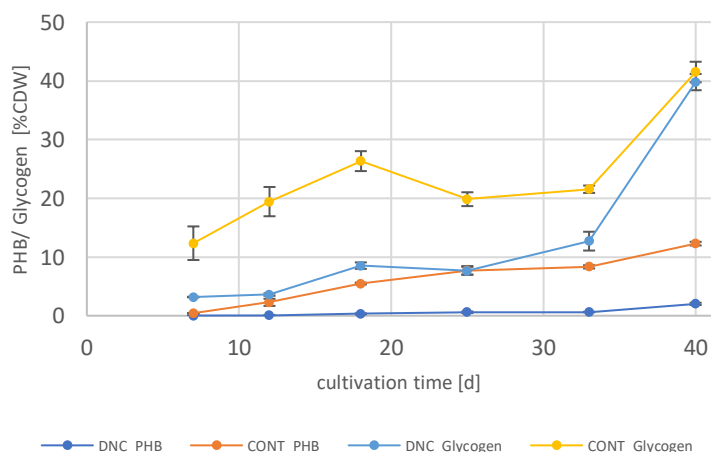
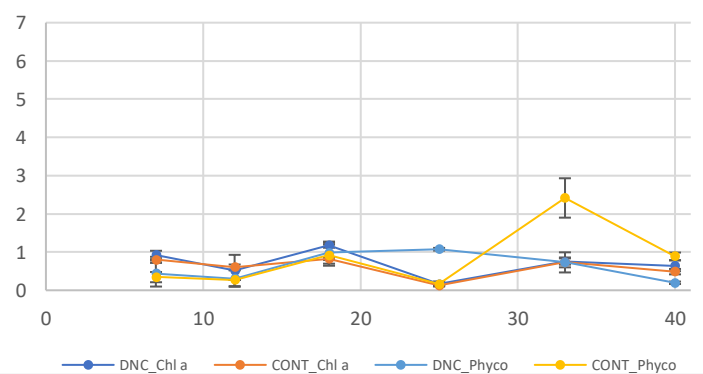
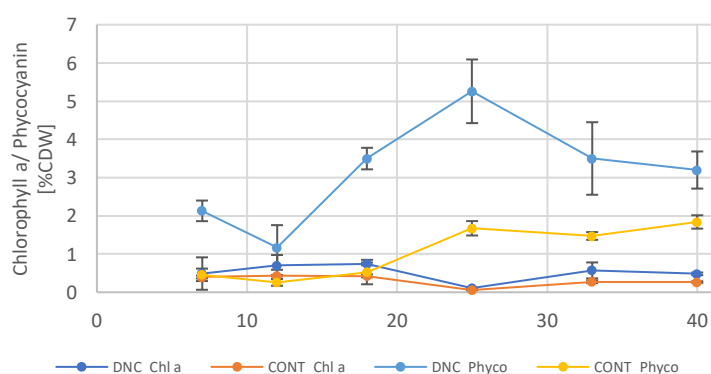
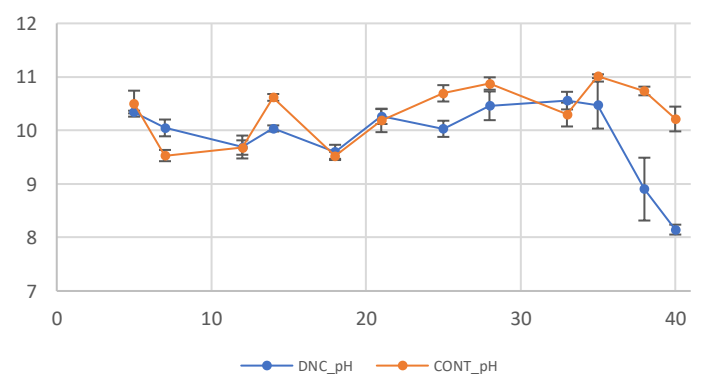
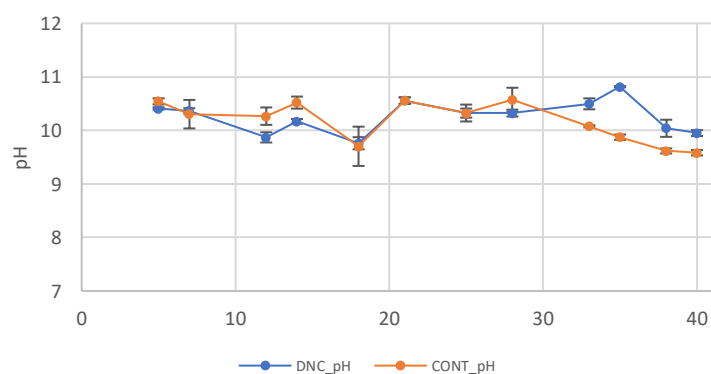
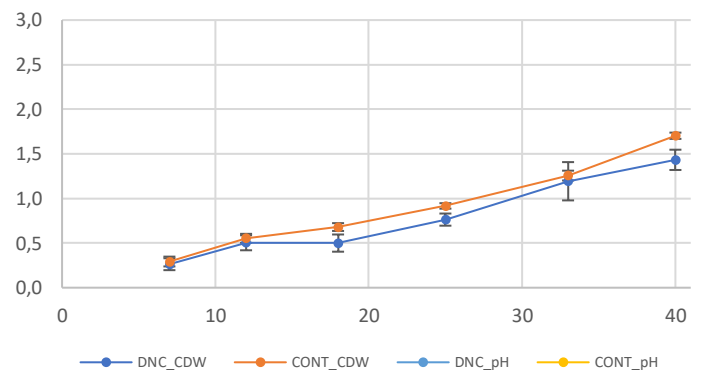
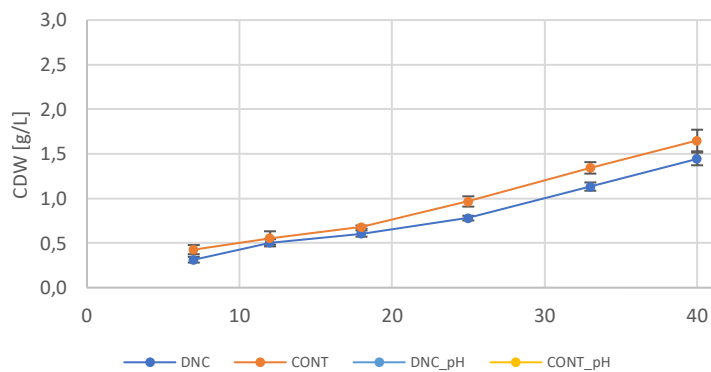
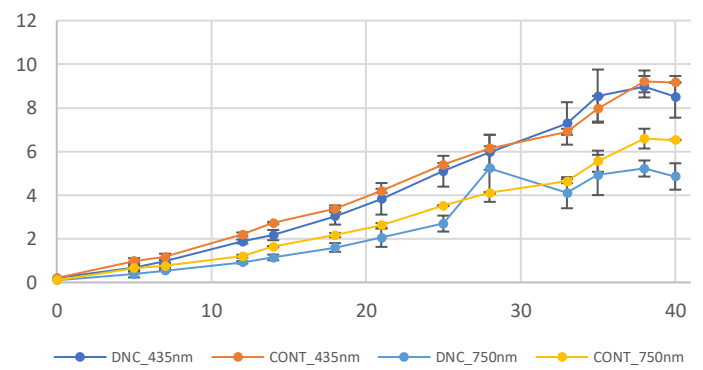


Figure 26: Analytical data representing the physiological state of the cultures cultivated at DNC and CONT. On the left S.192, on the right S.6803 at 3000lux.

Overall the S.192 strain at CONT conditions displayed the highest cell content of the measured analytes and also the most PHB content (Figure 27).

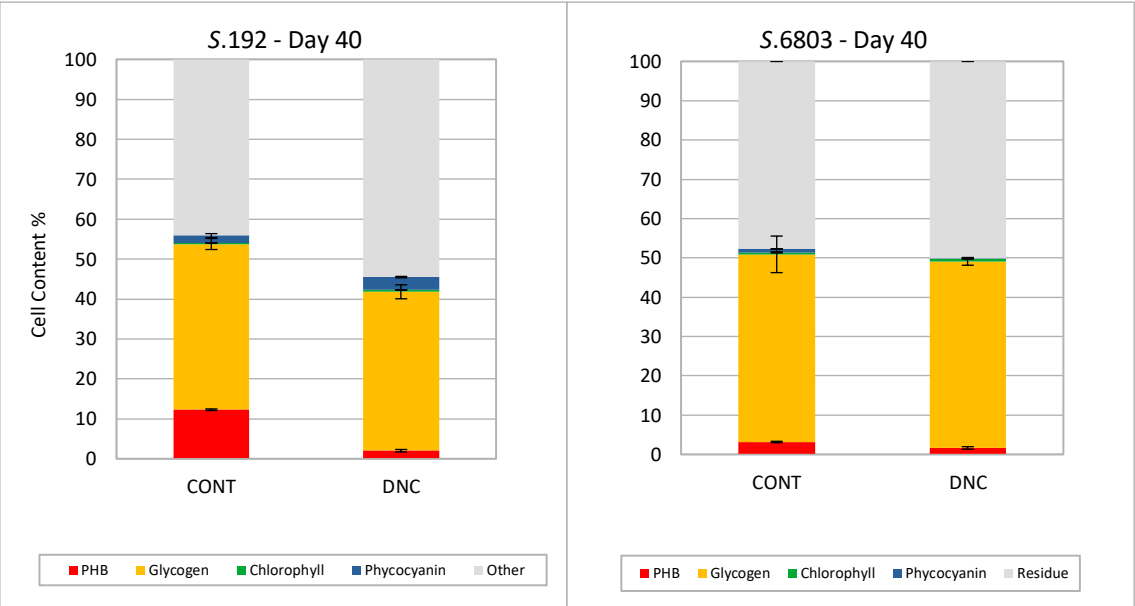


Figure 27: Cell content of S.192 and S.6803 in %CDW on day 40 at DNC and CONT illumination at 3000lux.

Confocal scanning microscope images revealed that in both strains the continuous illumination resulted in a bigger cell size (Figure 28 &29). The cells from the CONT cultures were almost 50% larger compared to the cells from the same strain at DNC. The cell size of the S.192 CONT cells was $2.75\pm0.35\mu\text{m}$ on average and only $1.88\pm0.27\mu\text{m}$ at DNC. For the S.6803 the cell size of the cells cultivated at CONT conditions was $2.46 \pm 0.41\mu\text{m}$ and $1.83 \pm 0.39\mu\text{m}$ at DNC.

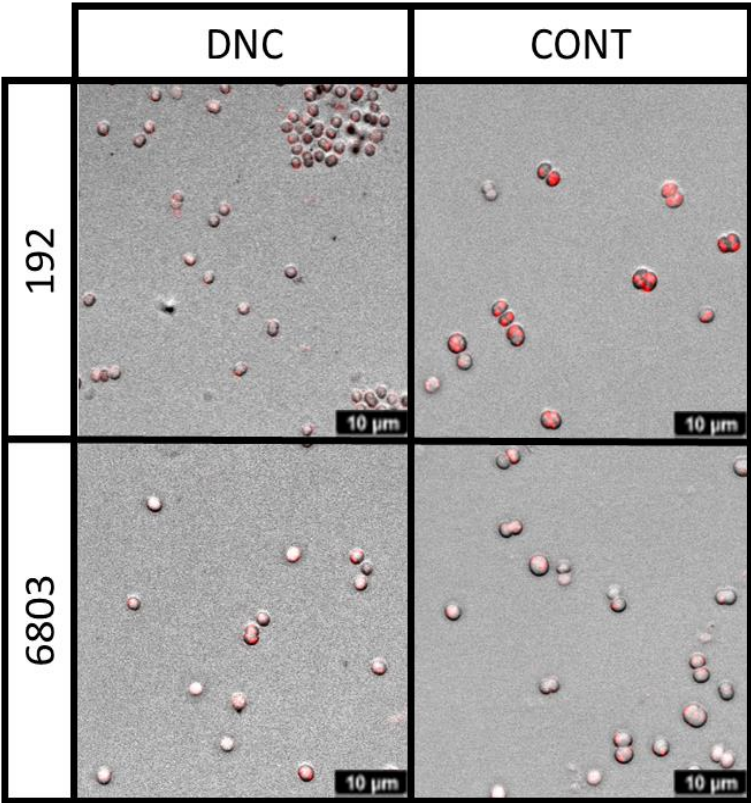


Figure 28: Microscopic images of the S.192 and S.6803 cells at 3000lux stained with Nile-red and taken with a confocal scanning microscope

While the cells at CONT conditions were much bigger, the cell number at DNC conditions was much higher (Figure 29, right graph). The cell density of the S.192 DNC culture was 3 times as high as in the CONT culture, with 590million and 196million cells/mL, respectively. The difference in the S.6803 strain was not as big, but there were still 1.3 times as many cells in the DNC compared to CONT cultures, with 436 and 328million cells/mL, respectively.

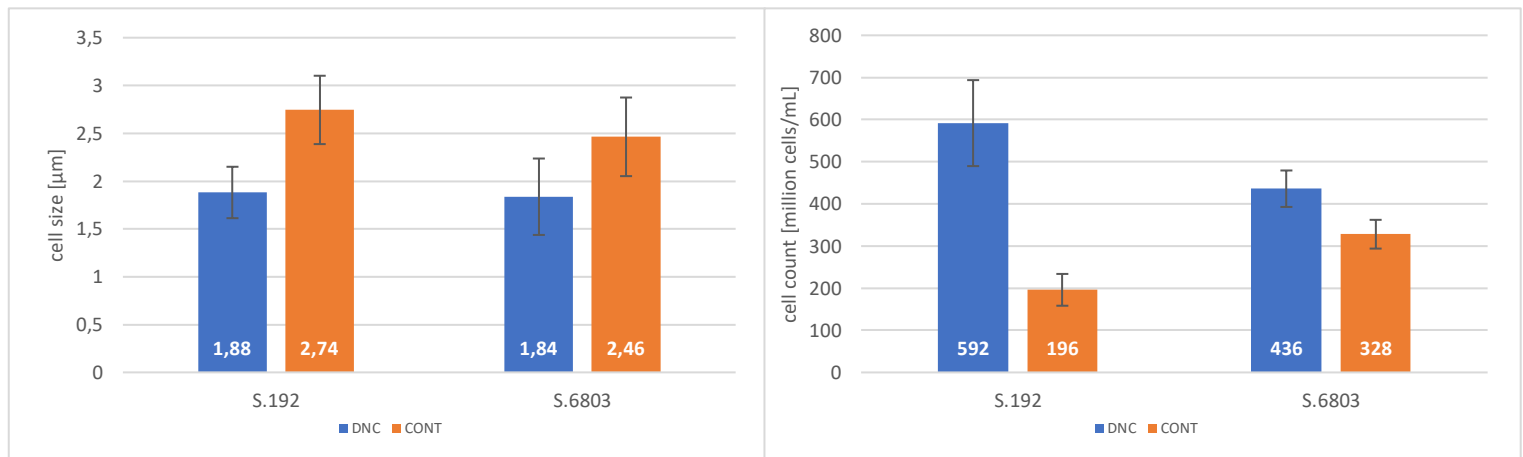


Figure 29: Cell count and cell size at 3000lux for S.192 and S.6803. On the left the cell size of S.192 and S.6803 at DNC and CONT conditions. On the right the corresponding cell count in million cells per mL.

The remaining nitrate levels in the medium were measured photometrically on day 40. The initial concentration of nitrate in the media was 332mg/L, after 40 days of cultivation only 0.6 to 1.2% of the initial nitrate was left in the culture (Figure 30). The lowest nitrate levels were measured in the S.192 CONT culture with 2.2mg/L and the highest level in the S.6803 CONT culture with 3.9mg/L. All cultures had similar low nitrate levels in their medium and therefore all cultures reached nitrate starvation at the end of the experiment on day 40. This implies that the differences in the PHB content between CONT and DNC cultures was not due to differences in the nitrate availability. Only the nitrate concentration was measured on the last day, therefore no statement about the nitrate development or its eventual formation can be made. Also, other nitrogenous compounds like ammonia were not measured.

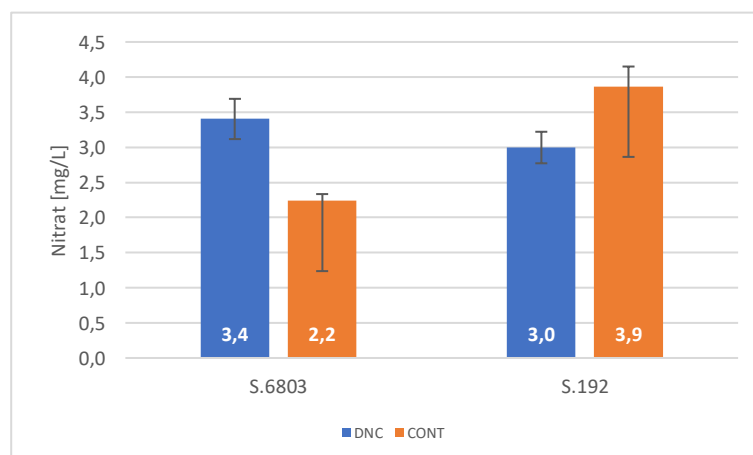


Figure 30: Remaining nitrate levels in the medium of experiment 1 measured on day 40.

8.3 Continuous illumination at 3000lux S.192 and IFA (Exp.2)

In experiment 2 triplicates of the S.192 and IFA strains were cultivated at DNC and CONT conditions. The temperature and light intensity were monitored with a data logger as in experiment 1 and the mean values were calculated (Table 8). The temperature of the continuous illuminated set-up was again slightly higher compared to the DNC, but the illumination of the CONT was other than in the previous experiment 1 slightly higher. These differences were minor and were not expected to have any significant influence on the cultures. Therefore experiment 1 and 2 had comparable conditions.

Table 8: Cultivation conditions in experiment 2 monitored with a HOBO data logger.

Condition	Temperature [°C]	HOBO Data logger Light intensity [lux]	Voltcraft Light intensity [lux]
DNC	22.93±0.52	2109±122	3100
CONT	23.56±0.55	2217±262	2900

Photos of the cultures were taken before every sampling, see Figure 31. The strains IFA and S.192 at DNC displayed the same colour succession. While S.192 started to lighten from day 21 on and showed clear signs of chlorosis on day 40. IFA kept a strong dark green colour until day 21, but also reached chlorosis on day 40. Also, at DNC both strains displayed a similar colour succession. The CONT cultures never reached an as dark green colour as the DNC. The DNC cultures of both strains reached the darkest colouration sooner than the CONT cultures on day 14. Afterwards they decreased in colour because of chlorosis. None of the cultures reached a clear yellow chlorosis coloration like the S.6803 on day 38 in the previous experiment 1. The S.192 strains expressed a similar, but not identical growth and colour succession over the duration of the experiment. In experiment 1 they displayed an overall darker colour. This could be due to the fact, that the culture was from the start denser and greener. This was due to different inoculum densities resulting in different inoculation volumes of 12mL in experiment 1 and 14mL in experiment 2.

The phenotypic appearance of the strains S.192 in experiment 1 and 2 and IFA displayed similar colour patterns over the 40 days of cultivation with only S.6803 differing substantially at both conditions from the other cultures.

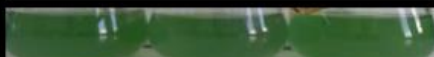


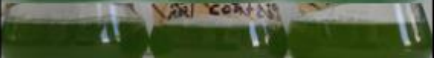


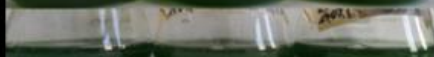
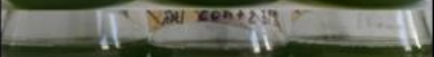















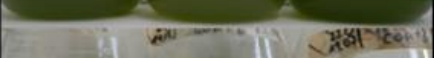
	DNC			CONT			Day
192							0
							6
							14
							21
							28
							40
IFA							0
							6
							14
							21
							28
							40
	K1	K2	K3	K1	K2	K3	Day

Figure 31: Visual appearance of S.192 and IFA at 3000lux. Left cultivated with a day-night-cycle and on the right cultivated under continuous illumination.

Analytical measurements were conducted to represent the physiological state of the cultures, see Figure 32. The OD at 435nm of both strains at both conditions showed a similar steady increase until day 33, but then changed to a more exponential increase. This differed from the previous experiment where the OD growth rate decreased towards the end. The graph of the OD_{750nm} of the CONT strains on the other hand looked comparable, but also the DNC cultures displayed an increase and not a decrease at the end. Even though visually the cultures appeared denser and greener in experiment 1, the cultures in experiment 2 reached higher OD_{435nm} with 13.6 for the S.192 DNC as the highest value compared with 10.1 in experiment 1. This also applied to the other cultures, with all of them reaching a higher final OD at the end of experiment 2. The OD_{435nm} of the CONT cultivated S.192 and IFA was significantly lower during the whole experiment and differs from the S.6803. The pH fluctuated above 10 in experiment 2 but decreased from day 35 below pH10. At the end of the experiment, starting from day 25, the pH of the CONT cultures was significantly lower compared to the DNC.

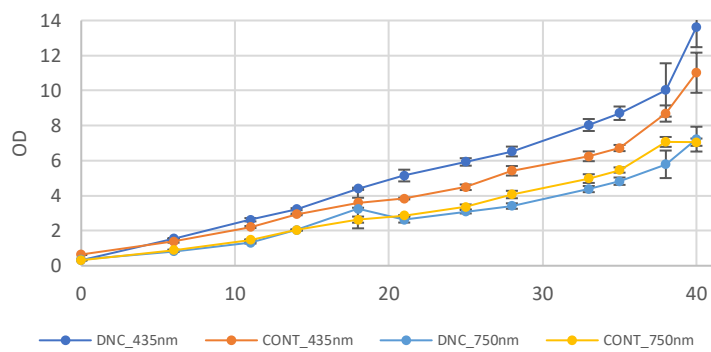
The S.192 strain accumulated comparable amounts of CDW in both experiments with a little less in the DNC with 1.65g/L in experiment 1 and 1.74g/L in experiment 2. The last two samples taken on day 33 and 40 showed a reversed trend in the IFA strain with higher CDW values in the DNC culture. The chlorophyll amount in the S.192 cultures decreased at first slightly and increased again at the end, but for the IFA cultures it was the other way around. In both strains there was more chlorophyll in the DNC cultures compared to CONT. This trend was even more pronounced in the IFA cultures, with also overall higher chlorophyll values than the S.192.

Also, the phycocyanin values were higher at DNC, but in the S.192 strain they first increased up to almost 4%CDW and thereafter decreased rapidly. In the IFA culture the phycocyanin content slightly decreased but increased again rapidly on day 25 reaching 5.4%CDW- Thereafter it decreased again rapidly. In the continuous cultures the phycocyanin content was overall lower. In the S.192 culture it decreased continuously until day 25 to below 0.1% and thereafter displayed stable values around 0.1%. In the CONT IFA culture this was reversed with the phycocyanin content increasing from 0.85%CDW up to almost 1.5%CDW on day 40. This was more concurrent with the values of the S.192 cultures in experiment 1 that were even higher on day 40.

The most pronounced difference between the CONT and DNC cultures was the PHB content. The S.192 CONT culture reached the highest value with 11.25%CDW PHB on day 40, the more than 7-fold of the DNC cell content. The IFA CONT culture only reached 4.6%CDW PHB on day 40 which was 3.8 times as much as in the DNC culture. The PHB content increased in all cultures linearly, similar to experiment 1.

The glycogen content was more or less stable in all cultures until day 25, with the DNC displaying lower levels around 5%CDW and the CONT cultures between 15% and 18%CDW. After day 25 the glycogen rapidly increased in all cultures, but the increase in the CONT cultures stopped on day 33 and stayed stable at around 35%CDW glycogen content while the DNC glycogen content further increased until day 40 bypassing the CONT cultures.

S.192



IFA

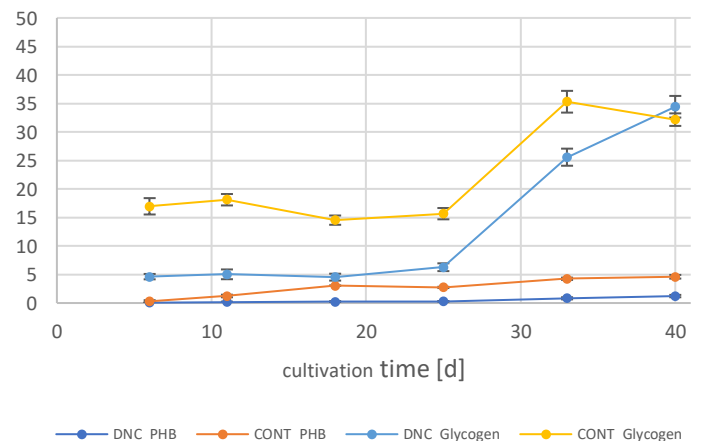
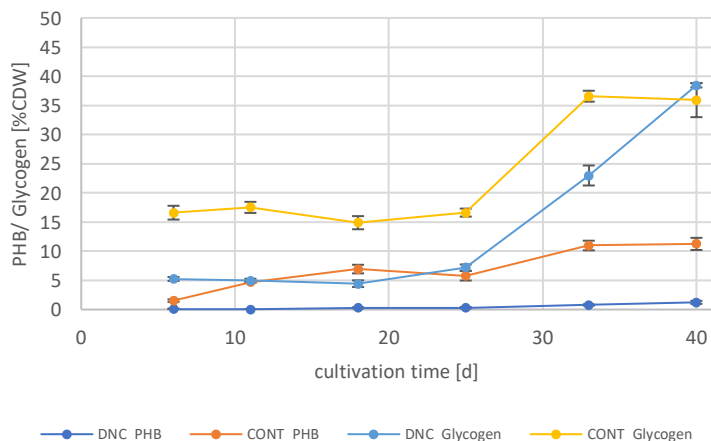
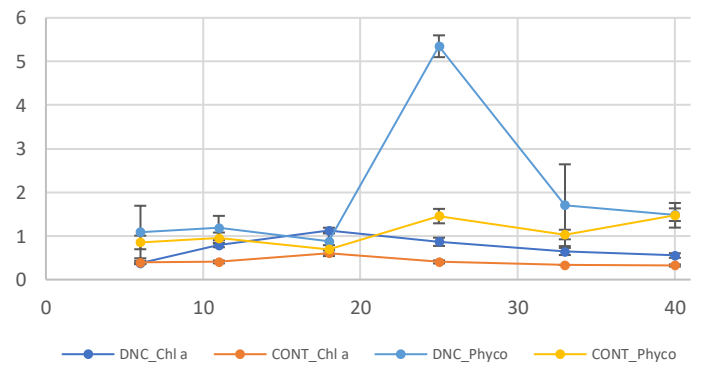
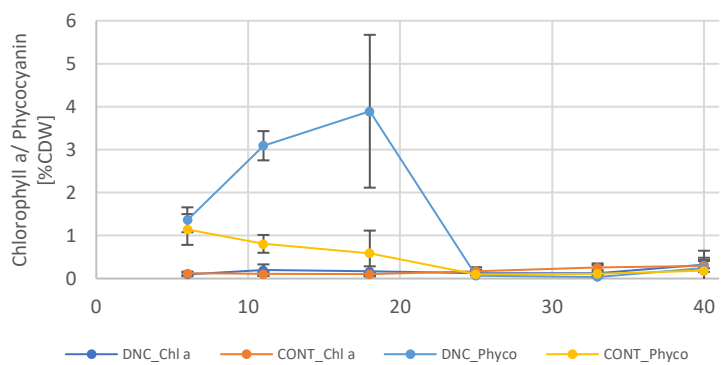
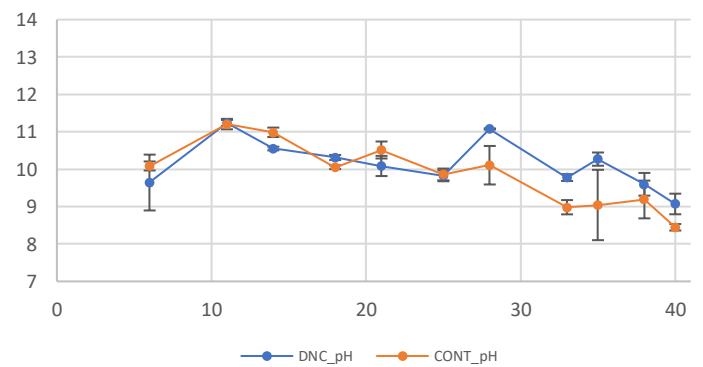
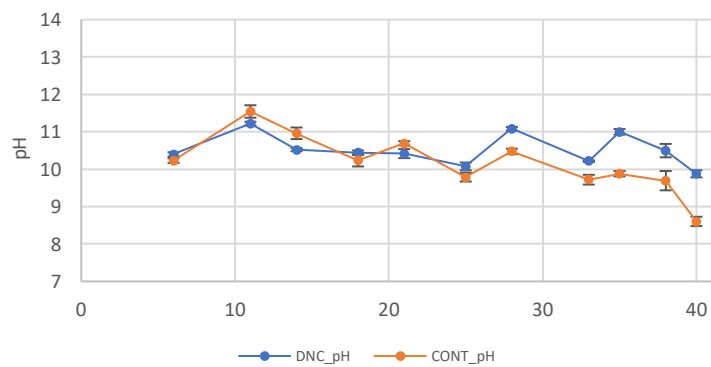
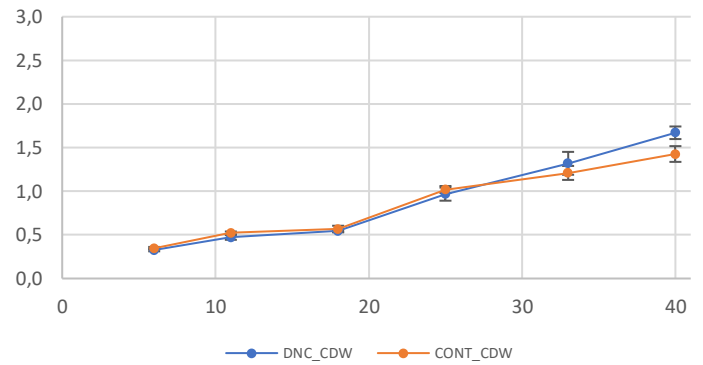
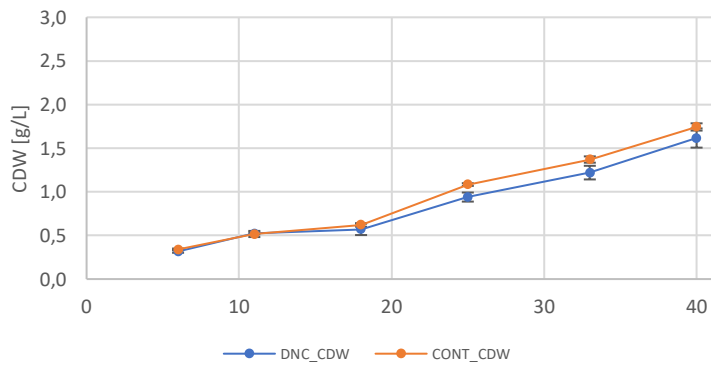
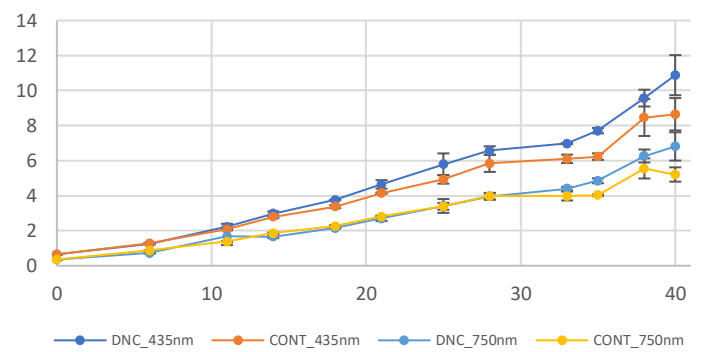


Figure 32: Analytical data representing the physiological state of the cultures cultivated at DNC and CONT. On the left S.192, on the right IFA at 3000lux.

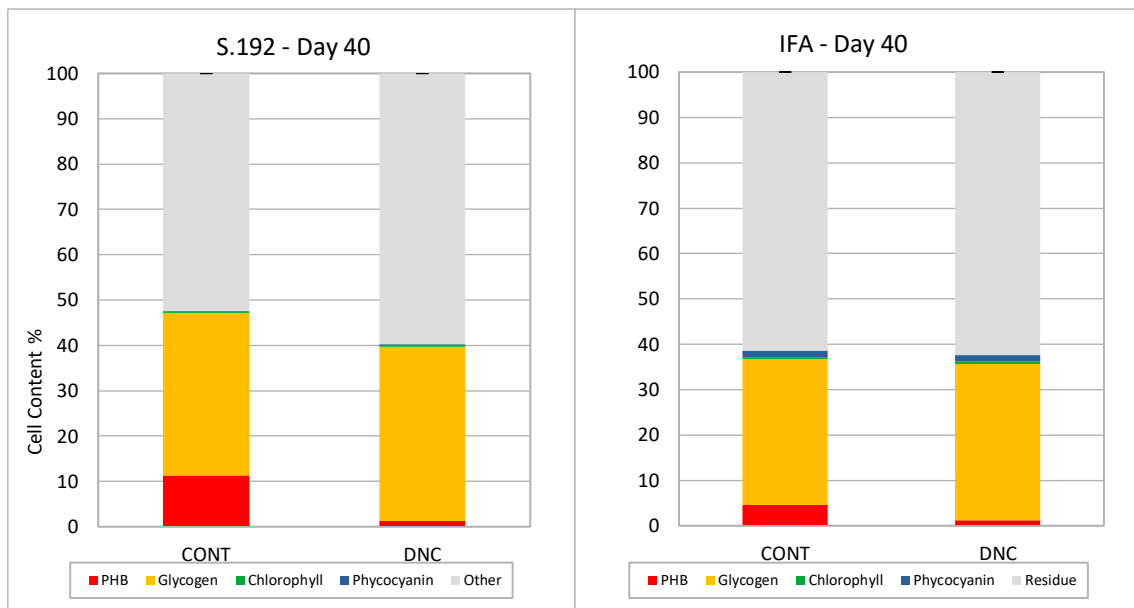


Figure 33: Cell content of S.192 and IFA in %CDW on day 40 at DNC and CONT illumination at 3000lux.

The overall cell content (Figure 33) was less compared to experiment 1, with no culture reaching 50%. In the strain S.192 the difference in PHB content between the DNC and CONT cultivation conditions was most pronounced, but also applied to the IFA strain. The content of phycocyanin and chlorophyll was higher in the IFA cultures, but they displayed overall a lower content of the analysed cell components of below 40%CDW. The S.192 CONT culture was able to build up more of the cell components compared to the DNC, while there was no significant difference in the IFA cultures, only the distribution differed between the CONT and DNC culture.

As in the previous experiment, cells obtained from the cultures cultivated at CONT conditions were clearly bigger than cells exposed to DNC (Figure 34). The cell size of the S.192 CONT culture was even bigger compared to the previous experiment 1 reaching $2.9 \pm 0.39 \mu\text{m}$ (Figure 35). At the same time the DNC cell size was smaller with $1.7 \pm 0.23 \mu\text{m}$. The CONT cells increased their cell size by 67% compared to the DNC cultures. For the IFA cultures the difference in cell size was also apparent, but not as big. The IFA DNC culture had an average cell size of $2.10 \pm 0.25 \mu\text{m}$ and the CONT culture was enlarged by a factor of 1.25 compared to the DNC with an average of $2.37 \pm 0.88 \mu\text{m}$. The increase of the cell size by 25% in the CONT culture of the IFA strain was much less, but still a significant change in cell morphology induced by continuous illumination.

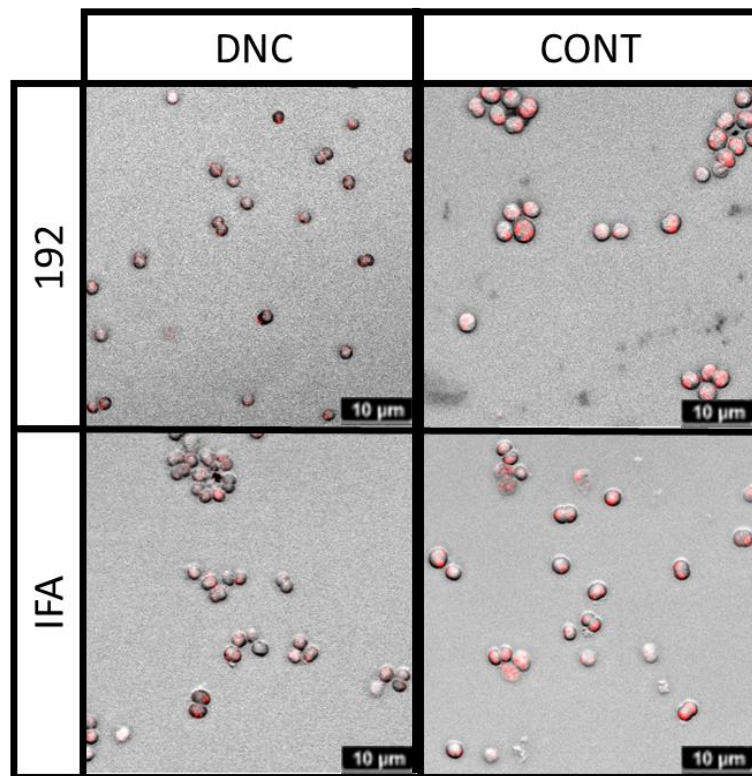


Figure 34: Microscopic images of the S.192 and IFA cells at 3000lux stained with Nile-red and taken with a confocal scanning microscope.

The cell count displayed a reversed trend (Figure 35, graph on the right). While the cell size in the CONT cultures was enlarged in the DNC the cell density was much higher. For the S.192 strain 539 ± 26 million cells/mL were counted at DNC and only 158 ± 23 million cells/mL in the CONT culture. This equates to more than 3 times as many cells in the S.192 DNC. In the IFA strain the difference was again not as high, but still significant. In the DNC culture the cell density was with 443 ± 50 million cells/mL approximately 1.5 times larger compared to 304 ± 59 million cells/mL in the CONT culture.

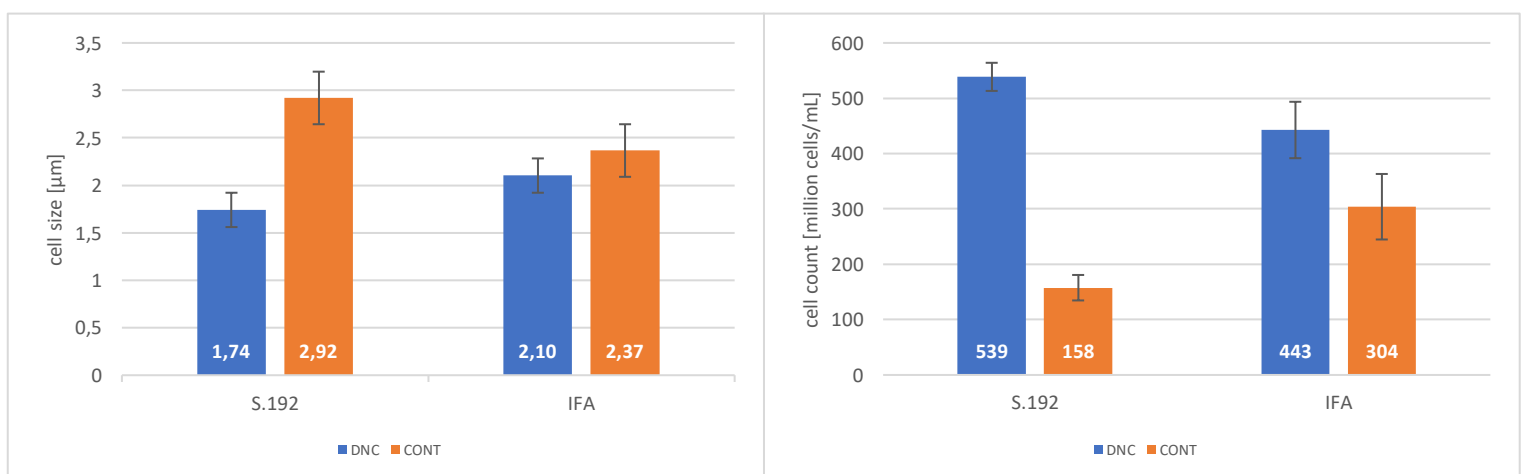


Figure 35: Cell count and cell size at 3000lux for S.192 and IFA. On the left the cell size of S.192 and IFA at DNC and CONT conditions. On the right the corresponding cell count in million cells per mL.

The nitrate levels at the end of the experiment on day 40 are depicted in Figure 36. The nitrate levels at DNC were slightly higher compared to the CONT cultures and the nitrate levels in the S.192 cultures were still higher than in the IFA culture. Compared to the previous experiment 1, the nitrate levels were slightly higher, but in the same range between 3.7mg/L and 5.0mg/L. Until the end of the experiment the initial 332mg/L nitrate was used up and only between 1.13% to 1.51% of the initial nitrate remained in the culture medium. All cultures reached nitrate limitation until the end of the experiment and no obvious difference was found between the CONT and DNC cultures.

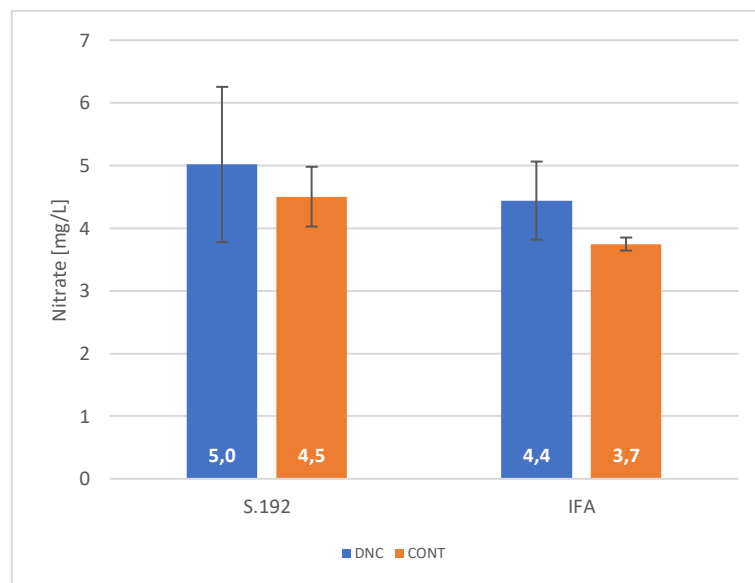


Figure 36: Remaining nitrate levels in the medium of experiment 2 measured on day 40.

8.4 Continuous illumination at 6000lux with 3 different *Synechocystis* strains (Exp.3)

In experiment 3 the light intensity was doubled by adding additional LEDs to the previous set-up resulting in about 6000lux (Table 4). In the DNC set-up 5648lux were measured with the Voltcraft luxmeter and in the CONT set-up 6168lux. The temperature and light intensity were monitored with data loggers and the average was calculated, see Table 9. The measured light intensity of the data logger was much lower because they were placed on the bottom of the boxes resulting in a higher distance to the LEDs compared to the distance of the cultures placed on the shaker.

Table 9: Cultivation conditions in experiment 3 monitored with a HOBO data logger.

Condition	Temperature [°C]	HOBO data logger Light intensity [lux]	Voltcraft Light intensity [lux]
DNC	23,07±0,85	3155±637	5648
CONT	23,79±0,38	3237±757	6168

The temperature was slightly increased in the CONT set-up compared to the 3000lux experiments 1&2 and was stable over the whole duration of the experiment except for the end of the experiment, where an increase above 25°C was observed due to unknown reasons. In the DNC set-up no significant change could be observed.

The light intensity in the CONT set-up was stable, but in the DNC experiment several light failures occurred between day 6 and 18 (Figure 37). The temperature fluctuated, because of the day night cycle between approximately 22.2°C and 24.3°C. Due to the light failures the average temperature of the DNC was reduced and would have been higher without any failures. It was assumed, that the temperature would have been slightly higher in the 6000lux experiment compared to the 3000lux experiment due to higher energy uptake.

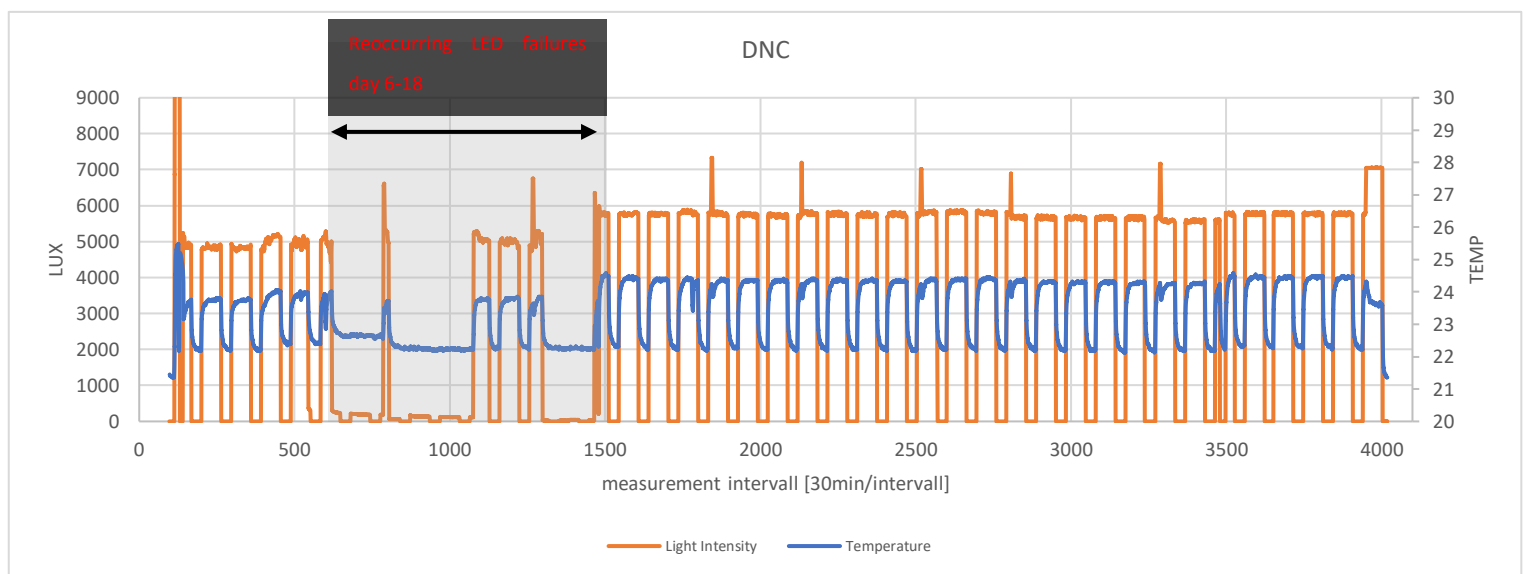


Figure 37: Temperature and illumination profile of the DNC culture of experiment 3 over 40 days at 6000lux, with the reoccurring LED failures indicated.

In the following Figure 38 the visual appearance of the cultures of the three strains S.192, S.6803 and IFA is depicted from day 6 until day 40. The light failures in the DNC set-up also led to an altered growth of the cultures. This can be seen in one of the S.192 DNC culture (indicated by a red arrow) which displayed a yellow colour on day 21 but turned dark green again after the failures stopped. The S.192 strain reacted more sensitive to the prolonged darkness since its cultures never reached the same dark green coloration, as the cultures of the other strains. Therefore, it was decided to additionally sample the two S.192 DNC cultures cultivated for PHB production. By increasing the sample size from duplicate to quadruplicate, the outlier due to the light failure didn't have such a big impact on the data reliability. This also meant no PHB samples of the S.192 DNC cultures at 6000lux were available for PHB extraction and analysis.

The other strains S.6803 and IFA displayed no disturbance by the light failures. Their growth parameters looked very similar to their growth in the previous experiments with only a slightly lower growth rate which led to the same dark green colour on day 21 instead of 14 (compare to Figure 31). After

the cultures reached the darkest green colour on day 21, the cultures became increasingly damp and reaching a brownish colour on day 40 indicating chlorosis.

The CONT cultures reached a dark green colour sooner compared to the DNC on day 14, but the cultures dampened from day 14 on and became brownish from day 35 reaching a brownish green colour on day 40. The chlorosis in the CONT cultures on day 40 was not as clearly visible as in the DNC cultures.

Only the IFA strain behaved differently as it never reached a dark green colour and displayed a brownish colour from day 14 on without any changes in colour until day 35, but a dark brown colour on day 40.





































	DNC		CONT		Day
192					6
					14
					21
					28
					35
					40
6803					6
					14
					21
					28
					35
					40
IFA					6
					14
					21
					28
					35
					40
	K1	K2	K1	K2	Day

Figure 38: Visual appearance of S.192, S.6803 and IFA at 6000lux.

The collected analytical data is represented in Figure 39 with the strain S.192 on the left, IFA on the right and S.6803 in the middle. The data is represented in graphs over the course of the experiment with the cultivation time on the x-axes.

The OD at 430nm showed a linear upward trend for all three strains, but for the S.192 the OD of the CONT culture was higher over the whole course of the experiment, while in the S.6803 it was the same until day 28, when the DNC started to increase and the CONT and DNC had about the same until day 40. In the IFA culture it was the other way around with the same OD until day 28, when the OD of the DNC became higher. This was diverging from the former experiments in which the OD_{435nm} of the DNC culture was predominantly above the CONT cultures.

The final OD_{435nm} of the CONT cultures at 6000lux was higher in the IFA and S.6803 cultures on day 40 compared to the 3000lux CONT cultures. For the S.192 strain it was not clear with an OD_{435nm} of 8.2 (Exp.1) and 11 (Exp.2) at 3000lux and an OD_{435nm} of 8.2 at 6000lux.

The measured CDW was higher in the CONT cultures over the whole course of the experiment with one exception, on day 28 it was higher throughout all of the DNC cultures. This could be a sign for a systematic error in the sampling or sample preparation on that specific day. The final CDW in all CONT cultures was about 1.7g/L, which was in the same range as the CONT cultures in experiment 1 and 2.

In the DNC cultures, a clear drop in the pH was visible from day 6 until day 18, when the values started to increase again. This pH drop happened during the light failures and prolonged darkness. Without light the cultures were missing energy for CO₂ fixations from the media and since CO₂ forms with water the carbonic acid (H₂CO₃) the stopped consumption of dissolved CO₂ by the cultures resulted in the pH drop. Once the photosynthesis restarted the pH levels rose again to a pH above 10 similar as in the CONT cultures, but dropped again at the end of the experiment, when photosynthesis was reduced due to chlorosis.

In the DNC cultures the phycocyanin content dropped from 2%, 9% and 5% in the S.192, S.6803 and IFA respectively down to below 2% and stayed low until the end of the experiment. In the CONT cultures on the other hand the phycocyanin increased at first with peaks on day 35 in the S.192 culture and on day 28 in the S.6803 and IFA cultures with 3.1%, 4.2% and 1.3% respectively. After the peak the phycocyanin content dropped again in all cultures. The chlorophyll content in the DNC was always higher compared to the CONT cultures at above 1% until day 28, when the values dropped from the highest value at 1.4% in the S.6803 culture and 1.3% in the IFA culture below 1%. The S.192 strain was the exception with chlorophyll contents below 1% over the whole course of the experiment. In the CONT cultures the chlorophyll levels were overall much lower, but constant during the experiment with mean values of 0.5%, 0.8% and 0.4% per CDW in the strains S.192, S.6803 and IFA respectively.



Figure 39: Analytical data representing the physiological state of the cultures cultivated at DNC and CONT at 6000lux.

The glycogen content was similar to the experiments before. The glycogen content in the CONT cultures first rose above 20% CDW in the S.192 and IFA cultures and 17% in the S.6803 culture on day 21. Afterwards the values slightly decreased, but then exponentially increased to the highest glycogen level on day 40 with about 42%, 48% and 41% CDW in the strains S.192, S.6803 and IFA respectively. The PHB levels slowly increased at a steady rate in the CONT cultures until day 28, after which they increased at a higher rate reaching 11%, 4.3% and 5.5%CDW PHB on day 40, respectively. In the DNC cultures the PHB content increased linearly at much lower rates until day 40, when they reached 1.4% and 1.7% in the strains S.6803 and IFA, which was in both cases 3 times lower as in the CONT cultures. In the S.192 culture the PHB content linearly increased until day 28 resulting in the maximum of 5.4% and afterwards declined to 3.5% on day 40, which also was 3 times as much PHB content in the CONT culture compared to the DNC culture. Compared with the 3000lux cultures, the difference in PHB content was still significant between the CONT and DNC cultures, but the difference was not as pronounced anymore. This could have also been due to the light failure in the DNC set-up. The CONT culture of the S.192 strain reached a slightly lower PHB content, the S.6803 and the IFA culture a slightly higher content (about +1%) compared to the 3000lux cultures.

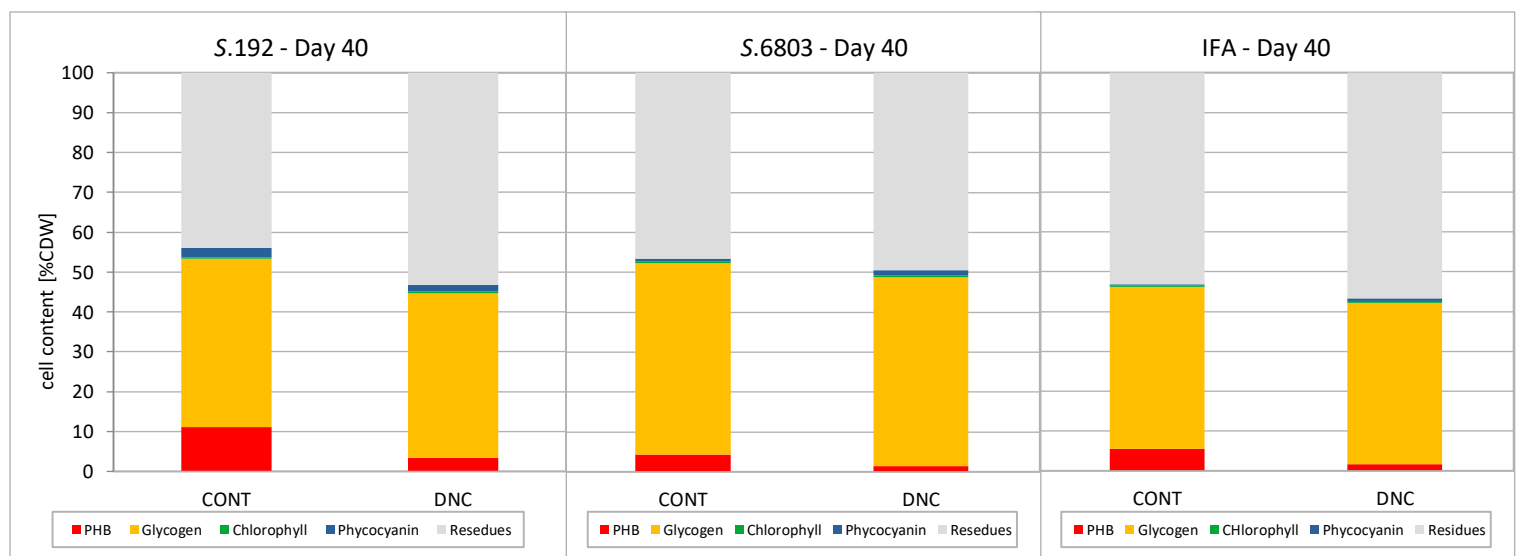


Figure 40: Cell content of S.192, S.6803 and IFA in %CDW on day 40 for the two cultivation conditions DNC and CONT at 6000lux.

In Figure 40 the overall cell content of the analysed cell components is shown. The analysed components made up more than 50% of the cells dried mass in the CONT cultures of the strains S.192 and S.6803 which was comparable to experiment 1. The PHB content was clearly much higher in the CONT cultures independent from the strain. This was most pronounced in the S.192 strain and least in the IFA strain. In this experiment was a difference in the total content of all analysed components visible between the CONT and DNC cultures. The DNC contained overall less of the analysed

components, even though the major fraction (glycogen) was about the same in CONT and DNC cultures.

For the cell size the same trend as in the previous 3000lux experiments was observed (Figure 41). The cells obtained from the cultures cultivated at CONT conditions were clearly bigger (right side) compared to the cells from DNC cultures. Also, the stained PHB granules displayed a better resolution and were more pronounced in the CONT cultures.

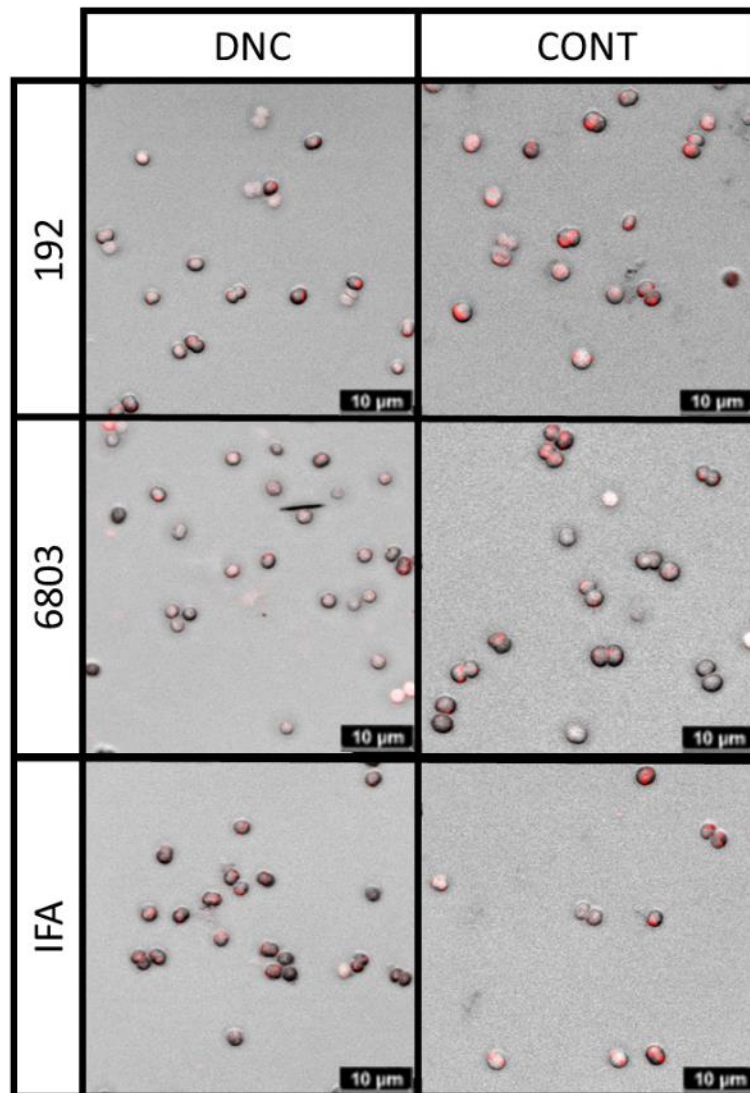


Figure 41: Microscopic images of the S.192, S.6803 and IFA cells at 6000lux stained with Nile-red and taken with a confocal scanning microscope.

The measured cell size of the CONT culture was larger compared to the DNC (Figure 42). The cells of the CONT S.192 cultures were most enlarged with cell sizes up to about $2.98 \pm 0.38 \mu\text{m}$, which was 1.4 times larger than DNC cells (40% increase). The S.6803 culture cells did not reach this size with only $2.53 \pm 0.37 \mu\text{m}$, the same as the IFA cultures with $2.48 \pm 0.51 \mu\text{m}$. Therefore, the IFA and S.6803 CONT cultures were only about 20% larger compared to the DNC. The DNC cells were about the

same size in all three strains with around 2.1µm, which was also larger than in the previous experiments where the DNC at 3000lux had a cell size between 1.74µm and 2.1µm.

In the strains S.6803 and IFA the cell count was again higher in the DNC, but in the S.192 strain the cells density in the CONT culture was higher with 459 million cells/mL compared to 374 million cells/mL in the DNC. This was a tremendous difference to the previous experiments with 550-600million cells/mL in the DNC cultures and 150-200million cells/mL in the CONT cultures. The cell count in the S.6803 and IFA cultures at 6000lux was less compared to the 3000lux except the S.6803 CONT culture had a little higher cell density, but the ratio between the CONT and DNC cultures remained about the same.

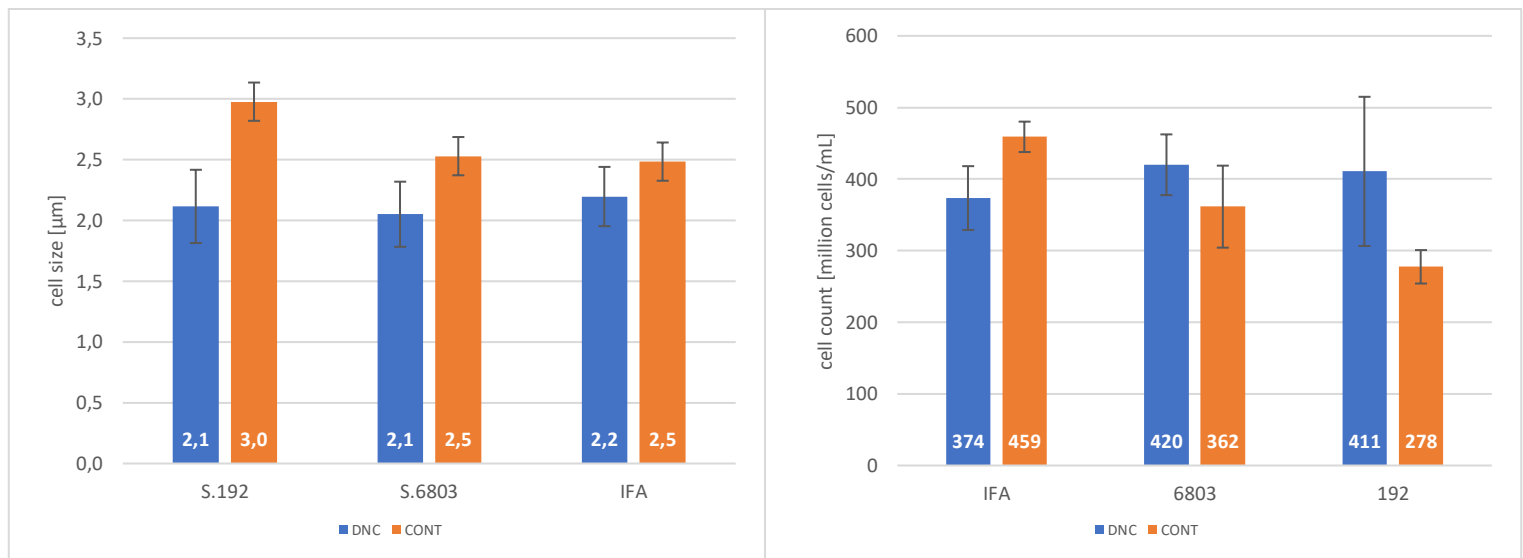


Figure 42: Cell count and cell size at 6000lux for S.192, S.6803 and IFA. On the left the cell size at DNC and CONT conditions. On the right the corresponding cell count in million cells per mL.

In the following Figure 43, the cell size distribution is represented for the CONT cultures on the left and the DNC cultures on the right. The DNC cell size distribution was much narrower, while the CONT distribution was broadened. The maxima for the DNC cultures centred around 2.0 to 2.4 µm, while the CONT cultures showed higher deviations. The S.192 CONT cultures had their maxima between 3.0 and 3.2µm, S.6803 at 2.2 to 2.4µm the same as the DNC as well as the IFA culture with the maxima at 2.0 to 2.2µm. In all CONT cultures cell sizes above the 2.4µm were overrepresented and in the DNC, there were barely any cells larger than 2.8µm. On the contrary in all CONT cultures there have been cell sizes measured as large as 3.8µm, which was almost double the size of the average 2.0µm at standard conditions. In the IFA and S.6803 cultures the cell size distribution was much broader, but still with most cells in the range of the standard cell size. The S.192 CONT culture displayed a completely shifted cell size distribution rather than a broadening.

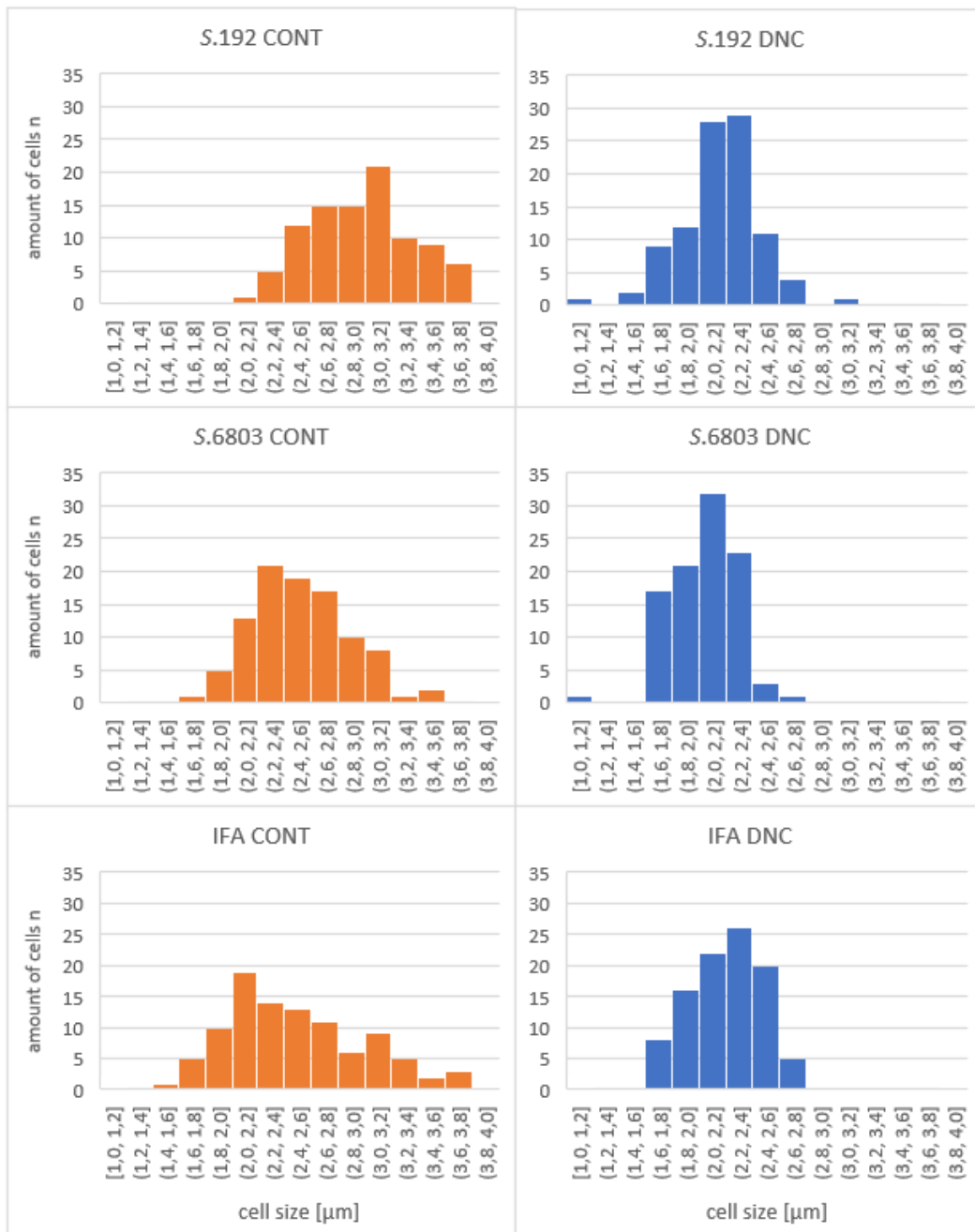


Figure 43: Cell Size distribution of the three strains S.192, S.6803 and IFA at 6000lux and two different cultivation conditions, CONT and DNC.

8.5 Continuous illumination at 10000lux with 3 different *Synechocystis* strains (Exp.4)

In experiment 4 the light intensity was further increased by adding additional LEDs to the previous set-up resulting in about 10000lux (Table 4). In the DNC set-up 10800lux were measured and in the CONT set-up 10180lux. The temperature and light intensity were monitored with a data logger and the average was calculated, see table 10. The measured light intensity of the data logger differed from the Voltcraft measurement due to the difference in the measurement distance.

Table 10: Cultivation conditions in experiment 4 monitored with a HOBO data logger.

Condition	Temperature [°C]	HOBO data logger Light intensity [lux]	Voltcraft Light intensity [lux]
DNC	23,75±1,00	5303±403	10800
CONT	24,87±0,22	5203±240	10180

In the CONT set-up the temperature was considerably higher compared with the previous experiments at lower light intensities, with almost 25°C. The temperature and light intensity were stable over the course of the experiment.

Unfortunately, another light failure in the DNC set-up between day 22 and 24 (Figure 44) occurred. The temperature and light intensity were, besides the failure, stable over the course of the experiment. The average temperature was about 1°C lower compared to the CONT set-up but fluctuated according to the day-night-cycle. The temperature dropped to approximately 22.3°C during darkness and increased to almost 25°C during light. The light intensity dropped continuously over the whole course of the experiment, maybe because of wearing off effects of the continuously turned-on LEDs.

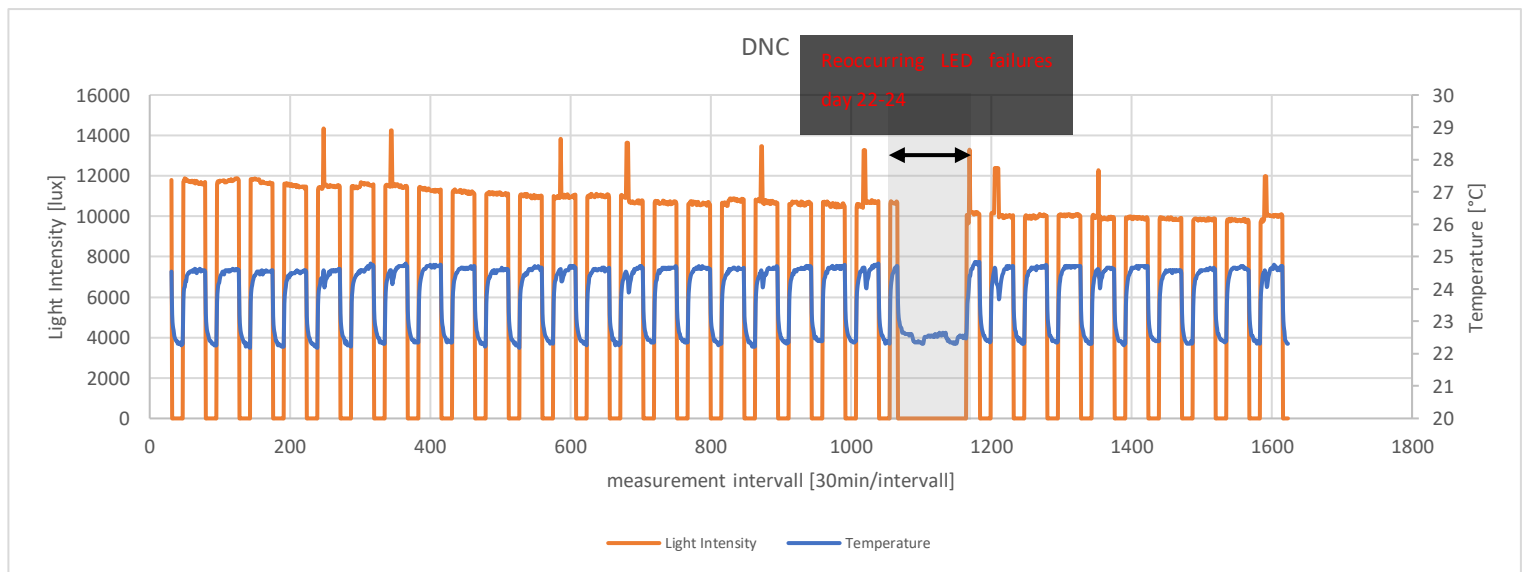


Figure 44: Temperature and light intensity measured with the HOBO data logger in the DNC 10000lux set-up.

The colour of the cultures was monitored, and photos were taken each sampling (Figure 45). In the DNC cultures the darkest green colouration was reached in all strains on day 14. This was much sooner compared to the previous experiments. After day 14 the DNC cultures started to become olive to brownish in colour. The strain S.192 started to become yellow on day 33. In the CONT cultures of the strain S.192 and S.6803 the maxima in green colour was reached even earlier on day 7. Only the strain IFA displayed it's darkest colouration also on day 14, the same as the DNC culture. After their maxima of green colouration, the CONT cultures decoloured rapidly. The cultures reached a state of colouration that was assumed to indicate a concerning state of culture vitality, for example

in Figure 45 strain S.6803 CONT on day 33. For this reason, it was decided to prematurely abort the experiment before reaching day 40.

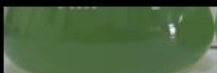
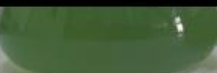






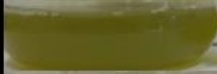


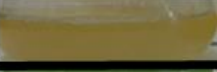
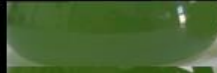
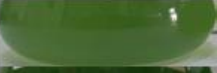








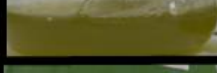
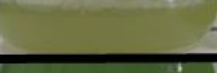










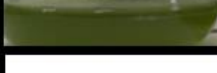
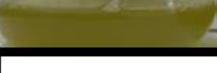
	DNC		CONT		Day
192					0
					7
					14
					21
					25
					33
6803					0
					7
					14
					21
					25
					33
IFA					0
					7
					14
					21
					25
					33
	K1	K2	K1	K2	Day

Figure 45: Visual appearance of S.192, S.6803 and IFA at 10000lux.

Microscopic images were taken to monitor the culture state on cell level and control for any contaminations. On day 33, when the experiment was aborted, the accompanying flora of the cultures already had taken over and heterotrophic bacteria were dominating the culture in cell number. Cell components were related to the cell dry weight to compare the different strains and conditions, but

because of the massive growth of the heterotrophic bacteria the CDW on day 33 was biased. Microscopic images revealed, that on day 25 the fraction of heterotrophic bacteria was still minor compared to the cyanobacteria. Therefore day 25 was taken for comparison to prevent any influence of the heterotrophic cell dry mass on the final values. In the following Figure 46, the microscopic images of the three strains at the two conditions are shown for day 33 and day 25. The bright white cells were cyanobacteria at a magnification factor of 40x using a phase contrast. The smaller dark cells were heterotrophic bacteria. On the right side in the images of day 33, the overrepresentation of the heterotrophic bacteria can be seen compared to the images of day 25 where only a few heterotrophs can be seen.

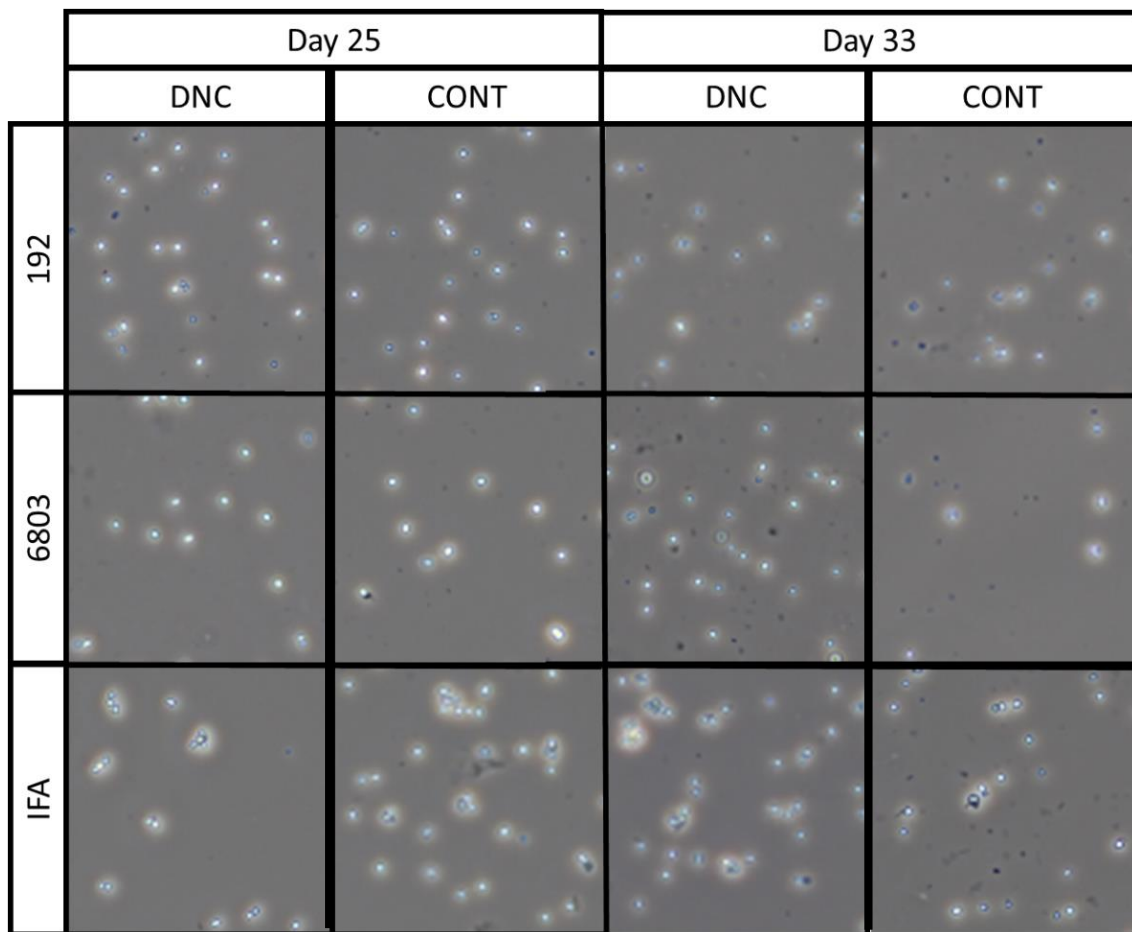


Figure 46: Microscopic images at 40x magnification and contrast filter on day 25 and day 33 for all three strains used at DNC and CONT conditions

In the Figure 47, representing the summary of all the analytical data compiled for the three strains at the two differing conditions, it can also be seen that after day 25 most values were dropping indicating instable cultures. The OD_{435nm} values of the DNC and CONT cultures increased at first linearly, but the graph started to flatten on day 18 for the DNC cultures and on day 14 for the CONT cultures. The cultures reached their maxima OD_{435nm} on day 25. The only exception was the DNC IFA culture which reached the maxima on day 21. The OD_{435nm} was significantly lower in the CONT cultures of the strains S.192 and S.6803, but in the IFA strain it was reversed.



Figure 47: Analytical data representing the physiological state of the cultures cultivated at DNC and CONT at 10000lux.

The OD_{750nm} displayed the same graph form, but the values were much lower. Also, in the OD_{750nm} the DNC cultures displayed the higher values.

With an overall OD_{450nm} maxima of about 4, the cultures at 10000lux conditions only archived half of the OD compared to the 6000lux experiment and only about a third of the OD compared to the 3000lux experiment.

About 0.65g/L CDW was reached in all cultures, only the IFA CONT culture reached higher values and the IFA DNC culture less. The CDW grew slowly until day 18 and stayed at about the same level until the end of the experiment, except the IFA cultures increased further until day 25. None of the cultures reached a CDW as in the experiments before of above 1g/L. At 3000lux and 6000lux the cultures never reached a plateau in the CDW graph, as seen at 10000lux, but grew continuously at a constant rate until the end of the experiment.

The pH values also behaved differently in the 10000lux experiment compared to the previous experiments. The pH started at 11 and dropped to pH 10 on day 12. On day 14 a spike in the pH was visible, but this could have been a measurement or calibration error, because afterwards the pH further decreased to a pH between 8 and 9 on day 21-25. The pH stayed this low until the end of the experiment. In all three strains the pH of the CONT culture was higher at first, but from day 14 to 18 the pH of the CONT culture dropped beneath the pH of the DNC culture. This was also about the time when the OD_{435nm} of the CONT cultures enter the plateau. The pH showed very precisely when the cultures stopped taking up CO₂ from the media due to the suspension of photosynthesis.

This was also seen in the chlorophyll content. The chlorophyll content of the DNC cultures increased until day 12 and the strains S.6803 and IFA almost reached 1% CDW chlorophyll. After day 12 the chlorophyll content slowly decreased to around 0.5% on day 33. The S.6803 and IFA CONT cultures displayed the same trend but at about half the chlorophyll content of the DNC cultures. Only the chlorophyll in the S.192 strain behaved differently. The chlorophyll content increased in the S.192 DNC culture until day 12 up to 0.5%CDW but stayed at this level until day 33. In the S.192 CONT culture the chlorophyll content started at 0.5% and linearly decreased from there to 0.14%CDW on day 33.

The phycocyanin content increased until day 18 in all cultures from below 0.2% up to around 1.5% in the CONT and 2% in the DNC culture. In the S.192 and S.6803 cultures the phycocyanin content was higher in the CONT cultures, but in the IFA cultures it was the other way around. After day 18 the phycocyanin levels dropped to between 0.5 and 1%.

In the S.192 strain the glycogen content increased from 6.2% and 2.7% in the CONT and DNC culture respectively up to 26.5% and 28%CDW glycogen on day 18. The glycogen content of the DNC culture was above those of the CONT culture the whole time but decreased in both cultures from day 18 onwards below 20%. In the other two strains the trend was the same, except they reached higher values and their maxima were on day 25. S.6803 reached 47.7% and 10.2% while IFA reached 34.6% and 33% for the DNC and CONT cultures respectively.

The PHB values in the S.192 cultures were again the highest and the CONT culture had throughout the experiment significantly higher values. The same trend was observed in the IFA cultures, but the values were below the S.192 culture. The S.192 CONT and DNC cultures reached a final PHB content of 8.89% and 4.33% respectively, while the IFA cultures reached 4.04% and 1.36%. The S.6803 cultures displayed a different behaviour. The PHB content of the S.6803 CONT culture slowly increased up to 0.59% on day 18 and afterwards decreased until day 33. The PHB content of the DNC cultures slowly increased until day 33 and reached a final PHB content of 2.49%CDW PHB. All of these values were much lower compared to the previous experiments conducted at lower light intensities.

When comparing the values, it is important to keep in mind, that the values considered the CDW. The CDW on day 33 was biased by the fraction of heterotrophic bacteria. Therefore, only until day 25 the values can be assumed to be comparable without any systematic error.

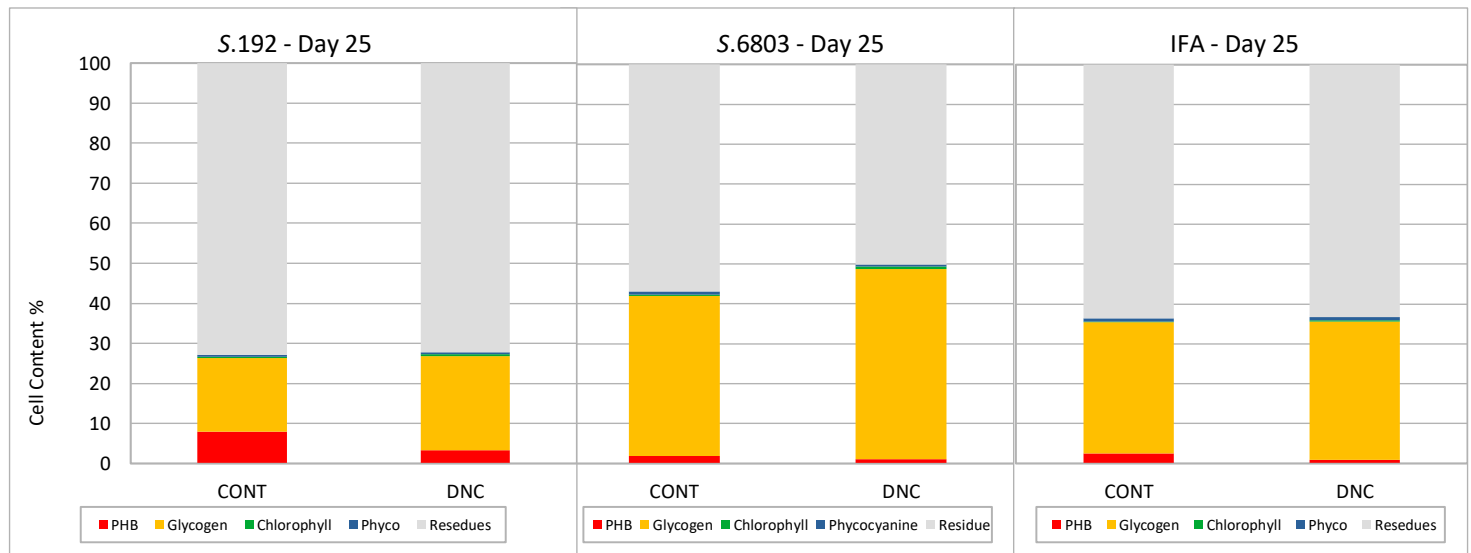


Figure 48: Cell content of S.192, S.6803 and IFA in %CDW on day 25 for the two cultivation conditions DNC and CONT at 10000lux.

In the Figure 48 the overall cell content of the measured cell components is represented. The CDW of the DNC cultures had the highest fraction of analytes, but least of it was PHB in contrast to the CONT cultures. The strain S.6803 showed the highest analyte content in percentages with glycogen representing the biggest fraction. The strain S.192 displayed the lowest values, but the highest fraction of PHB. The analyte content more than halved compared to the previous experiment in all strains from about 65% to below 30% in the CONT and from 55% down to below 30% in the DNC cultures. In the other cultures the overall content also decreased, but not as massively as in the S.192 cultures. For the S.6803 DNC culture the overall content of the analytes stayed about the same.

On day 33 Nile-red stained cultures were examined with a confocal scanning microscope and images were taken and analysed (Figure 49, 50 and 51). In the following Figure 49 the images of the DNC and CONT culture of all three strains are shown. Compared to the previous experiments the difference in cell size was not as obvious anymore. The fluorescent signal was only very weak, because

of the low PHB content. This caused difficulties in finding the right settings for contrast rich and well-focused images.

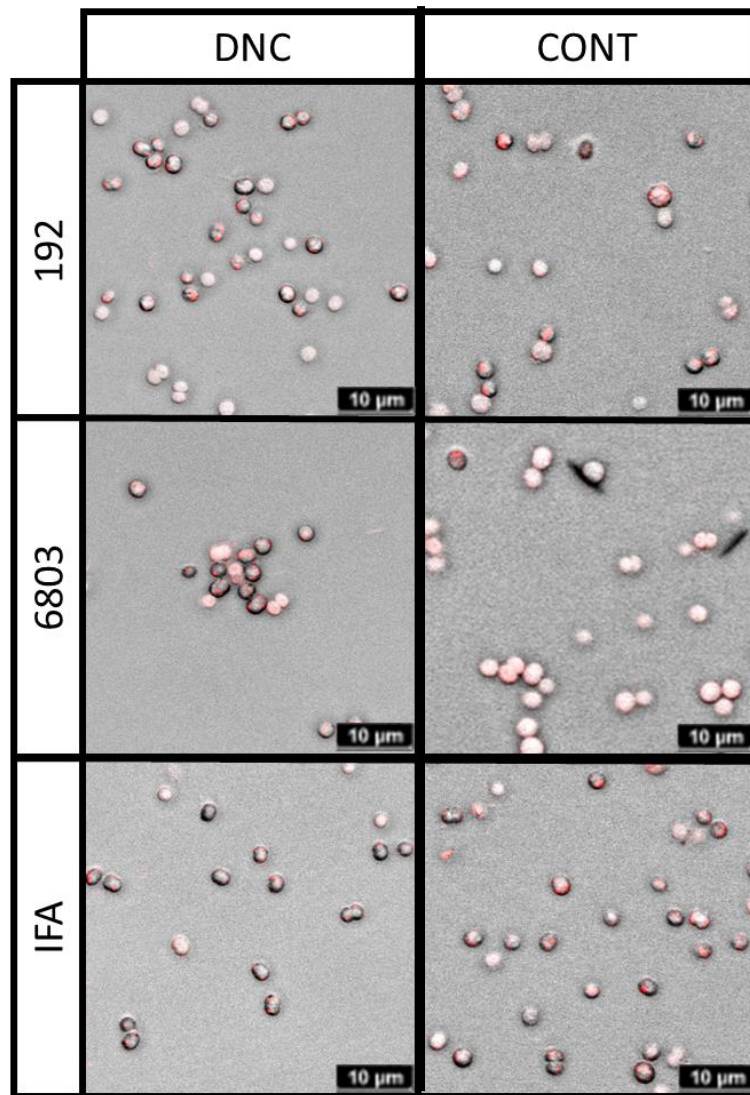


Figure 49: Microscopic images of the S.192, S.6803 and IFA cells at a10000lux stained with Nile-red and taken with a confocal scanning microscope.

Not only the visual difference in cell size decreased in the 10000lux experiment, but also the measured cell size (Figure 50). Before, the strain S.192 displayed the biggest difference in cell size between the CONT and DNC cultures, but at this light intensity the cell size of the DNC culture increased slightly compared to the 6000lux experiment from 2.1 to 2.3µm, but greatly compared to the 3000lux experiments. The cell size of the CONT cultivated cells on the other hand decreased from 3µm (6000lux) to 2.7µm (10000lux). In the S.6803 strain the cell size of both the DNC and the CONT culture increased massively up to 2.7 and 3.0 respectively, compared to the previous experiments. At these conditions the S.6803 CONT cultures for the first time displayed the largest measured cell size of 3µm. The cell size of the CONT IFA strain stayed the same, but also here the DNC culture cells displayed an increased cell size compared to cultivation at lower light intensities. The cell size

at both conditions was enlarged compared to the cell size of $2.1\mu\text{m}$ measured in the temperature experiment and an increase in cell size could be measured in some cultures even though the PHB content in this experiment was found to be the lowest of all the illumination experiments. Similarly, the overall content of the analytes decreased compared to the previous experiments.

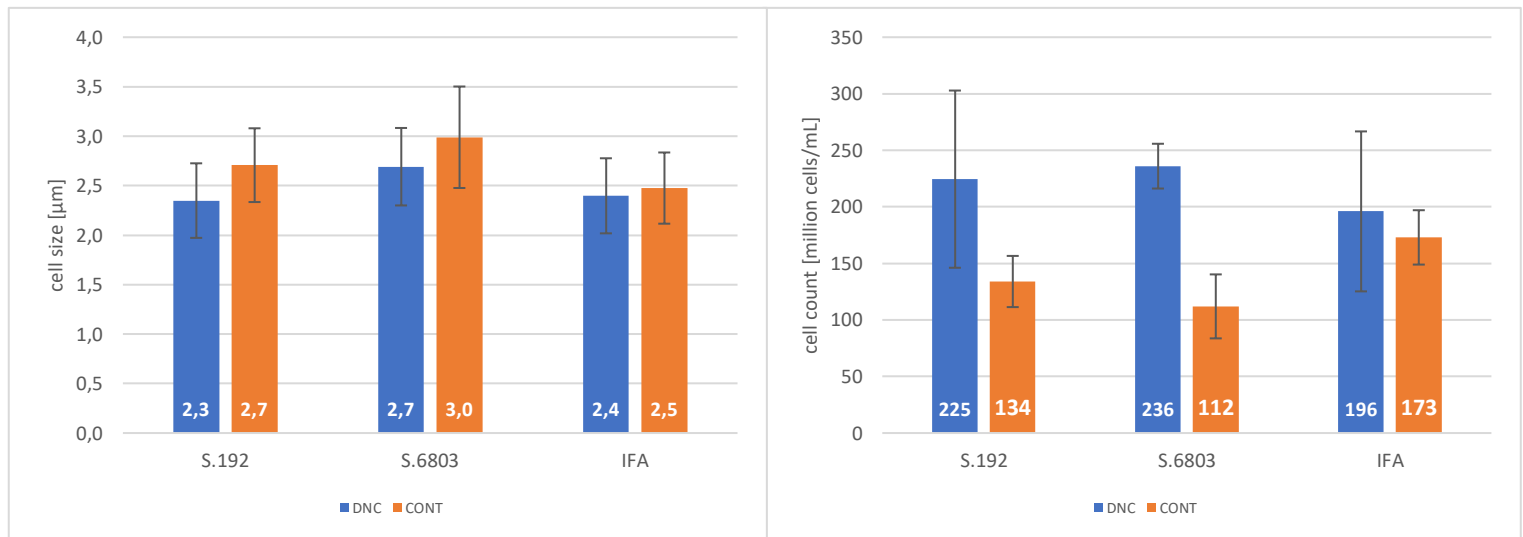


Figure 50: Cell count and cell size at 10000lux for S.192, S.6803 and IFA. On the left the cell size at DNC and CONT conditions. On the right the corresponding cell count in million cells per mL.

The cell density decreased at both conditions compared to the 6000lux experiment. This was more pronounced in the CONT cultures. In the S.192 strain the cell count decreased from 459 million cells/mL down to 134 million cells, a decrease of 70%. In the DNC culture it was only a decrease of 40%. The same trend was also seen in the other two strains. The difference in cell count between the CONT and DNC cultures became greater, except for the IFA cultures where the difference became less. For the S.192 and S.6803 the cell count of the DNC cultures was approximately double of the cell count of the CONT cultures. The difference between the two conditions in cell count was even higher in the S.192 strain in the 3000lux experiment, where the cell count of the DNC cultures was three times and even 3.75 times as much. This discontinuity could have also been due to the light failures in the 6000lux experiment.

In the following Figure 51 the cell size distribution is depicted for all three strains at CONT and DNC conditions. On the left side the CONT cultures are represented as orange bars and on the right side the DNC cultures are represented as blue bars. The S.192 DNC and IFA DNC culture had a peak between 2.2 to $2.4\mu\text{m}$ and 2.0 and $2.2\mu\text{m}$ respectively. The S.6803 DNC cultures did not have a peak and displayed a rather uniformly cell size distribution. The CONT were also more uniformly distributed compared to the DNC cultures, but again their distribution was slightly shifted to a bigger cell size. Compared to the 6000lux experiment the cell size distribution was also less pronounced between the two conditions, but this could have been caused by the prolonged light failure in the 6000lux DNC set-up leading to a bias. Still, when only comparing the distribution of

the CONT cultures the distribution in the 10000lux experiment was less shifted to a larger cell size and the distribution was more uniformly without any pronounced peaks.

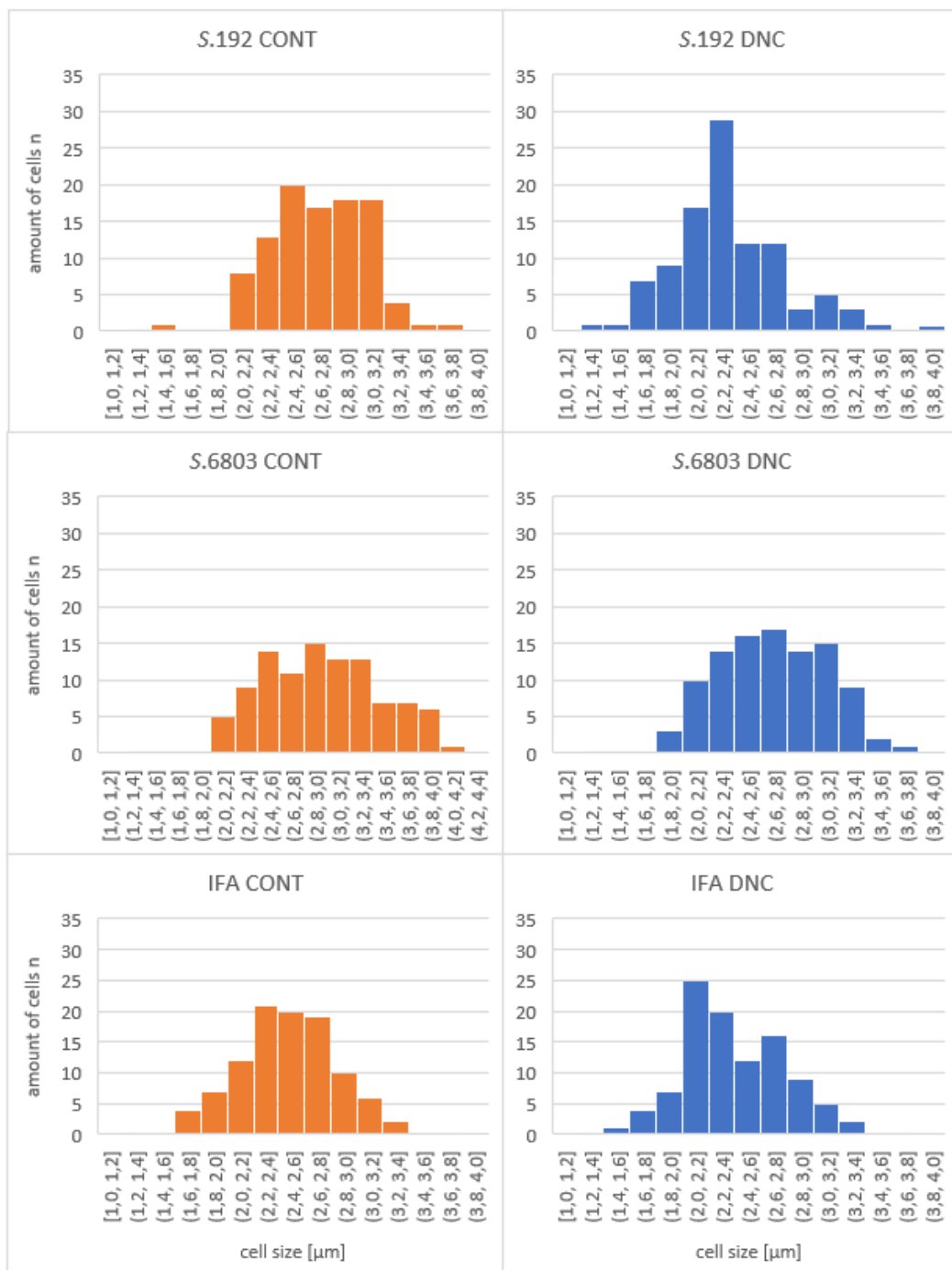


Figure 51: Cell Size distribution of the three strains S.192, S.6803 and IFA at 10000lux and two different cultivation conditions, CONT and DNC.

The nitrate levels were measured at day 25 and day 33 to monitor for nitrogen depletion. The measured nitrogen levels are depicted in the following Figure 52. On the left side for day 25 and on the right side for day 33. From the initial 332mg/L nitrate present in the media the S.6803 strain only used up about half until day 33. In the S.192 cultures still about 100mg/L was left on day 25

and this value barely changed until day 33. The CONT IFA culture displayed the lowest nitrate level with 37mg/L on day 33 and 92mg/L in the DNC culture. The nitrate levels in the IFA cultures only decreased a little from day 25 to day 33. The difference to the 3000lux experiment was enormous where only between 5 to 2.2mg/L nitrate were left in the media. The cultures at 10000lux were not exposed to nitrogen starvation and nevertheless showed signs of chlorosis and synthe-

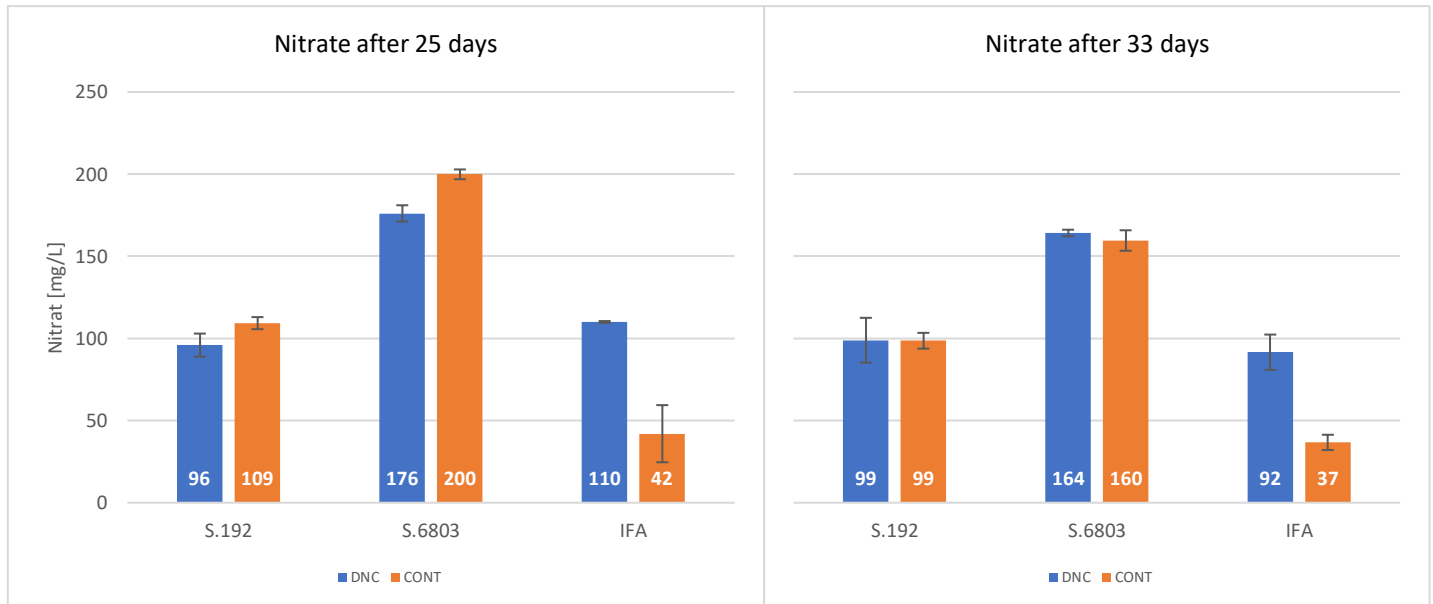


Figure 52: Remaining nitrate levels in the medium of experiment 4 measured on day 25 and 33 in the cultures of the strains S.192, S.6803 and IFA at two different illumination regimes.

sized notable amounts of PHB.

8.6 Comparison of three different *Synechocystis* strains at 3000, 6000 and 10000lux

The following sections are a comparison of the previous presented effects of the three different light intensities on the three different used *Synechocystis* strains.

Monitoring with the data logger showed fluctuations in the temperature due to the difference in energy input during light and dark phase. The measured light intensity also fluctuated, probably caused by the movement of the shaker, the logging device, and the light source. These fluctuations in temperature and light intensity were observed in all experiments posing a potential source for errors. Since this effect was observed in all the experiments the effects on the cultures were the same and the effects on the data for comparison was neglected. Providing a completely stable system for these experiments could have only been reached by undertaking enormous efforts, which would not have been in relation with the gain in data quality considering the errors caused by handling and measurement.

8.6.1 Effects of different light intensities on the strain S.192

In Figure 53 the collected analytical data of the strain S.192 at 3000lux (3k), 6000lux (6k) and 10000lux (10k) is represented. On the left side for the cultures cultivated at DNC conditions in blue. The colour darkness in the graphs increases with the light intensity from light blue representing 3k to dark blue representing 10k. The same applies to the data of the CONT cultures on the right side of the Figure, represented in orange colours.

The optical density at 435nm increased linearly at a higher rate in the S.192 DNC 3k culture compared to the 6k culture which had a lower growth rate in the beginning because of the light failures. The shape of the 3k and 6k graph was similar, but the shape of the 10k graph was completely different. There was a strong increase in the beginning matching the 3k graph, but from day 14 onwards the graph flattened and stayed below the 3k graph reaching a plateau before the values decreased. In the CONT cultures the effects could be seen unbiased, without any light failures. The 3k graph showed the same growth profile as the DNC culture but with lower OD_{435nm} values. The 6k culture graph matched the 3k graph until day 21, when the values started to be slightly below the 3k values. The 10k curve also matched the other graph but started to deviate from them on day 18. In the 10k culture the increase stopped completely and the graph reached a plateau before the OD_{435nm} started to decrease again.

The OD_{750nm} showed the same shape as the OD_{435nm} only at lower values. In the DNC 10k culture the OD_{750nm} increased until day 25 before decreasing again. The ratio between OD_{435nm} and OD_{750nm} in the DNC cultures continuously decreased at very low rates. The ratio of the 10k cultures was below 3k and 6k. The decrease in the ratio represented an increase in the OD at 750nm compared to the OD at 435nm. The 750nm represents the general growth of the culture since it is not influenced by colour and only measures the turbidity of particles or cells. At 435nm chlorophyll-a was measured and therefore the decrease in the ratio could have been due to a decrease in chlorophyll per cell or an increase in heterotrophic cells. The microscopic assessment of the bacteria cultures only revealed an increase in heterotrophic cells in the 10k cultures at the end of the experiment, therefore this was ruled out as reason for the decline in the 435nm/750nm ratio. In the CONT cultures the ratio dropped at all light intensities from the beginning until day 5 and from there on stayed at about 1.5 in the 10k culture and further decreased in the 3k and 6k cultures to about 1.25.

The CDW showed the same plateau in the 10k cultures at DNC and CONT conditions starting on day 18 at about 0.75g/L and 0.68g/L respectively, while the 3k and 6k cultures were increasing linearly and reached almost 1.5g/L for the DNC and 1.65g/L for the CONT cultures.

Even though the other parameters decreased sooner in the 10k experiment, compared to the 3k and 6k, the PHB was continuously increasing until the end of the experiment. In the DNC culture the highest end value was reached with 4.3%CDW. In the CONT culture the PHB values at 10k were the highest in the beginning, but the 3k culture reached the same values later and had the overall highest value on day 40. The PHB development of the 6k culture stood out, because the PHB level

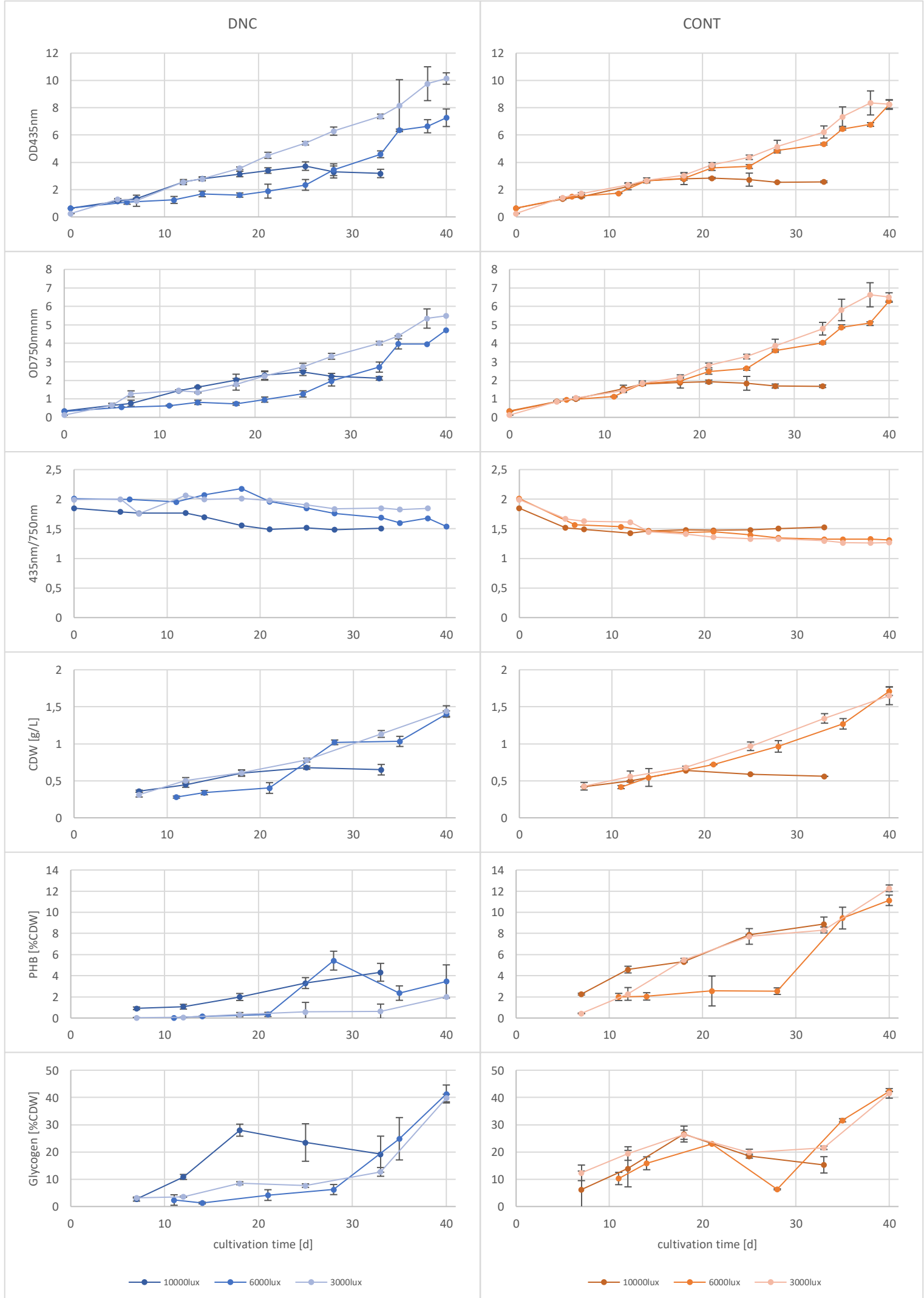


Figure 53: Collected analytical data of the strain S.192 at 3000lux, 6000lux and 10000lux.

stayed at around 2%CDW over a long period and then showed a very strong increase on day 28 until 40. It almost reached the same PHB amount above 12%CDW as the 3k culture on day 40. The development of the glycogen content differed strongly between the two conditions. The glycogen in the DNC cultures slowly increased at 3k and 6k, but the increase accelerated in the last quarter of the experiment until day 40 reaching about 40%CDW glycogen. The 10k culture differed strongly as it showed from the start a strong increase until day 18 reaching about 30%CDW glycogen and thereafter a decrease until day 33. The 10k DNC glycogen showed a strong increase until day 18 and a slow decline after. In the CONT cultures the trend in glycogen content did not deviate much between the three light intensities, but the 10k cultures had the lowest value on day 33, when the experiment was prematurely stopped.

All CONT cultures showed an initial increase in glycogen content until the end of the second quarter of the experiment. After the first peak at approximately 30%CDW glycogen around day 20, the glycogen levels decreased again. Between day 30 and 33 the glycogen content in the 6k and 3k cultures started to rapidly increase until day 40 to a final glycogen content above 40% which was a little higher compared to the DNC cultures. The 10k culture was stopped at day 33 and no rapid glycogen increase could be observed.

Concluding from all this data the CONT cultures at 3k and 6k have a higher turbidity indicated by a higher adsorption at 750nm, while in contrast the cell count revealed lower cell densities in the CONT cultures. The adsorption at 435nm was higher in the DNC cultures representing higher chlorophyll adsorption. The overall CDW of the CONT cultures was also higher except for the 10k culture. There were more similarities between the CONT and DNC cultures regarding the parameters representing culture growth. The CDW at both conditions and even at different light intensities was about the same. A big difference between DNC and CONT conditions was observed in the development of the glycogen content and in the PHB amount, that was significantly higher in the CONT cultures.

8.6.2 Effects of different light intensities on the strain S.6803

The S.6803 strain showed similar patterns in the collected analytical data as the S.192 strain (Figure 54). The 10k cultures had the same plateau in the DNC as well as the CONT cultures. The OD_{435nm} measurements were slightly higher, especially in the 6k DNC culture. The same applied to the OD_{750nm} and the OD_{435nm}/OD_{750nm} ratio. All cultures displayed the same behaviour as the S.192 cultures. The CDW in the S.6803 culture displayed the same behaviour as the S.192 cultures and also reached about the same final cell dry weight. Therefore, the two strains displayed no significant differences in their growth or in the reaction to increasing light intensities.

The glycogen and PHB content displayed significant differences. In the DNC cultures the highest PHB content was achieved by the 10k culture with 2.5%CDW. Also, the 10k culture of the S.192 strain contained the highest PHB amount, but the difference to 6k was minor. The S.192 cultures had much higher PHB values in all DNC and CONT cultures. The S.6803 strain reached the overall

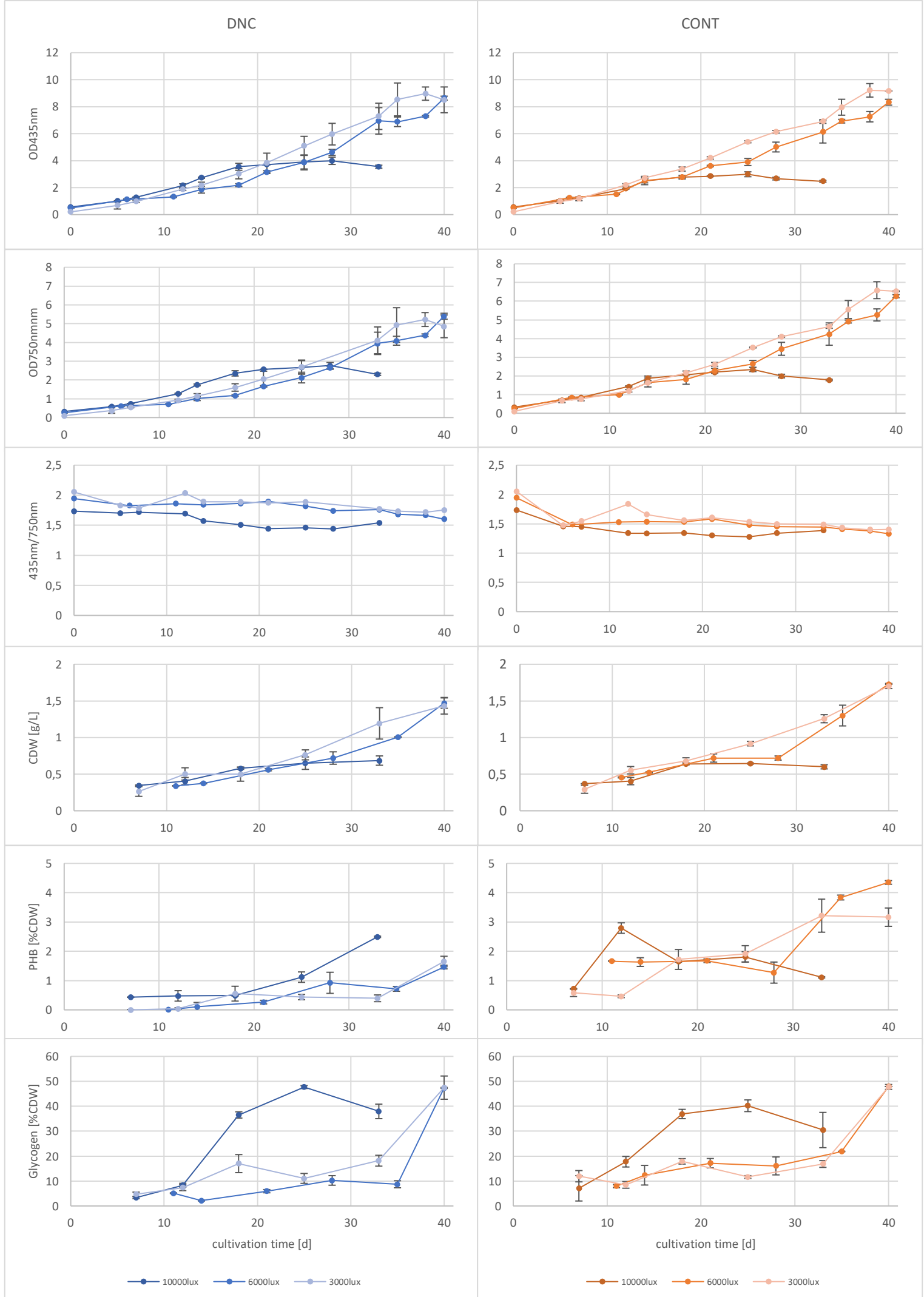


Figure 54: Collected analytical data of the strain S.6803 at 3000lux, 6000lux and 10000lux.

highest PHB content with 4.4%CDW PHB in the 6k culture at CONT conditions. Which was only a third of the 12.3%PHB produced by the S.192 3k CONT culture. In the S.6803 10k CONT culture the PHB content decreased from day 12. This was a big difference to the S.192 at same conditions displaying a continuous increase.

The Glycogen content also differed between the two strains. The S.6803 reached a higher glycogen content at all light intensities and both conditions. The 3k and 6k cultures reached almost 50% glycogen/CDW, which was almost 10% more compared to the S.192 strain. Also, the 10k cultures reached higher values. On day 25 at DNC conditions a maximum of 48% and 40% at CONT conditions was measured. The glycogen content decreased after the peak on day 25. The S.192 strain peaked on day 18 with a 20% lower glycogen content in the 10k DNC culture and 15% lower in the 10k CONT culture.

The S.6803 strain displayed an overall lower PHB content, but a higher glycogen accumulation potential compared to the S.192 strain at the same conditions and comparable growth patterns.

8.6.3 Effects of different light intensities on the strain IFA

Similar effects of increasing light intensity on the growth parameters as in the two previous presented strains S.192 and S.6803 are shown in Figure 55. The IFA cultures exposed to 10k illumination reached a plateau around day 18.

The OD_{435nm} values were slightly lower compared to the S.192 strains while the OD_{750nm} was slightly higher in the DNC cultures. In contrast, in the CONT cultures the values were about the same. The ratio of the OD_{435nm}/OD_{750nm} showed a comparable trend as in the S.192. The IFA DNC cultures started at a ratio of about 2 and decreased down to 1.5. So did the CONT cultures, but the decrease started at an earlier timepoint. The CDW of the IFA cultures also matched the CDW of the other cultures with about 1.5g/L in the 3k and 6k DNC and CONT cultures. The 6k cultures showed a slight slack between day 21 and 28 but continued to increase afterwards at a higher rate so on day 40 the same CDW was reached. The 10k cultures only reached 0.75g/L CDW on day 18 and 25 in the DNC and CONT culture respectively. All three strains displayed the same CDW at the same light intensity and illumination profile.

Even though there were no major differences found between the strains regarding their growth parameters, the PHB and glycogen content differed. The PHB content of the IFA strain was very low (below 2%CDW) at all light intensities in the DNC cultures compared with the other strains. In the CONT cultures on the other hand the PHB amount was much higher compared to the S.6803 strain. In both strains the 6k cultures reached the highest PHB content with 5.6% and 4.4% in the IFA and S.6803 culture respectively. This was still only half of the PHB amount accumulated in the S.192 CONT cultures. The IFA 10k CONT culture displayed no decrease in the PHB content as the S.6803 culture, but the same continuous increase as the S.192 strain.

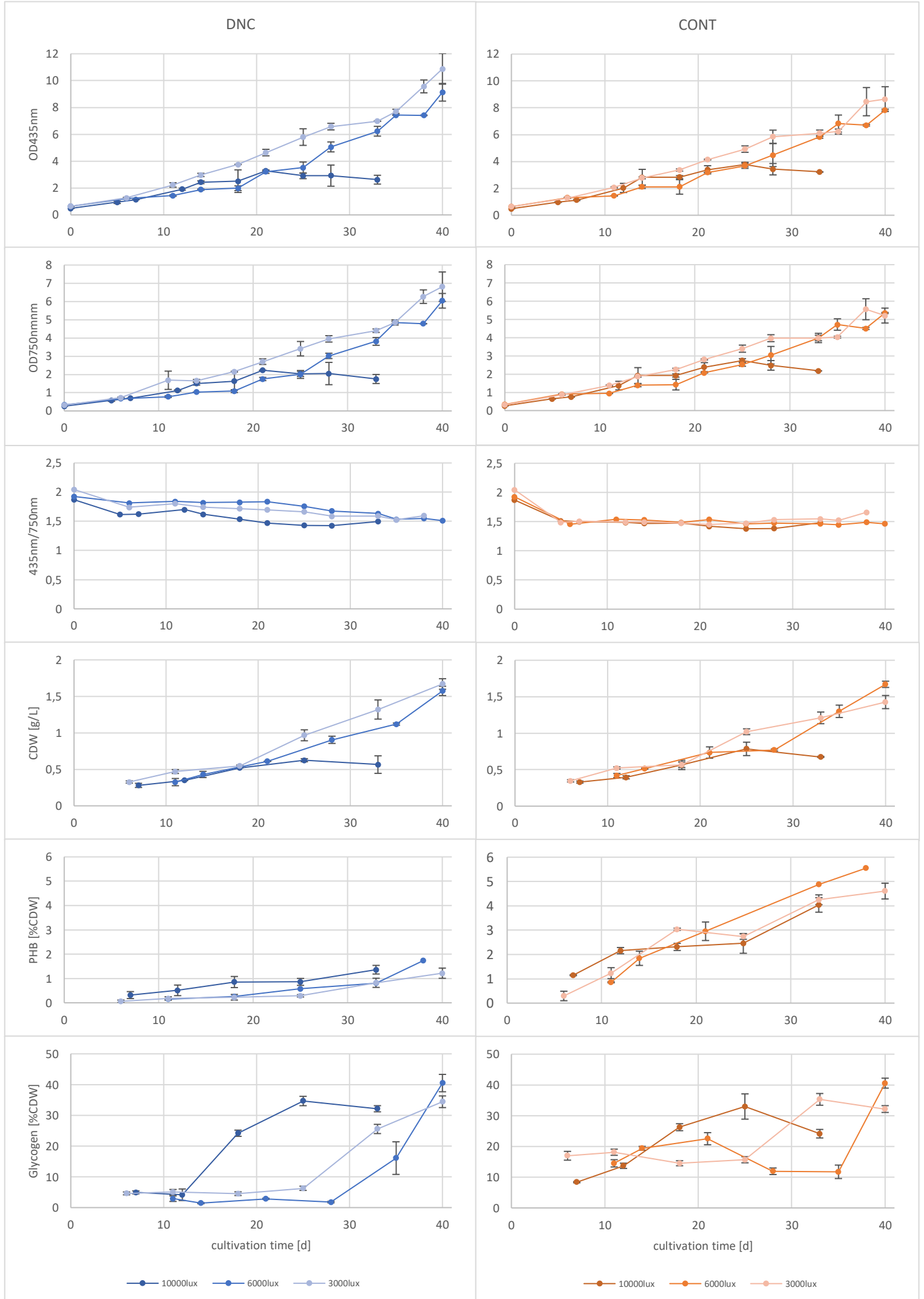


Figure 55: Collected analytical data of the strain IFA at 3000lux, 6000lux and 10000lux.

The form of the glycogen graph of the IFA cultures was similar to the S.6803 strain, but the glycogen content was comparable to the S.192 strain. At DNC and CONT condition the IFA cultures at 3k and 6k accumulated about 40%CDW. In the 10k cultures at DNC the IFA strain accumulated 35% and at CONT 32% glycogen. The graph shape matched the S.6803 cultures at 10k, but the values were lower. The glycogen content was above 30% which was still higher compared to the S.192 strain. Overall, the IFA strain performed better in the PHB production at CONT conditions than the S.6803 strain, but worst at DNC conditions. The glycogen content was higher compared to the S.192 strain, but lower compared to the S.6803 strain. All three strains differed in their PHB and content at the same conditions and light intensity, while the parameters for cell growth were more or less comparable.

8.6.4 Influence of different light intensities and illumination regimes on the cell size

The cell size of the three different strains is shown in Figure 56 at increasing light intensities. On the left side the DNC cultures and on the right side the CONT cultures. The cell size increased with the light intensity in the DNC cultures. The same trend was seen in all three strains and most pronounced in the S.6803 strain with the smallest cell size of 1.8 μ m at 3k and the largest cell size with 2.7 μ m at 10k. This was comparable to the enlarged cells of the CONT cultures with cell sizes between 2.5 μ m and 3.0 μ m. In the strain S.192 the DNC cultures increased their cell size by 0.2 μ m with each increase of the light intensity. This trend was also visible in the IFA strain, but less pronounced. In the CONT cultures the increase in light intensity showed no concurrent trend in all strains. The S.192 cells at 3k and 10k displayed the same cell size and at 6k the largest average cell size of 3 μ m was measured. The S.6803 strain reached a size of 3 μ m in the 10k culture, while at 3k and 6k the average cell size was 2.5 μ m. The light intensity showed no significant influence on the average cell size of the IFA cells. The IFA 3k CONT culture displayed the smallest cell size of all CONT cultures with 2.4 μ m and this value only increased to 2.5 μ m in the 6k and 10k cultures. Overall, the cell size in the CONT cultures was significantly larger compared to the DNC cultures, but the difference in cell size decreased with the increase in light intensity. Therefore, the increase in cell size was not simply induced by continuous illumination, but by the total luminous energy per time. The CONT cultures were illuminated 6 hours longer than the DNC cultures and the luminous energy was increased by 25% at

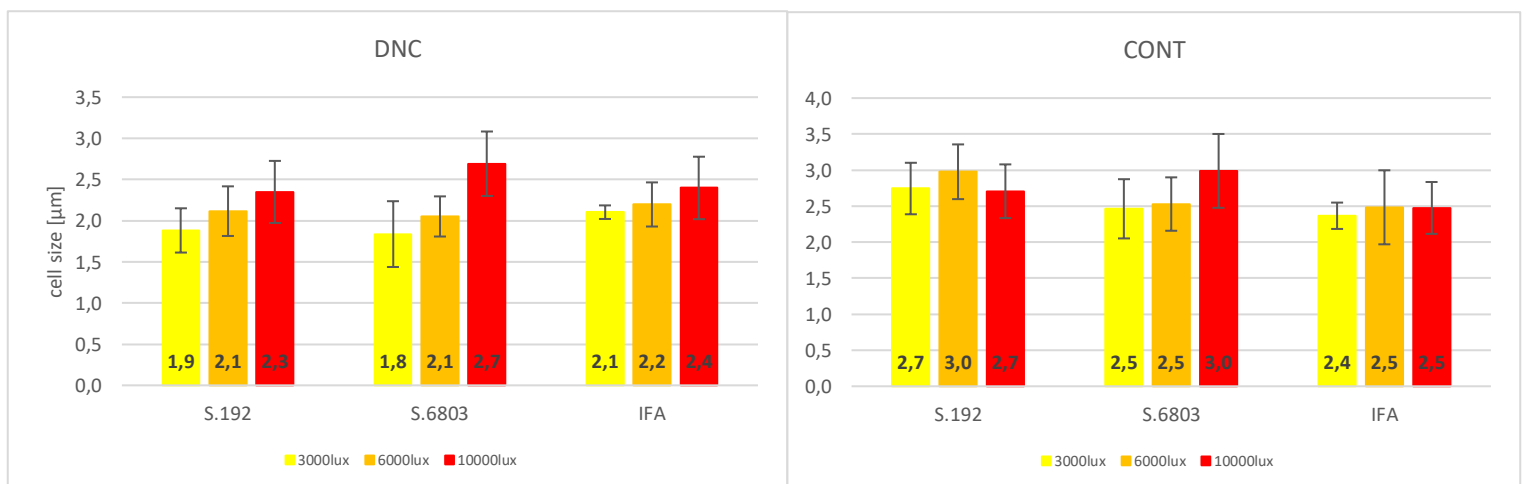


Figure 56: Measured cell size at three different light intensities for the two different illumination regimes, DNC and CONT.

the same time. The regeneration time in the dark phase could have supported the cells in maintaining their regular cell size. Even when the luminous energy was doubled in the DNC set-up to 6k, the cell size still didn't increase to the CONT culture cell size at 3k.

8.6.5 Influence of different light intensities and illumination regimes on cell density

The trend observed in the cell size reciprocally applied to the cell density (Figure 57). While the cell size increased with the light intensity in the DNC culture, the cell count decreased at the same time. This trend was most pronounced in the S.192 culture with a decrease from 592million cells/mL at 3k down to 225million cells/mL at 10k. This was a decrease by 62%. In the other strains the decrease was also observable, but not as drastic. The cell number of the S.192 DNC 3k culture was also especially high compared to S.6803 and IFA with cell counts of about 450million cells/mL. The cell density of the 6k and 10k cultures was for all strains in the same range.

In the CONT cultures the cell count increased with the illumination intensity from 3k to 6k, but strongly decreases from 6k to 10k by more than 50%. The cell number in the CONT cultures was always lower compared to their DNC counterpart. With 459million cells the CONT 6k IFA culture reached the highest cell density. The cell size and cell number in the CONT cultures didn't behave reciprocal as in the DNC cultures. The biggest cell size didn't necessarily result in the lowest cell density. In the CONT 6k S.192 culture the highest cell density and the biggest cell size was observed for this strain. The S.6803 strain at 10k had the overall lowest cell count of 112million cells/mL, but the largest cells of the strain at CONT conditions. In the IFA strain, the cell size of 6k and 10k was exactly the same, but the cell count of the 6k culture was 460million cells/mL. This was 2.65 times more compared to the 10k culture with only 173million cells/mL.

In the DNC cultures, the cell size increased with the light intensity and at the same time the cell number decreased. In the CONT culture such a trend was not observed, but the cell size of the CONT cultures was overall larger compared to the DNC cultures. The same applied to the cell densities, with the exception that the IFA CONT 6k culture had a higher cell count than the IFA DNC 6k culture.

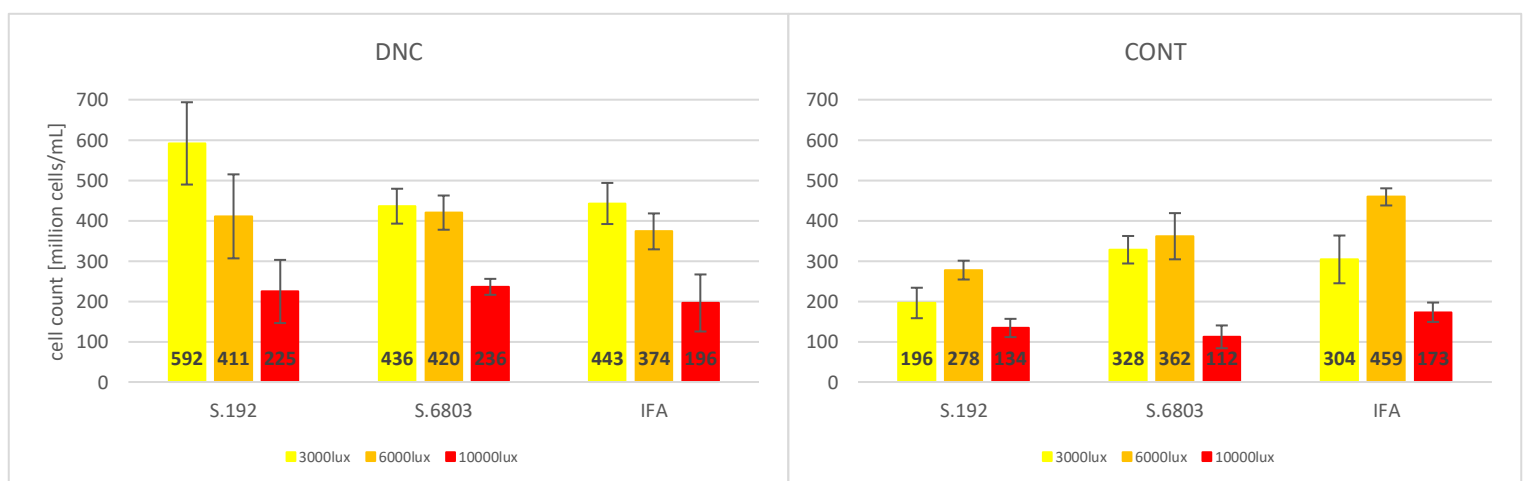


Figure 57: Numbers of cells counted at three different light intensities and for three different strains at CONT and DNC illumination regimes.

8.6.6 Remaining nitrate levels in the 3k and 10k cultures

Remaining nitrate in the culture broth is represented in Figure 58. The yellow bars represent the remaining nitrate in the 3k cultures, the red bars the 10k cultures and the grey bar the initial available nitrate in the media. In the 3k cultures only between 2.2mg/L and 4.4mg/L remained in the culture confirming the intended nitrate starvation in the cultures to boost PHB production. The nitrate levels in the DNC and CONT culture at 3k were in the same range and no trend was observed. In the 10k cultures the nitrate levels were still very high and, in the S.,6803 cultures less than 50% of the initial nitrate was consumed. Between the DNC and CONT cultures no difference was observed. In the S.192 culture the nitrate level was about 100mg/L in the DNC and CONT culture which was less than a third of the initial concentration. In the IFA cultures the DNC and CONT culture differed the most. The IFA 10k DNC culture still had 110mg/L left and the CONT culture with 42mg/L less than half of that.

The 3k cultures, independent of the strain and illumination regime, were exposed to nitrate limitation at the end of the cultivation, but the 10k cultures still had high concentrations of nitrate left in the culture even though they appeared chlorotic sooner (compare Figures 45, 31 and 25). The PHB accumulation in all strains and both conditions started at the beginning of the experiment and continuously increased until the end. The PHB accumulation was therefore not initiated by nitrate starvation. Chlorosis appeared not to be solely initiated by nitrate starvation as in the 3k cultures, but also by other unfavourable conditions as in the 10k cultures onset with still high nitrate levels.

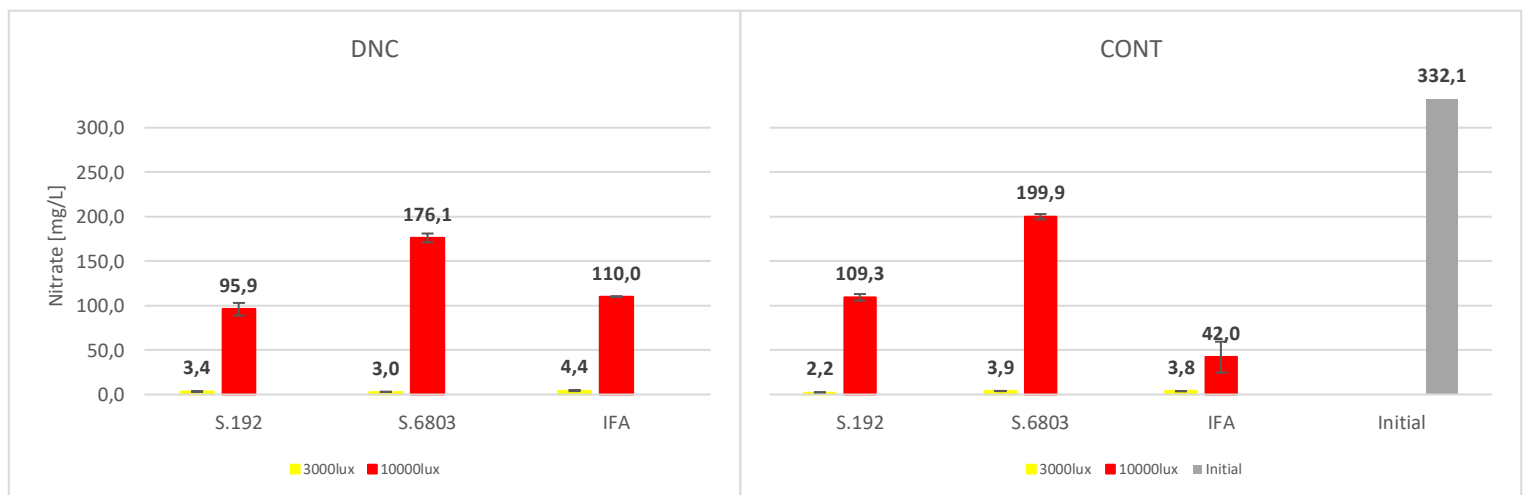


Figure 58: Remaining nitrate levels at 3k and 10k light intensity in three different strains for the two illumination regimes DNC and CONT.

8.7 Effects of illumination regimes on the cellular structures

In the following Figure 59 a single cell can be seen with indicated PHB granules. The inner and outer membrane were also visible as well as the membrane system of the thylakoids, lipid droplets and the nucleoid (compare to Figure 10). In the 3000lux illuminated S.192 cultures of experiment 1 and 2 the cultures were still green and showed no sign of chlorosis on day 40, when the sample was

taken. This coincides with the intact and high density of thylakoids. The cell didn't show any signs of disturbance or damage on day 40 at these conditions.

The TEM images of the DNC and CONT culture of the strain S.192 demonstrated again the big

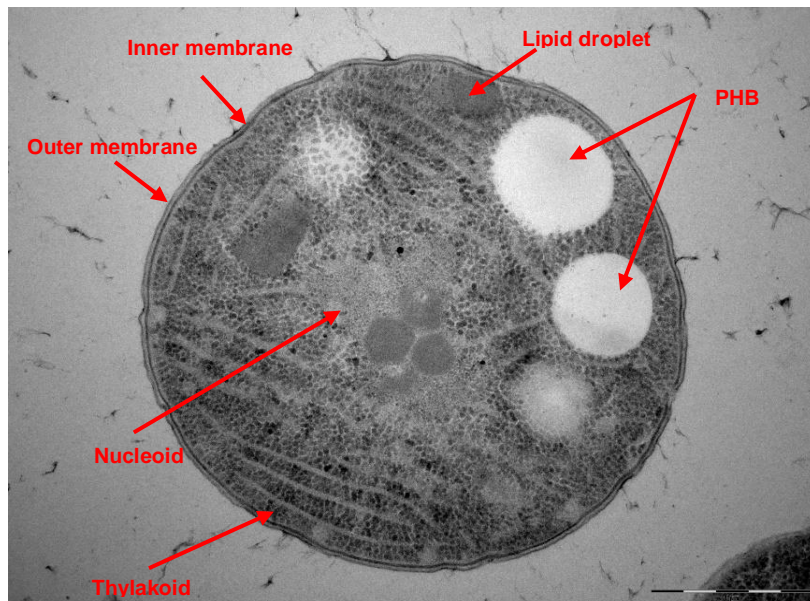


Figure 59: TEM image of a single cell of the strain S.192 cultivated at 3000lux and CONT illumination (image taken by Kateřina Mrázová).

difference in cell size between the two different illumination regimes (Figure 60). Additionally, the PHB granules were much bigger and there was a higher number of granules. Up to 7 PHB granules were counted in Figure 61 in the CONT culture cells. The cells of the CONT culture also displayed no disruption or change in their cell organelles, other than the PHB granules, compared to the DNC culture. Their thylakoids were intact, and no change was visible due to the incipient chlorosis.

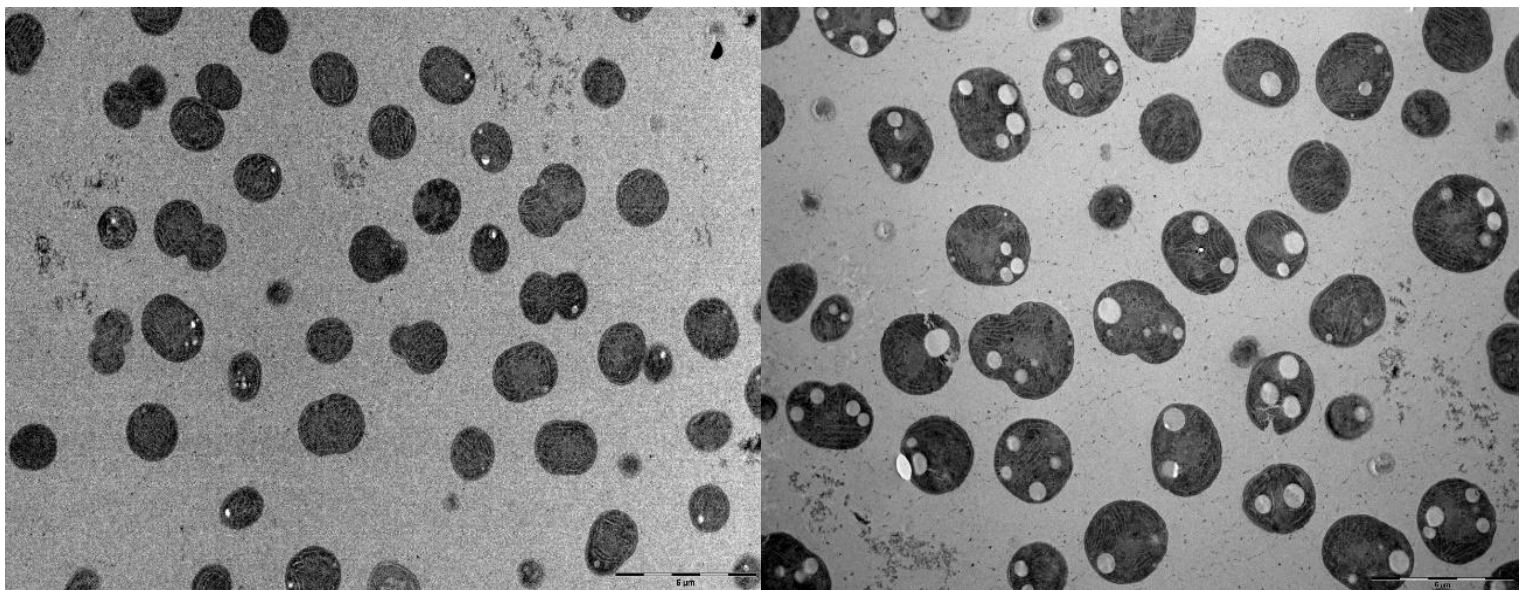


Figure 60: TEM image taken of the strain S.192 cultivated at 3000lux. On the left illuminated with DNC and on the right CONT (image taken by Kateřina Mrázová).

In the following Figure 61 several dividing cells can be seen and all of them showed an even distribution of the PHB granules to the new daughter cells.

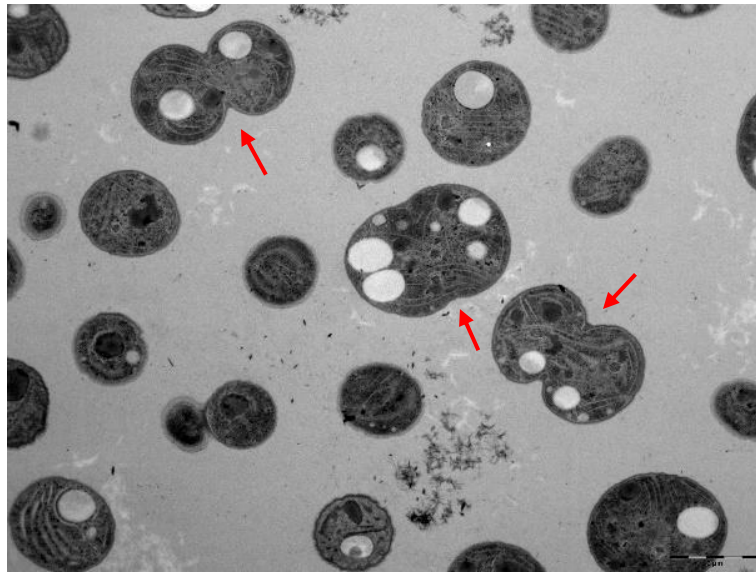


Figure 61: TEM image of several dividing cells indicated with a red arrow of a S.192 culture at 3000lux and CONT illumination (image taken by Kateřina Mrázová).

The CONT illumination of the strains S.6803 and IFA showed the same enlarged cells as the S.192 strain in the TEM imaging, but a significant lower number of PHB granules (Figure 62). The PHB granules were also larger in size compared to the DNC cultures (not shown).

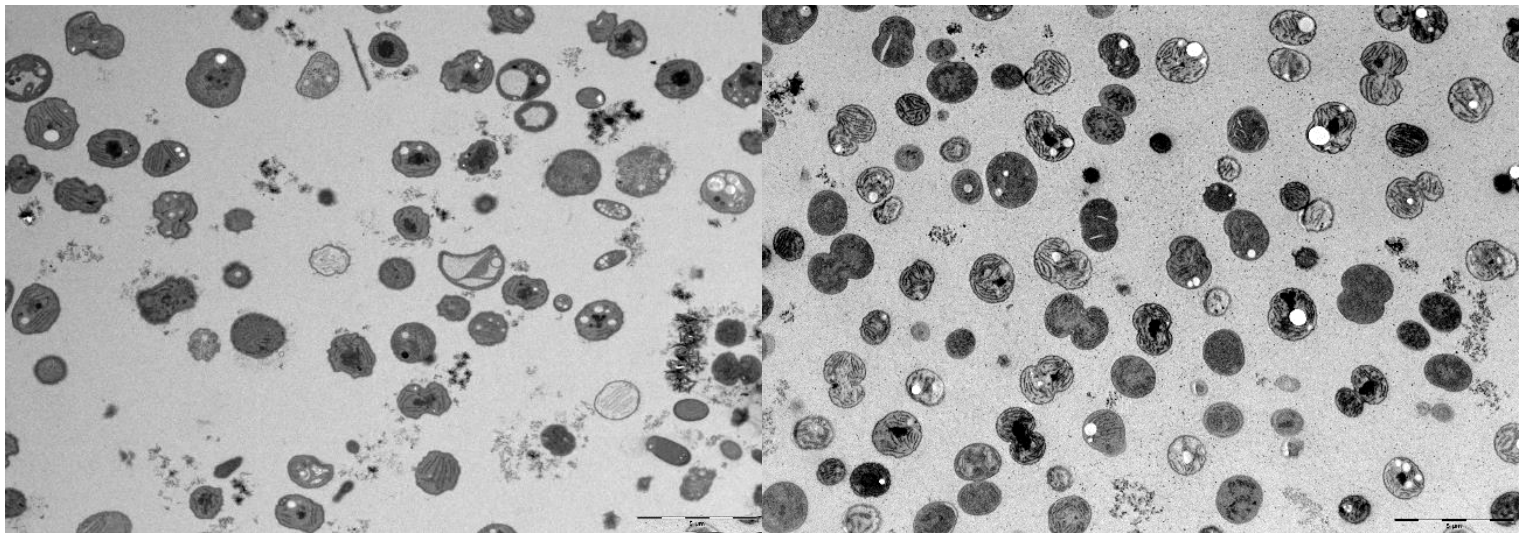


Figure 62: TEM images of two different strains cultivated at 3000lux at CONT conditions. On the left side the strain S.6803 and on the right-side IFA (image taken by Kateřina Mrázová).

8.8 PHB extraction and the influence of the cultivation regime on the quality

A novel approach for PHB extraction using EDGE was tested successfully (Figure 63). The method showed good extraction results and cut back the time expense from the previous method using a Soxhlet. Per sample the EDGE extraction only needed 15 minutes and the handling was much easier, at the same time less chemical waste was produced. The only drawback was the sequential processing of one sample at a time, while in the Soxhlet several samples can get extracted simultaneously. The extracted PHB samples were used for analysis with H-NMR and GPC.

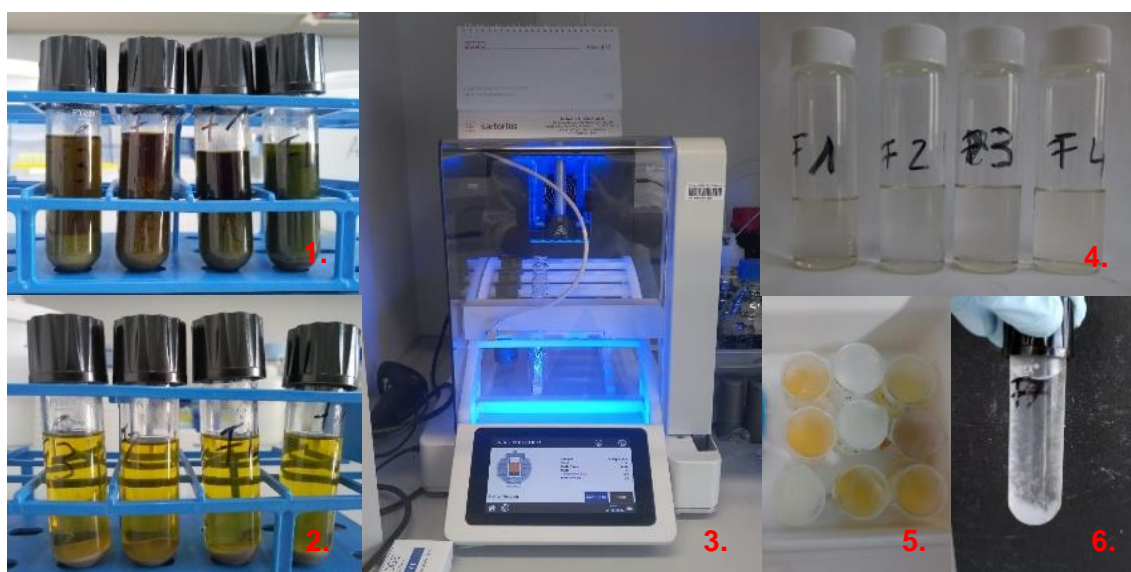


Figure 63: Photos of the PHB extraction procedure. 1.: Extraction of the dried cell pellet with ethanol. 2.: Extraction of the cell pellet with acetone. 3.: Extraction with chloroform with the EDGE. 4.: Extracts after the EDGE. 5. Precipitate in ethanol in the freezer. 6.: Precipitated PHB in ethanol.

8.8.1 H-NMR

With H-NMR analysis PHB was identified in the EDGE extract confirming the extraction as successful. The profile of the H-NMR spectrum fits to the molecular structure of PHB and the peaks were assigned to the corresponding hydrogen atoms (Figure 64). The spectra also matched the H-NMR spectra of PHB found in literature (Sindhu et al., 2011). The peak indicated with a star (*) corresponded to free hydroxy groups at the polymer tails or free water molecules in the sample.

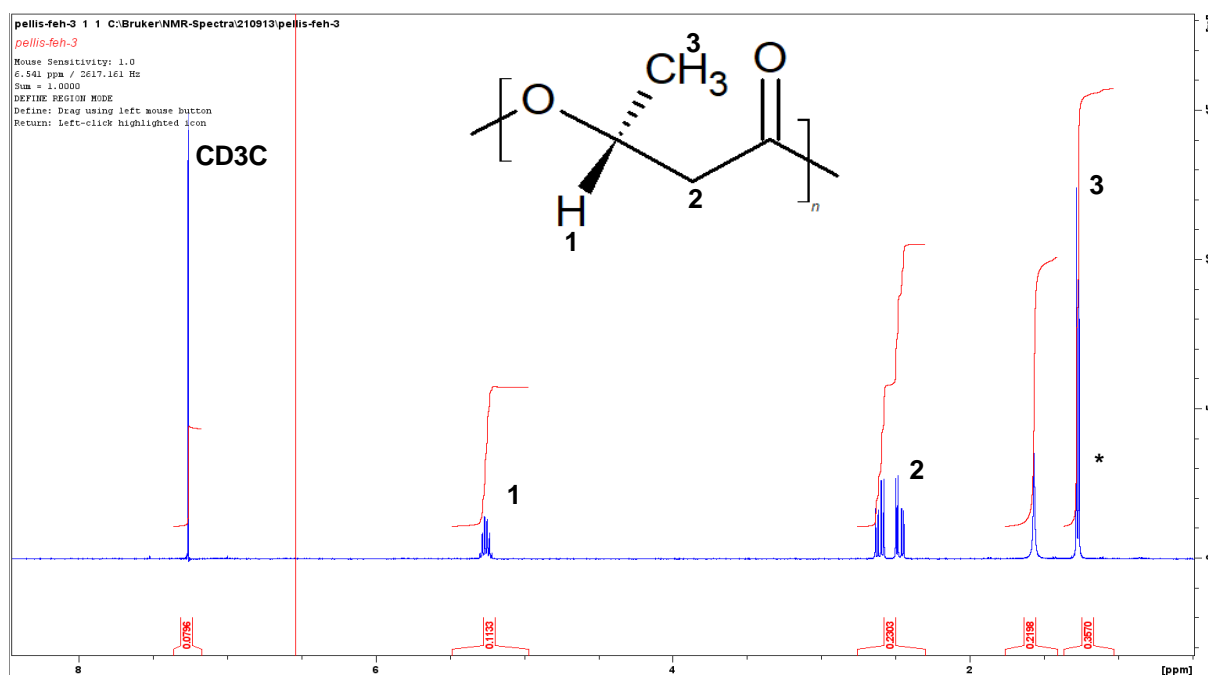


Figure 64: ¹H-NMR spectra of the PHB product extracted from S.192 cultivated at DNC.

8.8.2 PHB analysis with GPC

The used GPC set-up for the PHB analysis proved to be unsuccessful and delivered unreliable values. For this reason, the analysis was conducted by the project partner Michal Kalina at Bruno university of technology, faculty of chemistry. Only two samples could be analysed with the AF4-MALS method resulting in better results for the expected high Mw values. Unfortunately, the AF4 set-up did not work well, because of the used organic solvent leading to the blockage of valves and troubles with focussing. Therefore, the samples were analysed with the more robust SEC-MALS set-up. The compiled data was also not complete as many of the PHB samples did not reach the required concentrations for measurement, due to limited culture volumes. The data was still sufficient for the following comparisons.

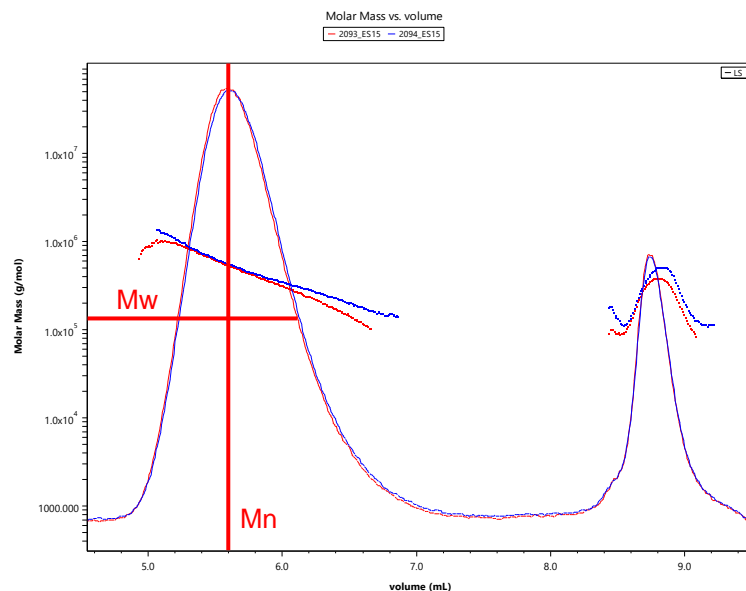


Figure 65: Mass weight distribution of PHB from the strain S.192 at 6000lux and DNC illumination regime analysed with SEC-MALS (provided by Michal Kalina).

The mass weight distribution can be seen as example for the PHB extracted from a S.192 culture at 6000lux cultivated at DNC (Figure 65). The Mw and Mn are indicated in red for the first peak representing the PHB fraction. All analysed samples had an additional second peak of yet unknown origin. The second peak indicated, that the chloroform PHB extracts did not only contain PHB, but probably also residual pigments, that could not be removed by the ethanol and acetone pre-treatment. The residual pigments varied among the extracts (Figure 66).



Figure 66: Different colours displayed by the extracts.

The pigments caused corruption of the result. Darker extracts resulted in bigger second peaks. The dark extracts reached Mw values above 1000kDa, and clear or slightly yellow appearing extracts resulted in Mw for the 2nd peak below 300kDa (Figure 67). This could have been caused by interactions of the sample with the column or by fluorescence interference shifting the measurement to much higher values.

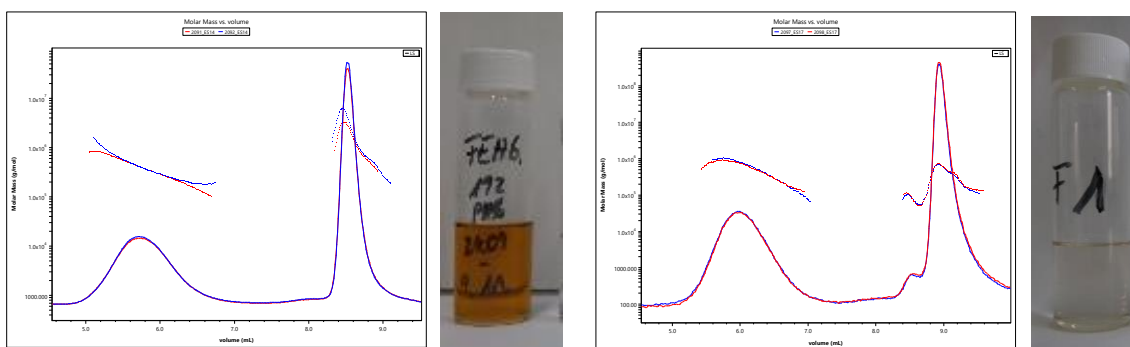


Figure 67: On the left the SEC-MALS result for the extract of the S.192 culture cultivated at 6000lux at DNC and next to it the image of the corresponding extract. The 1st peak has a Mw of 353,48kDa and the 2nd peak 1362,10kDa. On the right-side the SEC-MALS result of the S.192 culture cultivated at 3000lux at DNC and next to it the image of the corresponding extract. The 1st peak has a Mw of 457,65kDa 2nd peak 238,35kDa.

Two of the extracts were analysed with both methods with a significant mismatch in the results for the 1st peak. The AF4-MALS resulted in an Mw three times as high as the SEC-MALS results. From the limited data available the ratio between the two methods and the average was calculated. With the calculated factors the SEC-MALS results were corrected and compared to the uncorrected results in the Figures 68-70. This approach is very error prone and therefore the corrected SEC-MALS results have to be seen as a rough approximation of the real values.

Table 11: Comparison of the SEC-MALS and AF4-MALS results and calculation of the correction factors.

	Sample 1 of S.192 CONT 3000lux			Sample 2 of S.192 CONT 3000lux		
Method	Mn (kDa)	Mw (kDa)	Polydispersity (Mw/Mn)	Mn (kDa)	Mw (kDa)	Polydispersity (Mw/Mn)
SEC-MALS	317.8	415.55	1.3085	301.75	406.15	1.349
AF4-MALS	1213.75	1291.25	1.071	1208.7	1236.4	1.023
ratio	3.82	3.11	-	4.01	3.04	-
factor (ratio average):	3.91	3.076	-	-	-	-
% of AF4 method	26.18	32.18	-	24.96	32.85	-

From the available data the Mw and polydispersity index of the three strains S.192, S.6803 and IFA cultivated with DNC at 9500lux with a halogen-metal vapor lamp was compared (Figure 68). The Mw of the S.192 was lower compared to the other two strains, but the polydispersity was with 1.3 comparable to the IFA strain with 1.2. For all three strains the polydispersity of the corrected values was lower than the actual measured values.

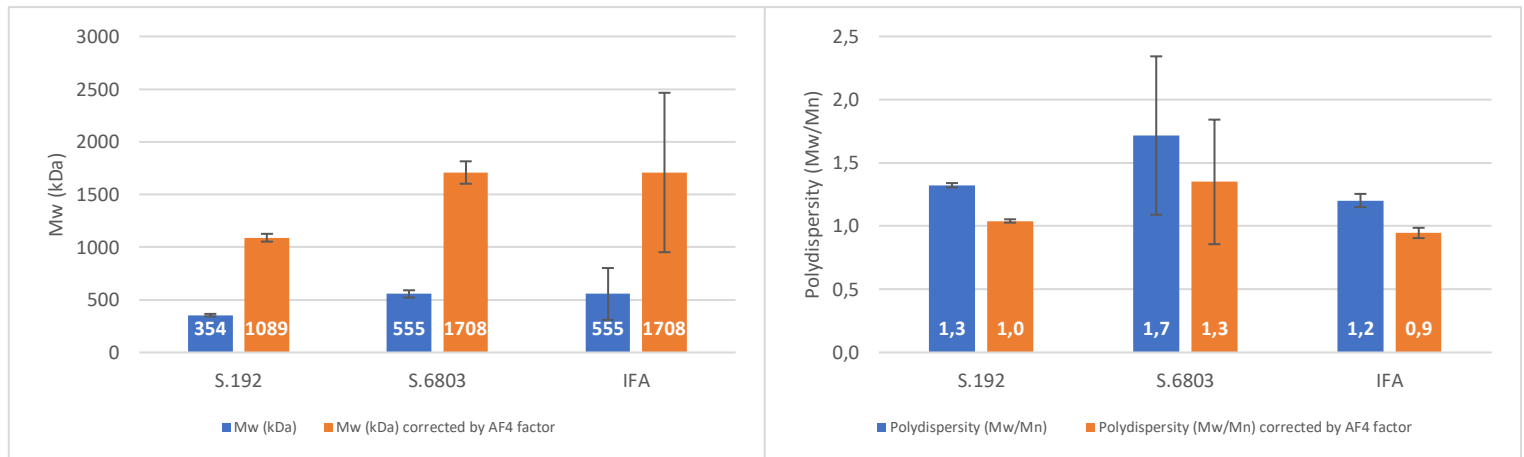


Figure 68: Comparison of the Mw of the three used strains cultivated at DNC with 9500lux of the halogen-metal vapor lamp on the left. The corresponding polydispersity is depicted on the right. The blue bars represent the measured values, and the orange bars represent the corrected values.

The comparison of the S.192 strain cultivated with DNC at 3000lux and 6000lux showed comparable Mw values, but a clear difference in the polydispersity (Figure 69). The polydispersity index for the PHB extracts of the culture at 6000lux was much lower. The corrected polydispersity values were again even lower than the original values.

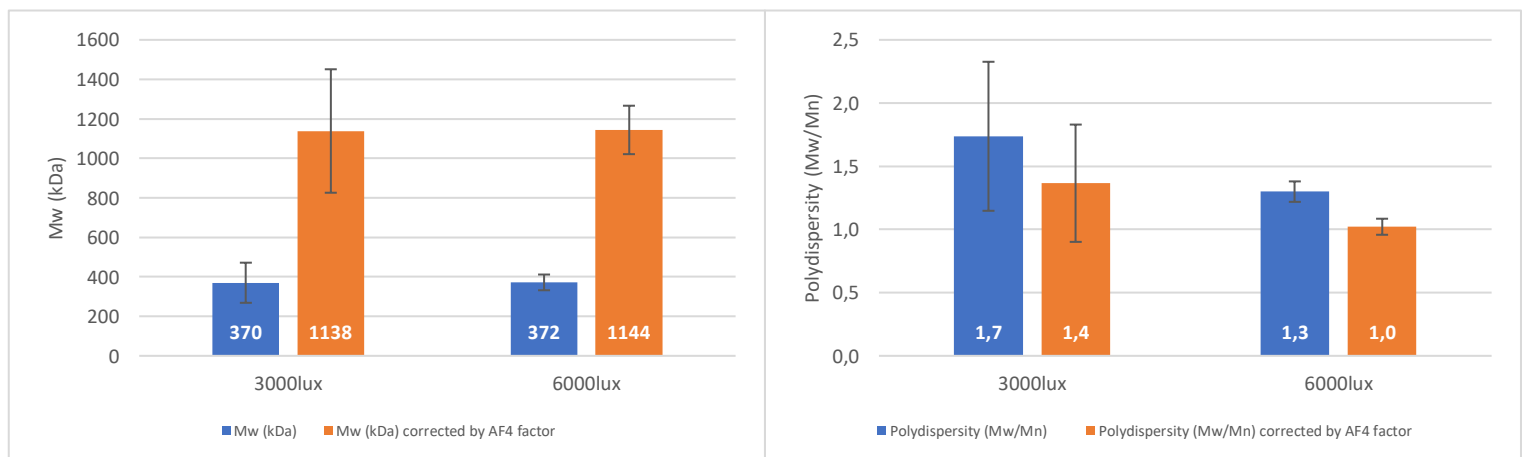


Figure 69: Comparison of the Mw of the strain S.192 cultivated at 3000lux and 6000lux both with DNC on the left. The corresponding polydispersity is depicted on the right. The blue bars represent the measured values, and the orange bars represent the corrected values.

In the following Figure 70 the difference between CONT and DNC illumination regime is depicted. The blue bars represent the DNC culture and the red the CONT culture. In the graph on the left side, the Mw at both conditions was comparable, but the difference increased with the corrected values. The polydispersity was exactly the same for both conditions in the original as well as for the corrected values. Again, the polydispersity decreased from the original 1.3 to 1.0 for the corrected values.

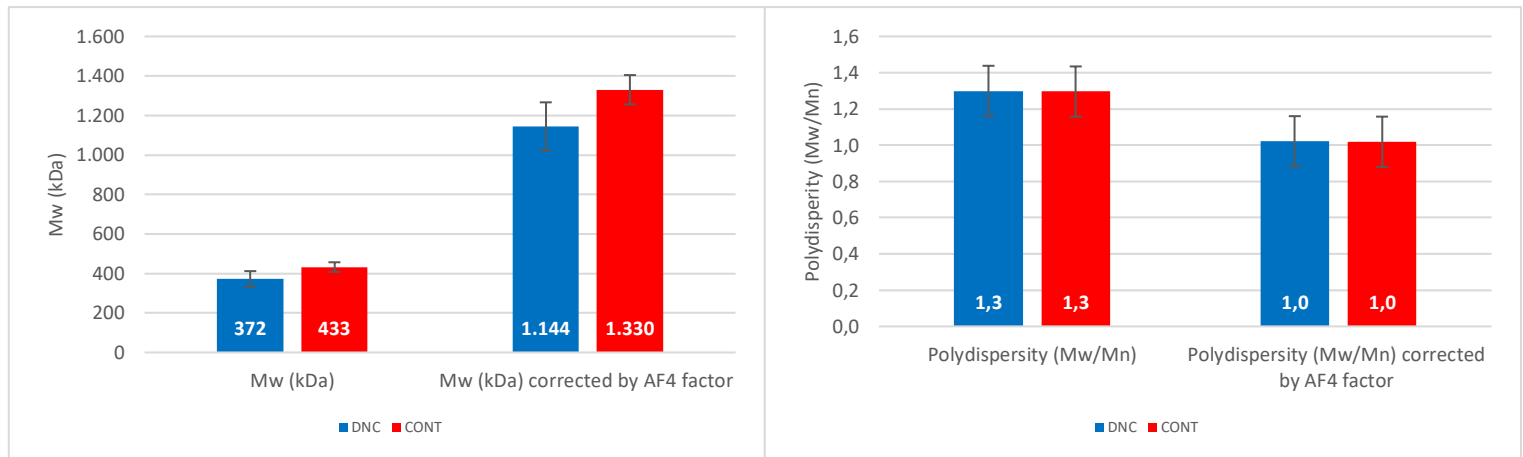


Figure 70: Comparison of the Mw of the strain S.192 cultivated at CONT and DNC at 6000lux on the left. The corresponding polydispersity is depicted on the right. The blue bars represent the DNC values, and the orange bars represent the CONT values.

Overall, the highest Mw value measured was 771.1kDa (corrected 2371kDa) and a polydispersity of 1.2 (corrected 0.9) in the extract of the IFA strain cultivated at DNC and 9500lux with the halogen-metal vapor lamp.

The lowest polydispersity index with 1.13 (corrected 0.88) was measured in the extract of the S.192 strain cultivated with DNC at 3000lux.

The only reliable values measured with the AF4-MALS in the extracts of the S.192 strain cultivated at 3000lux and CONT illumination regime reached an average Mn of 1211 ± 119 kDa and 1264 ± 79 kDa for Mw resulting in a polydispersity of 1.04 ± 0.06 .

9 Discussion

The strains S.192 and S.6803 were cultivated with a day-night-cycle at 1464 ± 259 lux (Data logger) at set temperatures of 20°C and 25°C. This temperature difference was very high compared to the differences in temperatures observed between day and night or between the DNC and the CONT cultures, with differences of not more than 1°C.

The effect of 5°C difference caused in the 25°C culture a reduced growth seen in the lower OD_{435nm} and CDW. This effect was stronger in the S.6803 strain and barely noticeable in the S.192 strain reaching the same CDW at both temperatures. The S.192 strain overall performed much better in growth and in PHB accumulation under these conditions.

The PHB accumulation was not influenced by the temperature difference. The PHB content started to increase linearly from day 18 on until day 40 reaching about 7.5%CDW in the S.192 strain and only 2%CDW in the S.6803.

The temperature had no significant influence on the cell size as well, which was about 2.1µm.

From this data it was concluded that the temperature differences observed in the illumination experiments didn't contribute to the differences found between continuous illuminated and day-night-cycle cultures.

In total four illumination experiments were conducted. In experiment 1 and 2 the cyanobacteria cultures were cultivated at rather low light intensities of about 3000lux in a CONT and DNC setup. The results of these experiment were replicated with all three cyanobacteria strains, S.192, S.6803 and IFA.

The DNC cultures showed better growth in the OD_{435nm} , but in the OD_{750nm} and in the CDW the CONT cultures reached higher values. All cultures showed no sign of a stationary phase until the end of the 40 days experiment. The CONT cultures showed clear signs of chlorosis in colour on day 40. All cultures reached about 1.5g/L CDW independent of strain or illumination regime.

The CONT illuminated cultures showed drastically enlarged cells especially the S.192 strain with almost reaching 3µm on average. This was compensated by the DNC cultures by reaching much higher cell counts, finally resulting in the same CDW.

The same effect was observed in experiment 3 at 6000lux and experiment 4 at 10000lux, even with the technical difficulties of light failures occurring in the DNC cultures.

At 6000lux the cultures also reached about 1.5g/L CDW. At 10000lux the cultures could only reach about 0.65g/L CDW and showed a batch culture growth profile in their OD and CDW values. A plateau was reached on day 18 until day 28, when the cell mass started to decrease entering the death phase.

At a very high light intensity of 10000lux, the difference in cell size was not as pronounced anymore and could not be observed by solely examining the cultures with the light microscope. The size difference could only be observed by measuring the cells with a software. This might be the reason

why this effect has not been reported yet in literature. Experiments with continuous illumination are usually conducted at high light intensities, but the results of this study show that the difference in size between continuous illumination and a day-night-cycle is especially pronounced at lower light intensities. Therefore, the effect could have been easily overlooked in the past.

The increase in cell size in the CONT cultures was accompanied by a much higher amount of intracellular accumulated PHB. Concluding that the increase in PHB also induces the increase in cell size would still be inadequate. For a genetically engineered *Synechocystis* strain accumulating 80%PHB/CDW no increase in cell size has been reported, but instead the rupture of the cell membrane was observed (Koch, Bruckmoser, et al., 2020). This clearly shows that the PHB amount in the cell does not influence the cell size control.

The cell size is one of the most defining parameters of a cell and is tightly controlled since it defines their volume to surface ratio and the cells have to maintain homeostasis by balancing the osmotic pressure. All cells throughout all living systems seem to follow the cell size scaling law, defined by the proportional relations between the cell dry mass, the nuclear size, and the cell size. This model implies, that the control of the cell volume is dominated by small osmolytes and not polymers like PHB. For example, the homeostasis between amino-acids and proteins originates from the enzymatic control of the amino-acid pool and explains the dry mass density homeostasis. When the homeostasis is disrupted by mRNA crowding or the pharmacological treatment with rapamycin, the protein content is saturated resulting in an increase of amino acid. This leads to an increase in the cell size and to dry mass dilution upon growth (Rollin et al., 2022).

Different mechanisms for the cell size control are currently under investigation, trying to answer the question how cells know their size and how populations of cells maintain their tight size homeostasis. This is achieved by balancing growth and division. The cell size of a new-born cell is determined by the size at which its parental cell divided. In single celled organisms the decision of a cell how big it should be is influenced by its nutritional status. The cell size is not directly maintained, but by a target nuclear-to-cytoplasmic (N:C) ratio. This lead in bacteria to the observation, that even under a wide range of growth rates, the DNA replication is initiated at a constant cell size to maintain the balance between cell size and genome number (Rhind, 2021).

According to Rhind (2021) the adder models, from all the different suggested models for cell size control, seem to fit the best for bacteria. Instead of dividing at a constant size, bacterial cells will grow independent from their birth size for a constant amount of time. This adder model suggests that a division-protein has to be synthesized until a certain concentration is reached, similar to the replication initiation by a critical number of DnaA protein molecules. Rhind proposed the FtsZ protein, assembling into the contractile ring protein, for regulating the size at division. The adder mechanism only works in actively growing cells and therefore only works for single celled organisms that are either growing or nutrient limited.

The nutrient availability is the primary external modulator for cell size because it directly influences the growth rate. For *E. coli* it has been proven, that cultivation in nutrient rich media lead to a cell size three times larger than under nutrient-poor conditions (Pierucci, 1978). The cell size increases with the growth rate which is dependent on the nutrient availability. Nutrients directly impact the biosynthesis and with it the cell growth and cell cycle progression. This correlation between the nutrient depended growth rate and the cell size is referred to as 'growth law'.

But it has been shown that other factors influencing the growth rate like the temperature (Kjeldgaard, 1958) or the chemical inhibition of the growth rate (Vadia et al., 2017) didn't influence the cell size. This means that the cell size is not dictated by the growth rate but rather by the nutrient availability. This is in line with the findings of this study, where no significant influence of the temperature on the cell size could be observed (Figure 24). Therefore, nutrient availability and the metabolic state are the mediators for the cell size, independent of their contribution to the growth rate.

Under nutrient-rich conditions cells add more material per generation compared to cultures in nutrient-poor conditions. Nutrient downshift experiments by Ferrezuelo et al. (2012). suggest a nutrient-dependent size threshold. Rapidly growing cells undergo cell cycle entry at a larger size compared to slow-growing cells at nutrient-poor conditions. The shift to nutrient-rich conditions triggered an increase in the threshold amount of growth required for cell division (Kellogg & Levin, 2022).

The cells were larger under continuous illumination. This size difference between CONT and DNC cells could be explained by a delay in cell cycle progression in the CONT cultures. This allowed them to reach the newly required size threshold for division. Or in other words the CONT culture cells divide later and since division is the primary determinant of cell size, they were larger. This is also consistent with the adder model. Under nutrient-rich conditions cells must grow a longer period of time and become larger to accumulate sufficient FtsZ to support the assembly of the division machinery (Kellogg & Levin, 2022). The cell diameter of the CONT cells is larger and therefore requires a larger cytokinetic ring and a higher number of division proteins. This means that continuous illumination has the same effects on the cyanobacteria culture as nutrient-rich conditions.

Even though the mechanisms controlling cell size remain poorly understood, the findings so far indicate that the enlarged cells observed in the CONT cultures were a result of their growth at conditions comparable to nutrient-rich conditions. Nutrient-rich and nutrient-poor can be misleading since both cultures have the same amounts of dissolved nutrients available in the media. But cyanobacteria fix carbon using photosynthesis and as the CONT cultures had more light available they were able to continuously fix carbon. This could be seen as growth under carbon-rich conditions, while the DNC culture cells are limited by the period of darkness. Therefore, the cell size difference between continuous illumination and day-night-cycle was a result of the illumination time and not different PHB accumulation.

This effect has not been observed in the comparison of DNC and CONT illumination by Koch et al. (2020). The light intensity of $\sim 50\mu\text{E}$ used in their experiment was lower compared to the $\sim 90\mu\text{E}$

(Experiment 1&2), ~200 μ E (Experiment 3) and ~350 μ E (Experiment 4) in this study. This could mean that the difference in the total amount of light received by the cells was not big enough in their experiment to produce an observable effect on the cell size.

The largest average cell size was 3 μ m measured in the CONT cultures S.192 at 6000lux and S.6803 at 10000lux. In the DNC cultures the cell size increased in all three strains with the increase of the light intensity at the same time decreasing the difference in cell size to the CONT cultures. The biggest difference was observed in the S.192 strain cultivated at 6000lux with the CONT cells being about 1.4 times bigger than the DNC cells, that only reached 70% of the CONT cell size.

Since the DNC cells did not need to grow to the size of the CONT cells, they divided sooner and therefore more often over the duration of the experiment resulting in a higher cell density. What is most peculiar about these results is that the differences in cell number and cell size seem to compensate each other in the end. The CONT and DNC cultures reach similar CDW values of about 1.5g/L at 3000lux and 6000lux, but only about 0.65g/L in the 10000lux cultures.

Concluding the increased cell size in the CONT cultures is no response to light stress, but to carbon-richness because of high light availability. This finding suggests that smaller cell size in the DNC cultures is a response to growth under carbon limitation caused by insufficient light availability.

The other significant difference caused by the different illumination regimes was seen in the amount of PHB and glycogen.

The glycogen showed less differences at the end of the experiments compared to PHB. Over the course of the experiments the glycogen content in the DNC cultures was significantly lower compared to CONT cultures. They reached comparable high values on day 40 in experiment 1,2 and 3. Only in experiment 4 at 10000lux the last day of the experiment did not display the highest glycogen amount, because of the massive growth of heterotrophic bacteria. A peak in glycogen content was observed between day 18 and 25. Before this turning point the CONT cultures displayed higher glycogen values and after the DNC cultures displayed a slower decrease in glycogen content and therefore higher levels. The glycogen content did not differ between 3000lux and 6000lux, but greatly to 10000lux cultures displaying a plateau with a thereafter decrease.

The highest measured glycogen content was in the S.6803 strain cultured at 3000lux and 6000lux at DNC and CONT almost reaching 50%CDW of glycogen. This is concurrent with the work of (Klotz et al., 2016) reporting glycogen amounting for up to 50% of cell dry weight in chlorotic cells.

Glycogen is known to be a carbon and energy storage for bacterial cells, but is also found throughout many other organisms and also humans (Prats et al., 2018). Under growth-limiting conditions the excess carbon is synthesized to glycogen and accumulated inside the cell. When energy and carbon supply is insufficient to maintain growth and viability, the glycogen storage is degraded to sustain cell survival under transient starvation conditions (Klotz & Forchhammer, 2017). The greatest

amounts of glycogen is accumulated in non-diazotrophic cyanobacteria like *Synechocystis* under nitrogen starvation conditions (Preiss, 1984).

In this study nitrogen limited media was used in the experiments to induce nitrogen starvation. The limiting conditions lead to the synthesis of glycogen, independent of the illumination regime or light intensity. When nitrogen depletion is reached, the carbon-nitrogen-balance is disturbed, and growth cannot be supported any longer. A genetically determined survival program is initiated leading to the rapid accumulation of glycogen. It functions as excess carbon sink. The survival program also induces the degradation of the light-harvesting complexes a process called chlorosis. This avoids the production of excess energy and reduction equivalents by the photosynthesis that cannot be consumed any longer by the anabolism (Doello et al., 2018; Doello, Neumann, & Forchhammer, 2021). The electron microscopic images in section 8.7 suggests, that the degradation of the photosynthetic machinery has only an influence on the coloration of the bacteria culture turning from green to brown or orange, but not on the intracellular thylakoidal membrane system. The cells maintain their intracellular order during dormancy and only change the biochemical make up. The as green perceived chlorophylls and as blue received phycocyanin responsible for trapping the photons are degraded, but the carotenoids, which have not been measured in this study, that are also responsible for protection against UV-radiation can still be observed as the brown to orange colouration of the cultures. Once a nitrogen source is reintroduced, photosynthesis is paused and the dormant cells solely rely on their glycogen storage to produce energy and metabolic intermediates in their catabolism restarting vegetative growth (Doello et al., 2018).

The synthesis of glycogen does not only function as a storage for energy and carbon, but is important to sustain homeostasis of the photosynthetic cell as shown by Cano et al. (2018) for the *Synechocystis* sp. PCC6803. As photosynthetic organisms use solar energy or release energy from stored chemical bonds to drive their biosynthetic reactions and life processes, they generate ATP and NADPH. Their generation must be regulated under changing environmental conditions, mainly the availability of nutrients and light. Therefore, they have developed mechanisms to balance their energy levels. These mechanisms intervene on the level of the photosynthetic electron transport chain regulating the light sensing and harvesting by photosynthetic rearrangements and photoprotection (Eberhard et al., 2008; Kirilovsky & Kerfeld, 2013; Montgomery, 2014).

The synthesis and use of glycogen, as carbon storage, is a common mechanism adapting to changing light and nutrient availability. It has been shown, that the synthesis of glycogen occurs in the daytime in accordance with light availability (Zilliges, 2014). Experiments conducted by Cano et al. (2018) showed that during darkness the cells managed to restore a high energy charge correlating to increased ATP levels by the catabolism of stored glycogen. During illumination the increasing ATP levels were balanced by the anabolism of glycogen consuming ATP. This glycogen cycle enables an efficient ATP consumption during illumination, attenuating excessive reduction of electron carriers which would otherwise lead to an overload of the photosynthetic electron transport chain (Hackmann

& Firkins, 2015; Russell, 2007). Balancing their energy charge is of high importance for the cell to keep the metabolism and catabolism flowing. The excess in photosynthesis is the driving force for the glycogen cycle allowing cyanobacteria to balance their energy charge by Glycogen synthesis/degradation (Cano et al., 2018).

These two effects on the glycogen level have been observed in the comparison of DNC and CONT cultivated cultures. The glycogen levels in the CONT cultures were much higher compared to the DNC cultures over the duration of the experiments 1,2 and 3. The CONT illumination leads to an ATP overflow by photosynthesis which is balanced by producing glycogen all the time. In the DNC cultures glycogen is produced during illumination and consumed during darkness balancing the ATP pool. At the end of the first three experiments nitrogen depletion was reached triggering the cells to produce glycogen as carbon and energy storage to restart their metabolism after dormancy. This can be seen in the in figures 26,32 and 39 as a sudden and massive increase in the glycogen content at the end of the experiments (around day 25 to 35 depending on light intensity and strain). This finding is also in line with the work of Orthwein et al. (2021) observing a steep increase in cellular glycogen levels after the removal of the nitrogen source.

Only in the cultures cultivated at 10000lux the glycogen content starts to decrease, which happens faster in the CONT cultures resulting in higher glycogen levels in the DNC cultures. At this light intensity, no nitrogen depletion was reached as described in Figure 52. In regards of the colour of the cultures (Figure 45) they seem to have entered chlorosis much sooner, starting at about day 21. This dormancy was not induced by nitrogen depletion, but by the stress reaction to high light intensity.

The content of other synthesized polymer PHB was significantly higher in the CONT cultures. This finding is in contradiction with the literature, where no difference (Kamravamanesh et al., 2017) or higher PHB amounts were found in DNC cultures (Koch, Bruckmoser, et al., 2020; Panda et al., 2006).

The highest PHB amount was found in the S.192 strain cultivated at 3000lux and CONT illumination with an amount of 12.3%CDW of PHB compared to only 2%CDW PHB in the DNC culture. The PHB content increase with the increase in light intensity in the DNC cultures, but for the CONT cultures there was no clear difference between the different illumination intensities.

Synechocystis produce PHB under nutrient limited conditions (Wu et al., 2001) and it has been hypothesized, that it serves next to glycogen as carbon and energy storage. The physiological functions of PHB are still unknown, but as glycogen in cell metabolism is much more than a simple storage the same could also apply to PHB.

The glycogen homo biopolymer $[C_6H_{10}O_5]_n$ has a calculated degree of reduction of $\gamma=4$, the repeating unit of PHB $[C_4H_6O_2]_n$ on the other hand has a much higher degree of reduction of $\gamma=9$, making it better suited as electron sink then a storage. Batista et al. (2018) already mentioned that PHB could

serve as an electron sink eliminating a surplus of reducing equivalents. This function has been shown by Van Gernerden (1968) in the anoxygenic phototrophic bacterium *Chromatium vinosum* converting glycogen to PHB. This way the strain experiences no carbon loss compared to the secretion of fermentation products.

Additionally, it has been shown by Hauf et al. (2013), that an excess of NADPH under nitrogen depletion supports PHB accumulation. The reaction catalysed by PhaB is converting one NADPH to NADP. This reaction, yielding hydroxybutyryl-CoA, is strongly favoured during nitrogen starvation when NADPH pools are increased.

This suggests that PHB is serving as an intracellular pool for electrons under excess reduction equivalents buffering the redox potential of the cell in an analogous manner as the glycogen cycle buffering the ATP and energy levels of the cell.

Such excess electron conditions would be the cultivation at high amounts or intense light, since photosynthesis continuously supplies NADPH which has to be recycled. For the PHB synthesis on the other hand NADPH is needed, reducing it to NADP⁻.

The redox potential of cyanobacteria can be monitored by measuring their photocurrent, the generated light induced current with an extracellular electrode. This photocurrent correlates to cellular redox state (Hatano et al., 2022).

The two central energy metabolisms, respiration and photosynthesis, in cyanobacterial cells take place in the same environment, as they do not develop any organelles and therefore share many metabolic intermediates and electron transport components (Binder, 1982; Mullineaux, 2014; Peschek et al., 2004). Even though the respiration rate is 10 times lower than the photosynthetic oxygen evolution rate, both depend on the shared NADPH pool (Bolychevtseva et al., 2015; Pils & Schmetterer, 2001).

The NADPH produced during illumination by the photosynthetic electron transport is mainly consumed in the reductive Calvin-Benson-Bassham (CBB) cycle. In darkness NADPH is produced by the pentose phosphate pathway (OPP) and thereafter consumed by the respiratory transport chain (Welkie et al., 2019). By measuring the photocurrent, Hatano et al. (2022) found that the NAD(P)H fluorescence immediately increased upon inducing light and remained constant under illumination. Once the light was turned off the fluorescence rapidly decreased again. The fluorescence representing the NAD(P)H clearly showed the light responsive rapid change in the NADPH production and consumption by the photosynthetic linear electron transport and CBB cycle, respectively (Tanaka et al., 2021).

This can also be applied to the results of this study, as more PHB was found in the CONT cultures compared to the DNC cultures, even before nitrogen depletion was reached. In the CONT illuminated cultures, the photosynthetic linear electron transport provides a constant oxidation of NADP⁻, which has to be recycled by reduction. To balance their internal redox potential, the unconsumed NADPH₂⁺ could be used for PHB synthesis. As the DNC cultures are only exposed to a fraction of the light,

they also produce a much lower fraction of PHB in the time they are illuminated. The same effect can be seen when light intensity is increased. Over the whole course of the experiment the DNC cultures at higher light intensity produced a higher PHB content compared to lower light intensities. In the CONT cultures this effect nor a trend caused by increased light intensity was observed. This could be due to different compositions in the photopigments, that can be adjusted by the cell to fit to the light intensity and spectral composition (Shevela et al., 2013).

This theoretical explanation however is weakly supported by the collected data, as the chlorophyll and phycocyanin data show no trends or reproducible behaviour during the experiments and therefore stays inconclusive.

Another characteristic of the cyanobacterial culture is the enormous light attenuation along the light path. The light reaching the surface of the culture is absorbed along the light path resulting in a light gradient. The cyanobacterial cells additionally absorb light and simply shade cells beneath them. This may cause a dark zone depending on the culture concentration, cell pigmentation, light path, and light intensity. The cultures are actively mixed by a shaker and the cells travel between the saturated light on the surface and the shaded darker depth of the culture. This means that even the continuously illuminated culture experiences a flashing light regime. It has been experimentally proven, that flashing light leads to an optimal growth. This can be explained by the photoinhibition due to the continuous emission of photons occurring under continuous illumination. At a flashing light regime the same high photon dosage can be utilized by the cyanobacteria without undergoing times of photoinhibition and therefore the light energy can be utilized more efficiently (Abu-Ghosh et al., 2016).

As energy and redox potential of a cell are the most defining parameters for cell metabolism, an interaction between the glycogen and PHB cycles as buffering systems for ATP and NADPH could be expected.

In a study by Koch et al. (2019) clear evidence was found, that the intracellular glycogen pool provides the carbon for the PHB synthesis during nitrogen starvation resulting in a slow net change of the glycogen amount. This residual metabolism in nitrogen starved dormant cells is probably needed to repair essential biomolecules (DNA, RNA, etc.), osmoregulation, regulated shifts in metabolic pathways and the preparation for a quick response as soon as nutrients are available, ensuring their long-term survival. Therefore, the cells still need a constant supply of ATP and reduction equivalents. The PHB production is mainly achieved through the EMP pathway yielding the highest ATP among the carbon catalytic pathways. The OPP pathway is also involved in PHB synthesis providing metabolites for the repair of biomolecules and the maintenance (Koch et al., 2019).

Cyanobacteria constantly monitor their intracellular milieu to detect imbalances, caused by external factors. Maintaining the carbon/nitrogen (C/N) homeostasis is fundamentally important in cellular physiology. Cyanobacteria as photoautotrophic organisms especially have to tightly interconnect

CO₂ fixation and nitrogen assimilation. This connection is achieved with the P_{II} proteins interacting with the metabolite 2-oxoglutarate (2-OG) and ATP. This way cyanobacteria can monitor their energy level and their C/N-balance, as 2-OG is present as intermediate in the tricarboxylic acid cycle (TCA) and is the precursor for the ammonia incorporation by the glutamine-synthetase-glutamate-synthase (GS/GOGAT) (Forchhammer & Selim, 2020).

ADP and ATP compete for the occupation of the binding sites of PII. Binding of ATP creates a coordination sphere for the 2-OG effector. From the effector binding site a large and flexible target-binding loop protrudes, adopting different conformations depending on the bound effector (Forchhammer & Lüddecke, 2016). As response to the metabolic and energetic state of the cell many metabolic key enzymes, transcription factors and transport proteins activities are tuned in response to this signalling pathway. PII can directly interact among others with the acetyl-CoA carboxylase, the rate-limiting step in the fatty acid biosynthesis (Zhang et al., 2006), the phosphoenolpyruvate carboxylase, catalysing the anaplerotic carbon fixation (Scholl et al., 2020) and the glutamine-dependent nicotinamide adenine dinucleotide (NAD⁺) synthase (A. R. S. Santos et al., 2020). Besides its functions for tuning enzyme activity, PII can also regulate transport activities by protein-protein interactions, e.g. the ensemble of nitrogen transporters (Watzer et al., 2019). A different mechanism allows PII through binding to a small signalling mediator protein PipX (PII-interacting protein X) to modulate gene expression in response to the C/N ratio (Giner-Lamia et al., 2017). Connecting the ATP and NADPH pools and governing the carbon flux in *Synechocystis* is the PII interactor, named PirC (Orthwein et al., 2021). PirC binds to and inhibits the activity of the 2,3-phosphoglycerate-independent phosphoglycerate mutase (PGAM). This enzyme is with PII of most importance for the carbon flux, as it deviates newly fixed CO₂ toward lower glycolysis. Upon nitrogen starvation the metabolite 2-oxoglutarate (2-OG) is accumulated tuning PirC to either bind PII or PGAM. High 2-OG levels lead to the dissociation of the PirC-PII-complex promoting PirC to bind and inhibit PGAM leading to the accumulation of glycogen and PHB (Orthwein et al., 2021).

The same signalling pathway, but induced by different effectors, could also cause the PHB accumulation during continuous illumination and at high light intensity. As discussed above, the PII and PGAM system governs the carbon flux and regulates multiple enzymes, transport mechanisms and transcription, depending on the energy and metabolic state of the cell. This makes it best fit to balance rising ATP levels during illumination by the synthesise of glycogen and NADPH levels by the accumulation of PHB. Thus, making these two polymer cycles best fit for balancing the energetic state and the redox potential of the cells in the natural periodic fluctuation of light availability caused by day and night.

During the unnatural continuous illumination, the balancing polymers are continuously synthesized, and higher amounts are accumulated. The same applies for high light intensities causing higher energy input per time and therefore resulting in higher ATP and NADPH amounts per time that must be recycled balancing the energetic and redox state of the cells.

The polymer quality is often assessed by the dispersity index since it indicates the size homogeneity of a polymer. To guaranty consistent properties in a product, the polymer chains must be approximately of the same length. The length of the polymer chain length is the baseline for the plastic properties, besides its chemical properties. The longer the chains become the stiffer the plastic and the higher its melting temperature. Shorter chains on the other hand led to more flexible polymers. Therefore, a polydispersity index of below 1 is desirable, indicating polymer chain lengths in the same range. To investigate the effects of continuous illumination on the PHB quality and to compare differences between the three used strains, the PHB was extracted and analysed.

The newly tested extraction method using the EDGE has been proven to be successful. The PHB, extracted with this method in a first attempt, was analysed using H-NMR. The PHB extraction was proven by the results (Figure 66) and in the analysis no impurities were observed. The further analysis with gel permeation chromatography have shown to be difficult and due to unreliable results, the extracts were analysed by the project partners from the Bruno University of Technology. During the analysis with the AF4-MALS setup they experienced difficulties caused by the organic solvents and had to switch to a more robust SEC-MALS system. Between these two systems a substantial discrepancy in the results could be observed. In the AF4-MALS set up the polymer length was found to be 1200kDa at a dispersity index of about 1. This is considerably lower than the values ($M_n=1.52\text{MDa}$, $M_w=5.82\text{MDa}$, $PDI=3.8$) reported by Kovalcik (2017) for PHB produced by *Synechocystis salina*, but about double of the reported mass weight ($M_n=503\text{kDa}$, $PDI=1.74$) found by Koch et al. (2020). In their study the genetically manipulated overproducing strain synthesized PHB of higher M_n , indicating that *Synechocystis* rather elongates existing PHB chains then producing more short chains.

The numbers of PHB granules (See chapter 8.7) depends on the strain. Not more than 7 granules in total could be accounted for in any cell. With increasing PHB the number of granules also increases and at the same time the existing PHB granules increase in size. This means cultures with higher PHB values displayed a higher number of granules that were also larger in size. It was reported that once they reached a certain size, the granules merged (Koch, Bruckmoser, et al., 2020), but this could not be observed in this study as no such high PHB levels were reached.

Upon division of the cells, the PHB granules were evenly distributed between the emerging sister cells (Figure 63), but their size stayed the same. This explains cells containing granules with a big difference in their size. Newly formed granules and large granules inherited from the mother cell can be present.

This could also explain the big variance in the dispersity index. A young culture will be more homogeneous in their PHB polymer length compared to a culture after multiple divisions with coexisting new and old granules with a larger spectrum in their polymer length distribution.

In this study PHB was continuously produced over the whole duration of the experiment. For the PHB quality a short production period induced by an external stressor seems the more appropriate approach to guarantee consistent polymer quality.

In other studies, the induction is the nitrogen limitation by washing with a media missing a nitrogen source. In this study a media was used with a very low starting concentration of nitrogen to expose the cells to nitrogen depletion until the end of the experiment, but the PHB synthesis was present from the beginning of the experiment on and was not induced upon nitrogen depletion.

The CONT cultures synthesized longer polymer chains compared to the DNC cultures and they displayed more and larger PHB granules

The increase in light intensity from 3000lux to 6000lux did not influence the polymer length, but the dispersity index. It was larger at lower light intensity at DNC cultivation.

From the polymer quality aspect, the IFA strain performed the best, synthesizing chains of high Mw of 1708kDa (corrected) and the best PDI of 0.9 (corrected), but from the production point of view S.192 outcompeted the other strains by far building much more PHB under CONT and DNC conditions.

From this study and the comparison with the literature it can be concluded that the method of PHB analysis as well as the extraction procedure have a huge effect on the results. The newly tested extraction method resulted in a before not reported second peak, which could result from impurities such as pigments interacting with the column or interfering with the detection. As long as the cause of this effect have not been determined the here presented results for the mass weight and PDI have to be regarded with caution.

10 Conclusion and Outlook

The production of the biodegradable and biobased polymer PHB is a chance to substitute conventional petrol-based plastics. The use of PHB represents an eco-friendlier alternative as it is produced from a renewable resource that is additionally not competing for agricultural land. The biggest challenge in the economic feasibility of the production with cyanobacteria are the low cell densities and the low amounts of intracellular PHB resulting in huge volumes needed for producing considerable amounts of this polymer. Even though progress has been made in elucidating the involved cell control mechanisms as well as producing genetically engineered high output strains, further investigations have to be made to understand the complex and intertwined control mechanisms.

The simple case of PHB production could turn out to be on the interface of the most basic cell regulation points governing the energy and redox state of the cell essential for the cell homeostasis. This understanding could be used in future to combine genetical engineering and cultivation conditions to increase PHB yield and quality.

In order to investigate PHB synthesis as a possible redox balancing system of the cells, further studies have to be conducted combining PHB measurements with simultaneous NADPH and ATP monitoring. Future efforts should go towards the determination of the redox charge and the [ATP]/[NADP] ratio to unravel energy balancing at continuous illumination compared to day-night-cycles and with increasing light intensities.

This study helps to understand the effects of different light intensities and illumination cycles on *Synechocystis sp.*, however an increased sample size to confirm the results and out rule technical failures still is needed.

Besides the difficulties in the measurements the major hurdle for the PHB quality testing was the limited amounts in culture volume resulting in low amounts of PHB, that could be extracted. This greatly limited the possibilities in the analysis and the statistical accuracy because of lacking coverage. This should be considered in the planning of further experiments and the used cultivation volumes should be capable of producing higher PHB quantities.

11 Acknowledgements

First of all, I would like to thank my supervisor Prof. Werner Fuchs and my project leader Prof. Ines Fritz for giving me the chance to conduct this study as well as for their advice and continuous support. I would also like to thank my colleges for their support and advice in everyday lab work. Thank you, Christina for planning the experiments with me, thank you Antonia for your preliminary work especially assembling the used set-up, Dennis for filling in when I was on leave and of course Michi for keeping the lab running. Thanks to all employees and fellow students at IFA for creating a respectful and fun environment to work in. A special thanks to the project partners at the Brno University of Technology for their support and analyses. Thanks to the University of Natural Resources and Life Science Vienna and the project funding institution FWF for enabling this thesis.

Finally, I would also like to express my gratitude to my family and parents for their support. My appreciation also goes out to my friends for their encouragement and support all through my studies. I want to especially thank my partner in life Teresa for her tremendous encouragement in the past few years, her scientific input and help in our everyday family life.

I hope this study can contribute to a sustainable future and enables me to continue working towards solving the environmental problems of our time so my kids can raise families in a healthy environment.

12 References

References

- Abu-Ghosh, S., Fixler, D., Dubinsky, Z., & Iluz, D. (2016). Flashing light in microalgae biotechnology. *Bioresource Technology*, 203, 357–363. <https://doi.org/10.1016/j.biortech.2015.12.057>
- Akaraonye, E., Keshavarz, T., & Roy, I. (2010). Production of polyhydroxyalkanoates: the future green materials of choice. *Journal of Chemical Technology & Biotechnology*, 85(6), 732–743. <https://doi.org/10.1002/jctb.2392>
- Alpizar, F., Backhaus, T., Decker, N., Eilks, I., Escobar-Pemberthy, N., & Fantke (2019). UN Environment Global Chemicals Outlook II: From Legacies to Innovative Solutions: Implementing the 2030 Agenda for Sustainable Development.
- Alsiyabi, A., Brown, B., Immethun, C., Long, D., Wilkins, M., & Saha, R. (2021). Synergistic experimental and computational approach identifies novel strategies for polyhydroxybutyrate overproduction. *Metabolic Engineering*, 68, 1–13. <https://doi.org/10.1016/j.ymben.2021.08.008>
- Anderson, A. J., & Dawes, E. A. (1990). Occurrence, metabolism, metabolic role, and industrial uses of bacterial polyhydroxyalkanoates. *Microbiological Reviews*, 54(4), 450–472. <https://doi.org/10.1128/mr.54.4.450-472.1990>
- Anis, S. N. S., Mohamad Annuar, M. S., & Simarani, K. (2017). In vivo and in vitro depolymerizations of intracellular medium-chain-length poly-3-hydroxyalkanoates produced by *Pseudomonas putida* Bet001. *Preparative Biochemistry & Biotechnology*, 47(8), 824–834. <https://doi.org/10.1080/10826068.2017.1342266>
- Anitha, N., & Srivastava, R. K. (2021). Microbial Synthesis of Polyhydroxyalkanoates (PHAs) and Their Applications. In B. B. Mishra, S. K. Nayak, S. Mohapatra, & D. Samantaray (Eds.), *Environmental and Agricultural Microbiology* (pp. 151–181). Wiley. <https://doi.org/10.1002/9781119525899.ch7>
- Antipov, E. M., Dubinsky, V. A., Rebrov, A. V., Nekrasov, Y. P., Gordeev, S. A., & Ungar, G. (2006). Strain-induced mesophase and hard-elastic behaviour of biodegradable polyhydroxyalkanoates fibers. *Polymer*, 47(15), 5678–5690. <https://doi.org/10.1016/j.polymer.2005.04.111>
- Bajt, O. (2021). From plastics to microplastics and organisms. *FEBS Open Bio*, 11(4), 954–966. <https://doi.org/10.1002/2211-5463.13120>
- Barragán Campos, R. C., Strojnik, M., Rivas, A. R., Torales, G. G., & Contreras, F. J. G. (2018). Optical spectral characterization of leaves for *Quercus Resinosa* and *Magnolifolia* species in two senescent states, *Proceedings Volume 10765, Infrared Remote Sensing and Instrumentation XXVI*; 1076511, 35. <https://doi.org/10.1117/12.2321710>
- Batista, M. B., Teixeira, C. S., Sfeir, M. Z. T., Alves, L. P. S., Valdameri, G., Pedrosa, F. d. O., Sasaki, G. L., Steffens, M. B. R., Souza, E. M. de, Dixon, R., & Müller-Santos, M. (2018). Phb Biosynthesis Counteracts Redox Stress in *Herbaspirillum seropedicae*. *Frontiers in Microbiology*, 9, 472. <https://doi.org/10.3389/fmicb.2018.00472>

- Behera, S., Priyadarshane, M., Vandana, & Das, S. (2022). Polyhydroxyalkanoates, the bioplastics of microbial origin: Properties, biochemical synthesis, and their applications. *Chemosphere*, 294, 133723. <https://doi.org/10.1016/j.chemosphere.2022.133723>
- Bennett, A., & Bogorad, L. (1973). Complementary chromatic adaptation in a filamentous blue-green alga. *The Journal of Cell Biology*, 58(2), 419–435. <https://doi.org/10.1083/jcb.58.2.419>
- Bermejo, R. (2014). Phycocyanins. In N. K. Sharma, A. K. Rai, & L. J. Stal (Eds.), *Cyanobacteria* (pp. 209–225). John Wiley & Sons, Ltd. <https://doi.org/10.1002/9781118402238.ch13>
- Binder, A. (1982). Respiration and photosynthesis in energy-transducing membranes of cyanobacteria. *Journal of Bioenergetics and Biomembranes*, 14(5-6), 271–286. <https://doi.org/10.1007/BF00743057>
- Blankenship, R. E. (2002). Carbon Metabolism. In R. E. Blankenship (Ed.), *Molecular Mechanisms of Photosynthesis* (pp. 171–203). Blackwell Science Ltd. <https://doi.org/10.1002/9780470758472.ch9>
- Bolychevtseva, Y. V., Kuzminov, F. I., Elanskaya, I. V., Gorbunov, M. Y., & Karapetyan, N. V. (2015). Photosystem activity and state transitions of the photosynthetic apparatus in cyanobacterium *Synechocystis* PCC 6803 mutants with different redox state of the plastoquinone pool. *Biochemistry. Biokhimiia*, 80(1), 50–60. <https://doi.org/10.1134/S000629791501006X>
- Calcott, M. J., Ackerley, D. F., Knight, A., Keyzers, R. A., & Owen, J. G. (2018). Secondary metabolism in the lichen symbiosis. *Chemical Society Reviews*, 47(5), 1730–1760. <https://doi.org/10.1039/c7cs00431a>
- Cano, M., Holland, S. C., Artier, J., Burnap, R. L., Ghirardi, M., Morgan, J. A., & Yu, J. (2018). Glycogen Synthesis and Metabolite Overflow Contribute to Energy Balancing in Cyanobacteria. *Cell Reports*, 23(3), 667–672. <https://doi.org/10.1016/j.celrep.2018.03.083>
- Chakdar, H., & Pabbi, S. (2016). Cyanobacterial Phycobilins: Production, Purification, and Regulation. In P. Shukla (Ed.), *Frontier Discoveries and Innovations in Interdisciplinary Microbiology* (pp. 45–69). Springer India. https://doi.org/10.1007/978-81-322-2610-9_4
- Coca-Cola company (Ed.). *Coca-Colas 100% plant based plastic bottle*. <https://www.coca-colacompany.com/news/100-percent-plant-based-plastic-bottle>
- Costa, S. S., Miranda, A. L., Morais, M. G. de, Costa, J. A. V., & Druzian, J. I. (2019). Microalgae as source of polyhydroxyalkanoates (PHAs) - A review. *International Journal of Biological Macromolecules*, 131, 536–547. <https://doi.org/10.1016/j.ijbiomac.2019.03.099>
- Costa Coelho, V., Da Cleber, K. S., Ana, L. T., Jorge, A. V. C., & Michele, G. d. M. (2015). Polyhydroxybutyrate production by *Spirulina* sp. LEB 18 grown under different nutrient concentrations. *African Journal of Microbiology Research*, 9(24), 1586–1594. <https://doi.org/10.5897/AJMR2015.7530>
- Dai, W., Chen, M., Myers, C., Ludtke, S. J., Pettitt, B. M., King, J. A., Schmid, M. F., & Chiu, W. (2018). Visualizing Individual RuBisCO and Its Assembly into Carboxysomes in Marine

- Cyanobacteria by Cryo-Electron Tomography. *Journal of Molecular Biology*, 430(21), 4156–4167. <https://doi.org/10.1016/j.jmb.2018.08.013>
- Delwiche, C. F., & Palmer, J. D. (1997). The origin of plastids and their spread via secondary symbiosis. In D. Bhattacharya (Ed.), *Plant Systematics and Evolution. Origins of Algae and their Plastids* (Vol. 11, pp. 53–86). Springer Vienna. https://doi.org/10.1007/978-3-7091-6542-3_3
- Directorate-General for Environment (2021). Turning the tide on single-use plastics. Advance online publication. <https://doi.org/10.2779/800074>
- Doello, S., Burkhardt, M., & Forchhammer, K. (2021). The essential role of sodium bioenergetics and ATP homeostasis in the developmental transitions of a cyanobacterium. *Current Biology : CB*, 31(8), 1606-1615.e2. <https://doi.org/10.1016/j.cub.2021.01.065>
- Doello, S., Klotz, A., Makowka, A., Gutekunst, K., & Forchhammer, K. (2018). A Specific Glycogen Mobilization Strategy Enables Rapid Awakening of Dormant Cyanobacteria from Chlorosis. *Plant Physiology*, 177(2), 594–603. <https://doi.org/10.1104/pp.18.00297>
- Doello, S., Neumann, N., & Forchhammer, K. (2021). *Phosphorylation of phosphoglucomutase 1 on a peripheral site tunes its activity to regulate glycogen metabolism*. <https://doi.org/10.1101/2021.04.15.439997>
- Drosg, B., Fritz, I., Gattermayr, F., & Silvestrini, L. (2015). Photo-autotrophic Production of Poly(hydroxyalkanoates) in Cyanobacteria. *Chemical and Biochemical Engineering Quarterly*, 29(2), 145–156. <https://doi.org/10.15255/CABEQ.2014.2254>
- Ducat, D. C., Way, J. C., & Silver, P. A. (2011). Engineering cyanobacteria to generate high-value products. *Trends in Biotechnology*, 29(2), 95–103. <https://doi.org/10.1016/j.tibtech.2010.12.003>
- Durall, C., & Lindblad, P. (2015). Mechanisms of carbon fixation and engineering for increased carbon fixation in cyanobacteria. *Algal Research*, 11, 263–270. <https://doi.org/10.1016/J.AL-GAL.2015.07.002>
- Dutt, V., & Srivastava, S. (2018). Novel quantitative insights into carbon sources for synthesis of poly hydroxybutyrate in *Synechocystis* PCC 6803. *Photosynthesis Research*, 136(3), 303–314. <https://doi.org/10.1007/s11120-017-0464-x>
- Eberhard, S., Finazzi, G., & Wollman, F.-A. (2008). The dynamics of photosynthesis. *Annual Review of Genetics*, 42, 463–515. <https://doi.org/10.1146/annurev.genet.42.110807.091452>
- El-Malek, F. A., Khairy, H., Farag, A., & Omar, S. (2020). The sustainability of microbial bioplastics, production and applications. *International Journal of Biological Macromolecules*, 157, 319–328. <https://doi.org/10.1016/j.ijbiomac.2020.04.076>
- UN Environment Programme. (2022). *UN Environment Assembly opens with all eyes on a global agreement on plastic pollution*. United Nations. <https://www.unep.org/news-and-stories/press-release/un-environment-assembly-opens-all-eyes-global-agreement-plastic>

- European Bioplastics. Bioplastic - Facts and Figures. *Www.European-Bioplastics.Org*.
https://docs.european-bioplastics.org/publications/EUBP_Facts_and_figures.pdf
- European Union. (2019). *DIRECTIVE (EU) 2019/904 OF THE EUROPEAN PARLIAMENT AND OF THE COUNCIL: on the reduction of the impact of certain plastic products on the environment*.
<https://eur-lex.europa.eu/eli/dir/2019/904/oj>
- Ferrezuelo, F., Colomina, N., Palmisano, A., Garí, E., Gallego, C., Csikász-Nagy, A., & Aldea, M. (2012). The critical size is set at a single-cell level by growth rate to attain homeostasis and adaptation. *Nature Communications*, 3, 1012. <https://doi.org/10.1038/ncomms2015>
- Flombaum, P., Gallegos, J. L., Gordillo, R. A., Rincón, J., Zabala, L. L., Jiao, N., Karl, D. M., Li, W. K. W., Lomas, M. W., Veneziano, D., Vera, C. S., Vrugt, J. A., & Martiny, A. C. (2013). Present and future global distributions of the marine Cyanobacteria *Prochlorococcus* and *Synechococcus*. *Proceedings of the National Academy of Sciences of the United States of America*, 110(24), 9824–9829. <https://doi.org/10.1073/pnas.1307701110>.
- Forchhammer, K., & Lüddecke, J. (2016). Sensory properties of the PII signalling protein family. *The FEBS Journal*, 283(3), 425–437. <https://doi.org/10.1111/febs.13584>
- Forchhammer, K., & Schwarz, R. (2019). Nitrogen chlorosis in unicellular cyanobacteria - a developmental program for surviving nitrogen deprivation. *Environmental Microbiology*, 21(4), 1173–1184. <https://doi.org/10.1111/1462-2920.14447>
- Forchhammer, K., & Selim, K. A. (2020). Carbon/nitrogen homeostasis control in cyanobacteria. *FEMS Microbiology Reviews*, 44(1), 33–53. <https://doi.org/10.1093/femsre/fuz025>
- Fradinho, J. C., Domingos, J. M. B., Carvalho, G., Oehmen, A., & Reis, M. A. M. (2013). Polyhydroxyalkanoates production by a mixed photosynthetic consortium of bacteria and algae. *Bioresource Technology*, 132, 146–153. <https://doi.org/10.1016/j.biortech.2013.01.050>
- Fritz, I. (2019). *The ecological role of poly-hydroxybutyrate in cyanobacteria*. Institute for Environmental Biotechnology, BOKU Research Units. https://forschung.boku.ac.at/fis/suchen.projekt_uebersicht?sprache_in=en&menue_id_in=300&id_in=12649
- Garcia-Pichel, F., Belnap, J., Neuer, S., & Schanz, F. (2003). Estimates of global cyanobacterial biomass and its distribution. *Algological Studies*, 109(1), 213–227. <https://doi.org/10.1127/1864-1318/2003/0109-0213>
- GESAMP. (2016). *Sources, fate and effects of microplastics in the marine environment: part two of a global assessment*. www.imo.org
- Giner-Lamia, J., Robles-Rengel, R., Hernández-Prieto, M. A., Muro-Pastor, M. I., Florencio, F. J., & Futschik, M. E. (2017). Identification of the direct regulon of NtcA during early acclimation to nitrogen starvation in the cyanobacterium *Synechocystis* sp. Pcc 6803. *Nucleic Acids Research*, 45(20), 11800–11820. <https://doi.org/10.1093/nar/gkx860>
- Grigore, M. E., Grigorescu, R. M., Iancu, L., Ion, R.-M., Zaharia, C., & Andrei, E. R. (2019). Methods of synthesis, properties and biomedical applications of polyhydroxyalkanoates: A review.

Journal of Biomaterials Science. Polymer Edition, 30(9), 695–712.
<https://doi.org/10.1080/09205063.2019.1605866>

- Gründel, M., Scheunemann, R., Lockau, W., & Zilliges, Y. (2012). Impaired glycogen synthesis causes metabolic overflow reactions and affects stress responses in the cyanobacterium *Synechocystis* sp. Pcc 6803. *Microbiology*, 158(Pt 12), 3032–3043.
<https://doi.org/10.1099/mic.0.062950-0>
- Hackmann, T. J., & Firkins, J. L. (2015). Maximizing efficiency of rumen microbial protein production. *Frontiers in Microbiology*, 6, 465. <https://doi.org/10.3389/fmicb.2015.00465>
- Hatano, J., Kusama, S., Tanaka, K., Kohara, A., Miyake, C., Nakanishi, S., & Shimakawa, G. (2022). NADPH production in dark stages is critical for cyanobacterial photocurrent generation: A study using mutants deficient in oxidative pentose phosphate pathway. *Photosynthesis Research*. Advance online publication. <https://doi.org/10.1007/s11120-022-00903-0>
- Hauf, W., Schlebusch, M., Hüge, J., Kopka, J., Hagemann, M., & Forchhammer, K. (2013). Metabolic Changes in *Synechocystis* PCC6803 upon Nitrogen-Starvation: Excess NADPH Sustains Polyhydroxybutyrate Accumulation. *Metabolites*, 3(1), 101–118.
<https://doi.org/10.3390/metabo3010101>
- Hays, S. G., & Ducat, D. C. (2015). Engineering cyanobacteria as photosynthetic feedstock factories. *Photosynthesis Research*, 123(3), 285–295. <https://doi.org/10.1007/s11120-014-9980-0>
- Herrero, A., & Flores, E. (2008). *The cyanobacteria: Molecular biology, genomics, and evolution*. Caister Academic Press.
- Holland, H. D. (2002). Volcanic gases, black smokers, and the great oxidation event. *Geochimica Et Cosmochimica Acta*, 66(21), 3811–3826. [https://doi.org/10.1016/S0016-7037\(02\)00950-X](https://doi.org/10.1016/S0016-7037(02)00950-X)
- Iglesias, A. A., & Preiss, J. (1992). Bacterial glycogen and plant starch biosynthesis. *Biochemical Education*, 20(4), 196–203. [https://doi.org/10.1016/0307-4412\(92\)90191-N](https://doi.org/10.1016/0307-4412(92)90191-N)
- Jendrossek, D., & Handrick, R. (2002). Microbial degradation of polyhydroxyalkanoates. *Annual Review of Microbiology*, 56, 403–432. <https://doi.org/10.1146/annurev.micro.56.012302.160838>
- Kamravamanesh, D., Pflügl, S., Nischkauer, W., Limbeck, A., Lackner, M., & Herwig, C. (2017). Photosynthetic poly- β -hydroxybutyrate accumulation in unicellular cyanobacterium *Synechocystis* sp. Pcc 6714. *AMB Express*, 7(1), 143. <https://doi.org/10.1186/s13568-017-0443-9>.
- Kavitha, G., Rengasamy, R., & Inbakandan, D. (2018). Polyhydroxybutyrate production from marine source and its application. *International Journal of Biological Macromolecules*, 111, 102–108. <https://doi.org/10.1016/j.ijbiomac.2017.12.155>
- Kellogg, D. R., & Levin, P. A. (2022). Nutrient availability as an arbiter of cell size. *Trends in Cell Biology*. Advance online publication. <https://doi.org/10.1016/j.tcb.2022.06.008>
- Kirilovsky, D., & Kerfeld, C. A. (2013). The Orange Carotenoid Protein: A blue-green light photoactive protein. *Photochemical & Photobiological Sciences : Official Journal of the European*

Photochemistry Association and the European Society for Photobiology, 12(7), 1135–1143.
<https://doi.org/10.1039/c3pp25406b>

- Kjeldgaard (1958). Dependency on medium and temperature of cell size and chemical composition during balanced grown of *Salmonella typhimurium*. *Journal of General Microbiology*, 19(3), 592–606. <https://doi.org/10.1099/00221287-19-3-592>
- Klotz, A., & Forchhammer, K. (2017). Glycogen, a major player for bacterial survival and awakening from dormancy. *Future Microbiology*, 12, 101–104. <https://doi.org/10.2217/fmb-2016-0218>
- Klotz, A., Georg, J., Bučinská, L., Watanabe, S., Reimann, V., Januszewski, W., Sobotka, R., Jendrossek, D., Hess, W. R., & Forchhammer, K. (2016). Awakening of a Dormant Cyanobacterium from Nitrogen Chlorosis Reveals a Genetically Determined Program. *Current Biology : CB*, 26(21), 2862–2872. <https://doi.org/10.1016/j.cub.2016.08.054>
- Koch, M., Berendzen, K. W., & Forchhammer, A. K. (2020). On the Role and Production of Polyhydroxybutyrate (PHB) in the Cyanobacterium *Synechocystis* sp. Pcc 6803. *Life (Basel, Switzerland)*, 10(4). <https://doi.org/10.3390/life10040047>
- Koch, M., Bruckmoser, J., Scholl, J., Hauf, W., Rieger, B., & Forchhammer, K. (2020). Maximizing PHB content in *Synechocystis* sp. PCC 6803: development of a new photosynthetic overproduction strain. Advance online publication. <https://doi.org/10.1101/2020.10.22.350660>
- Koch, M., Doello, S., Gutekunst, K., & Forchhammer, K. (2019). Phb is Produced from Glycogen Turn-over during Nitrogen Starvation in *Synechocystis* sp. Pcc 6803. *International Journal of Molecular Sciences*, 20(8). <https://doi.org/10.3390/ijms20081942>
- Koller, M., Gasser, I., Schmid, F., & Berg, G. (2011). Linking ecology with economy: Insights into polyhydroxyalkanoate-producing microorganisms. *Engineering in Life Sciences*, 11(3), 222–237. <https://doi.org/10.1002/elsc.201000190>
- Kovalcik, A., Kucera, D., Matouskova, P., Pernicova, I., Obruča, S., Kalina, M., Enev, V., & Marova, I. (2018). Influence of removal of microbial inhibitors on PHA production from spent coffee grounds employing *Halomonas halophila*. *Journal of Environmental Chemical Engineering*, 6(2), 3495–3501. <https://doi.org/10.1016/j.jece.2018.05.028>
- Kovalcik, A., Meixner, K., Mihalic, M., Zeilinger, W., Fritz, I., Fuchs, W., Kucharczyk, P., Stelzer, F., & Drosig, B. (2017). Characterization of polyhydroxyalkanoates produced by *Synechocystis salina* from digestate supernatant. *International Journal of Biological Macromolecules*, 102, 497–504. <https://doi.org/10.1016/j.ijbiomac.2017.04.054>
- Kumar, K., Mella-Herrera, R. A., & Golden, J. W. (2010). Cyanobacterial heterocysts. *Cold Spring Harbor Perspectives in Biology*, 2(4), a000315. <https://doi.org/10.1101/cshperspect.a000315>
- Kumar, M., Rathour, R., Singh, R., Sun, Y., Pandey, A., Gnansounou, E., Andrew Lin, K.-Y., Tsang, D. C., & Thakur, I. S. (2020). Bacterial polyhydroxyalkanoates: Opportunities, challenges, and prospects. *Journal of Cleaner Production*, 263, 121500. <https://doi.org/10.1016/j.jclepro.2020.121500>

- Kwon, W., Kim, D., Kim, H.-Y., Jeong, S. W., Lee, S.-G., Kim, H.-C., Lee, Y.-J., Kwon, M. K., Hwang, J.-S., Han, J. E., Park, J.-K., Lee, S.-J., & Choi, S.-K. (2022). Microglial phagocytosis of polystyrene microplastics results in immune alteration and apoptosis in vitro and in vivo. *The Science of the Total Environment*, 807(Pt 2), 150817. <https://doi.org/10.1016/j.scitotenv.2021.150817>
- Lemoigne, M. (1926). Produits de dehydration et de polymerisation de l'acide β -oxobutyrique. *Bull Soc Chim Biol* 8, 770–782.
- Lewandowski, I., Gaudet, N., Lask, J., Maier, J., Tchouga, B., & Vargas-Carpintero, R. (2018). *Bioeconomy: Chapter 2: Context*. Springer International Publishing. <https://doi.org/10.1007/978-3-319-68152-8>
- Magdaong, N. C. M., & Blankenship, R. E. (2018). Photoprotective, excited-state quenching mechanisms in diverse photosynthetic organisms. *The Journal of Biological Chemistry*, 293(14), 5018–5025. <https://doi.org/10.1074/jbc.TM117.000233>
- Markou, G., & Nerantzis, E. (2013). Microalgae for high-value compounds and biofuels production: A review with focus on cultivation under stress conditions. *Biotechnology Advances*, 31(8), 1532–1542. <https://doi.org/10.1016/j.biotechadv.2013.07.011>
- Masood, F., Yasin, T., & Hameed, A. (2015). Polyhydroxyalkanoates - what are the uses? Current challenges and perspectives. *Critical Reviews in Biotechnology*, 35(4), 514–521. <https://doi.org/10.3109/07388551.2014.913548>.
- Meixner, K., Daffert, C., Dalnodar, D., Mrázová, K., Hrubanová, K., Krzyzanek, V., Nebesarova, J., Samek, O., Šedrllová, Z., Slaninova, E., Sedláček, P., Obruča, S., & Fritz, I. (2022). Glycogen, poly(3-hydroxybutyrate) and pigment accumulation in three *Synechocystis* strains when exposed to a stepwise increasing salt stress. *Journal of Applied Phycology*. Advance online publication. <https://doi.org/10.1007/s10811-022-02693-3>
- Meixner, K., Kovalcik, A., Sykacek, E., Gruber-Brunhumer, M., Zeilinger, W., Markl, K., Haas, C., Fritz, I., Mundigler, N., Stelzer, F., Neureiter, M., Fuchs, W., & Drosig, B. (2018). Cyanobacteria Biorefinery - Production of poly(3-hydroxybutyrate) with *Synechocystis salina* and utilisation of residual biomass. *Journal of Biotechnology*, 265, 46–53. <https://doi.org/10.1016/j.jbiotec.2017.10.020>
- Mergaert, J. (1992). Biodegradation of polyhydroxyalkanoates. *FEMS Microbiology Letters*, 103(2-4), 317–321. [https://doi.org/10.1016/0378-1097\(92\)90325-I](https://doi.org/10.1016/0378-1097(92)90325-I)
- Mierziak, J., Burgberger, M., & Wojtasik, W. (2021). 3-Hydroxybutyrate as a Metabolite and a Signal Molecule Regulating Processes of Living Organisms. *Biomolecules*, 11(3). <https://doi.org/10.3390/biom11030402>
- Mohapatra, S., Maity, S., Dash, H. R., Das, S., Pattnaik, S., Rath, C. C., & Samantaray, D. (2017). Bacillus and biopolymer: Prospects and challenges. *Biochemistry and Biophysics Reports*, 12, 206–213. <https://doi.org/10.1016/j.bbrep.2017.10.001>

- Mokhtarzadeh, A., Alibakhshi, A., Hejazi, M., Omid, Y., & Ezzati Nazhad Dolatabadi, J. (2016). Bacterial-derived biopolymers: Advanced natural nanomaterials for drug delivery and tissue engineering. *TrAC Trends in Analytical Chemistry*, 82, 367–384. <https://doi.org/10.1016/j.trac.2016.06.013>
- Montgomery, B. L. (2014). The Regulation of Light Sensing and Light-Harvesting Impacts the Use of Cyanobacteria as Biotechnology Platforms. *Frontiers in Bioengineering and Biotechnology*, 2, 22. <https://doi.org/10.3389/fbioe.2014.00022>
- Moore, C., Moore, S., Leecaster, M., & Weisberg, S. (2001). A Comparison of Plastic and Plankton in the North Pacific Central Gyre. *Marine Pollution Bulletin*, 42(12), 1297–1300. [https://doi.org/10.1016/S0025-326X\(01\)00114-X](https://doi.org/10.1016/S0025-326X(01)00114-X)
- Muhammadi, Shabina, Afzal, M., & Hameed, S. (2015). Bacterial polyhydroxyalkanoates-eco-friendly next generation plastic: Production, biocompatibility, biodegradation, physical properties and applications. *Green Chemistry Letters and Reviews*, 8(3-4), 56–77. <https://doi.org/10.1080/17518253.2015.1109715>
- Mullineaux, C. W. (2014). Co-existence of photosynthetic and respiratory activities in cyanobacterial thylakoid membranes. *Biochimica Et Biophysica Acta*, 1837(4), 503–511. <https://doi.org/10.1016/j.bbabi.2013.11.017>
- Napper, I. E., & Thompson, R. C. (2019). Environmental Deterioration of Biodegradable, Oxo-biodegradable, Compostable, and Conventional Plastic Carrier Bags in the Sea, Soil, and Open-Air Over a 3-Year Period. *Environmental Science & Technology*, 53(9), 4775–4783. <https://doi.org/10.1021/acs.est.8b06984>
- Nogia, P., Sidhu, G. K., Mehrotra, R., & Mehrotra, S. (2016). Capturing atmospheric carbon: biological and nonbiological methods. *International Journal of Low-Carbon Technologies*, 11(2), 266–274. <https://doi.org/10.1093/ijlct/ctt077>
- Noreña-Caro, D., & Benton, M. G. (2018). Cyanobacteria as photoautotrophic biofactories of high-value chemicals. *Journal of CO2 Utilization*, 28, 335–366. <https://doi.org/10.1016/j.jcou.2018.10.008>
- Obruča, S., Sedláček, P., Slaninova, E., Fritz, I., Daffert, C., Meixner, K., Šedrllová, Z., & Koller, M. (2020). Novel unexpected functions of PHA granules. *Applied Microbiology and Biotechnology*, 104(11), 4795–4810. <https://doi.org/10.1007/s00253-020-10568-1>
- Oren, A. (2014). Cyanobacteria: biology, ecology and evolution. In N. K. Sharma, A. K. Rai, & L. J. Stal (Eds.), *Cyanobacteria* (pp. 1–20). John Wiley & Sons, Ltd. <https://doi.org/10.1002/9781118402238.ch1>
- Orthwein, T., Scholl, J., Spät, P., Lucius, S., Koch, M., Macek, B., Hagemann, M., & Forchhammer, K. (2021). The novel PII-interactor PirC identifies phosphoglycerate mutase as key control point of carbon storage metabolism in cyanobacteria. *Proceedings of the National*

Academy of Sciences of the United States of America, 118(6).
<https://doi.org/10.1073/pnas.2019988118>

- Padermshoke, A., Katsumoto, Y., Sato, H., Ekgasit, S., Noda, I., & Ozaki, Y. (2005). Melting behavior of poly(3-hydroxybutyrate) investigated by two-dimensional infrared correlation spectroscopy. *Spectrochimica Acta. Part A, Molecular and Biomolecular Spectroscopy*, 61(4), 541–550. <https://doi.org/10.1016/J.SAA.2004.05.004>
- Padermshoke, A., Sato, H., Katsumoto, Y., Ekgasit, S., Noda, I., & Ozaki, Y. (2004). Thermally induced phase transition of poly(3-hydroxybutyrate-co-3-hydroxyhexanoate) investigated by two-dimensional infrared correlation spectroscopy. *Vibrational Spectroscopy*, 36(2), 241–249. <https://doi.org/10.1016/J.VIBSPEC.2003.11.016>
- Panda, B., Jain, P., Sharma, L., & Mallick, N. (2006). Optimization of cultural and nutritional conditions for accumulation of poly-beta-hydroxybutyrate in *Synechocystis* sp. Pcc 6803. *Biore-source Technology*, 97(11), 1296–1301. <https://doi.org/10.1016/j.biortech.2005.05.013>.
- Panda, B., Sharma, L., & Mallick, N. (2005). Poly-beta-hydroxybutyrate accumulation in *Nostoc muscorum* and *Spirulina platensis* under phosphate limitation. *Journal of Plant Physiology*, 162(12), 1376–1379. <https://doi.org/10.1016/j.jplph.2005.05.002>
- Persson, L., Carney Almroth, B. M., Collins, C. D., Cornell, S., Wit, C. A. de, Diamond, M. L., Fantke, P., Hassellöv, M., MacLeod, M., Ryberg, M. W., Søgaard Jørgensen, P., Villarrubia-Gómez, P., Wang, Z., & Hauschild, M. Z. (2022). Outside the Safe Operating Space of the Planetary Boundary for Novel Entities. *Environmental Science & Technology*, 56(3), 1510–1521. <https://doi.org/10.1021/acs.est.1c04158>
- Peschek, G. A., Obinger, C., & Paumann, M. (2004). The respiratory chain of blue-green algae (cyanobacteria). *Physiologia Plantarum*, 120(3), 358–369. <https://doi.org/10.1111/j.1399-3054.2004.00274.x>
- Peters, V., & Rehm, B. H. A. (2005). In vivo monitoring of PHA granule formation using GFP-labeled PHA synthases. *FEMS Microbiology Letters*, 248(1), 93–100. <https://doi.org/10.1016/j.femsle.2005.05.027>
- Pierucci, O. (1978). Dimensions of *Escherichia coli* at various growth rates: Model for envelope growth. *Journal of Bacteriology*, 135(2), 559–574. <https://doi.org/10.1128/jb.135.2.559-574.1978>
- Pils, D., & Schmetterer, G. (2001). Characterization of three bioenergetically active respiratory terminal oxidases in the cyanobacterium *Synechocystis* sp. Strain PCC 6803. *FEMS Microbiology Letters*, 203(2), 217–222. <https://doi.org/10.1111/j.1574-6968.2001.tb10844.x>
- Pötter, M., & Steinbüchel, A. (2005). Poly(3-hydroxybutyrate) granule-associated proteins: Impacts on poly(3-hydroxybutyrate) synthesis and degradation. *Biomacromolecules*, 6(2), 552–560. <https://doi.org/10.1021/BM049401N>

- Prashant Kumar Singh, Ajay Kumar, Vipin Kumar Singh, & Alok Kumar Shrivastava. (2020). *ADVANCES IN CYANOBACTERIAL BIOLOGY*. ELSEVIER ACADEMIC PRESS.
- Prats, C., Graham, T. E., & Shearer, J. (2018). The dynamic life of the glycogen granule. *The Journal of Biological Chemistry*, 293(19), 7089–7098. <https://doi.org/10.1074/jbc.R117.802843>
- Preiss, J. (1984). Bacterial glycogen synthesis and its regulation. *Annual Review of Microbiology*, 38, 419–458. <https://doi.org/10.1146/annurev.mi.38.100184.002223>
- Price, G. D. (2011). Inorganic carbon transporters of the cyanobacterial CO₂ concentrating mechanism. *Photosynthesis Research*, 109(1-3), 47–57. <https://doi.org/10.1007/s11120-010-9608-y>
- Rane, S. S., & Choi, P. (2005). Polydispersity Index: How Accurately Does It Measure the Breadth of the Molecular Weight Distribution? *Chemistry of Materials*, 17(4), 926. <https://doi.org/10.1021/cm048594i>
- Rhind, N. (2021). Cell-size control. *Current Biology : CB*, 31(21), R1414-R1420. <https://doi.org/10.1016/j.cub.2021.09.017>
- Ritchie, R. J. (2008). Universal chlorophyll equations for estimating chlorophylls a, b, c, and d and total chlorophylls in natural assemblages of photosynthetic organisms using acetone, methanol, or ethanol solvents. *Photosynthetica*, 46(1), 115–126. <https://doi.org/10.1007/s11099-008-0019-7>
- Rollin, R., Joanny, J.-F., & Sens, P. (2022). *Cell size scaling laws: a unified theory*. <https://doi.org/10.1101/2022.08.01.502021>
- Rudnik, E. (2013). Biodegradability Testing of Compostable Polymer Materials. In *Handbook of Biopolymers and Biodegradable Plastics* (pp. 213–263). Elsevier. <https://doi.org/10.1016/B978-1-4557-2834-3.00011-2>
- Russell, J. B. (2007). The energy spilling reactions of bacteria and other organisms. *Journal of Molecular Microbiology and Biotechnology*, 13(1-3), 1–11. <https://doi.org/10.1159/000103591>
- Samantaray, S., & Mallick, N. (2015). Impact of Various Stress Conditions on Poly-β-Hydroxybutyrate (PHB) Accumulation in *Aulosira fertilissima* CCC 444. *Current Biotechnology*, 4(3), 366–372. <https://doi.org/10.2174/2211550104666150806000642>
- Santos, A. R. S., Gerhardt, E. C. M., Parize, E., Pedrosa, F. O., Steffens, M. B. R., Chubatsu, L. S., Souza, E. M. de, Passaglia, L. M. P., Sant'Anna, F. H., Souza, G. A. de, Huergo, L. F., & Forchhammer, K. (2020). Nad⁺ biosynthesis in bacteria is controlled by global carbon/nitrogen levels via PII signaling. *The Journal of Biological Chemistry*, 295(18), 6165–6176. <https://doi.org/10.1074/jbc.RA120.012793>
- Santos, R. G., Machovsky-Capuska, G. E., & Andrades, R. (2021). Plastic ingestion as an evolutionary trap: Toward a holistic understanding. *Science (New York, N.Y.)*, 373(6550), 56–60. <https://doi.org/10.1126/science.abh0945>

- Sauvageau, M. C. (1892). Sur Les Algues D'Eau Douce Récoltées En Algérie Pendant La Session De La Société Botanique En 1892. *Bulletin De La Société Botanique De France*, 39(10), CIV–CXXVIII. <https://doi.org/10.1080/00378941.1892.10828721>
- Schließmann, U., Derwenskus, F., & Schmid-Staiger, U. (2018). *Bioeconomy: Chapter 6.4: Microalgae*. Springer International Publishing. <https://doi.org/10.1007/978-3-319-68152-8>
- Scholl, J., Dengler, L., Bader, L., & Forchhammer, K. (2020). Phosphoenolpyruvate carboxylase from the cyanobacterium *Synechocystis* sp. Pcc 6803 is under global metabolic control by PII signaling. *Molecular Microbiology*, 114(2), 292–307. <https://doi.org/10.1111/mmi.14512>
- Schopf, J. W. (2011). The paleobiological record of photosynthesis. *Photosynthesis Research*, 107(1), 87–101. <https://doi.org/10.1007/s11120-010-9577-1>
- Schwarz, R., & Forchhammer, K. (2005). Acclimation of unicellular cyanobacteria to macronutrient deficiency: Emergence of a complex network of cellular responses. *Microbiology*, 151(Pt 8), 2503–2514. <https://doi.org/10.1099/mic.0.27883-0>
- Sciuto, K., & Moro, I. (2015). Cyanobacteria: the bright and dark sides of a charming group. *Biodiversity and Conservation*, 24(4), 711–738. <https://doi.org/10.1007/s10531-015-0898-4>
- Shang, L., Jiang, M., & Chang, H. N. (2003). Poly(3-hydroxybutyrate) synthesis in fed-batch culture of *Ralstonia eutropha* with phosphate limitation under different glucose concentrations. *Biotechnology Letters*, 25(17), 1415–1419. <https://doi.org/10.1023/A:1025047410699>
- Sharma, N. K. (2014). *Cyanobacteria: An Economic Perspective // Cyanobacteria: An economic perspective*. Wiley-Blackwell.
- Shevela, D., Pishchalnikov, R., & Eichacker, L. (2013). Oxygenic Photosynthesis in Cyanobacteria. In A. Srivastava, A. Rai, & B. Neilan (Eds.), *Stress Biology of Cyanobacteria* (pp. 3–40). CRC Press. <https://doi.org/10.1201/B13853-3>
- Shih, P. M., Wu, D., Latifi, A., Axen, S. D., Fewer, D. P., Talla, E., Calteau, A., Cai, F., Tandeau de Marsac, N., Rippka, R., Herdman, M., Sivonen, K., Coursin, T., Laurent, T., Goodwin, L., Nolan, M., Davenport, K. W., Han, C. S., Rubin, E. M., . . . Kerfeld, C. A. (2013). Improving the coverage of the cyanobacterial phylum using diversity-driven genome sequencing. *Proceedings of the National Academy of Sciences of the United States of America*, 110(3), 1053–1058. <https://doi.org/10.1073/pnas.1217107110>
- Sindhu, R., Ammu, B., Binod, P., Deepthi, S. K., Ramachandran, K. B., Soccol, C. R., & Pandey, A. (2011). Production and characterization of poly-3-hydroxybutyrate from crude glycerol by *Bacillus sphaericus* NII 0838 and improving its thermal properties by blending with other polymers. *Brazilian Archives of Biology and Technology*, 54(4), 783–794. <https://doi.org/10.1590/S1516-89132011000400019>
- Singh, A. K., Sharma, L., Mallick, N., & Mala, J. (2017). Progress and challenges in producing polyhydroxyalkanoate biopolymers from cyanobacteria. *Journal of Applied Phycology*, 29(3), 1213–1232. <https://doi.org/10.1007/s10811-016-1006-1>

- Slaninova, E., Sedláček, P., Mravec, F., Mullerova, L., Samek, O., Koller, M., Hesko, O., Kucera, D., Marova, I., & Obruča, S. (2018). Light scattering on PHA granules protects bacterial cells against the harmful effects of UV radiation. *Applied Microbiology and Biotechnology*, 102(4), 1923–1931. <https://doi.org/10.1007/s00253-018-8760-8>
- Srivastava, A. K., Rai, A. N., Neilan, B. A., & Rai, A. N. (2013). *Stress Biology of Cyanobacteria // Stress biology of cyanobacteria: Molecular mechanisms to cellular responses*. Taylor & Francis.
- Stanier, R. Y., Deruelles, J., Rippka, R., Herdman, M., & Waterbury, J. B. (1979). Generic Assignments, Strain Histories and Properties of Pure Cultures of Cyanobacteria. *Microbiology*, 111(1), 1–61. <https://doi.org/10.1099/00221287-111-1-1>
- Steinbüchel, A., & Fuchtenbusch, B. (1998). Bacterial and other biological systems for polyester production. *Trends in Biotechnology*, 16(10), 419–427. [https://doi.org/10.1016/S0167-7799\(98\)01194-9](https://doi.org/10.1016/S0167-7799(98)01194-9)
- Steinbüchel, A., & Valentin, H. E. (1995). Diversity of bacterial polyhydroxyalkanoic acids. *FEMS Microbiology Letters*, 128(3), 219–228. <https://doi.org/10.1111/j.1574-6968.1995.tb07528.x>
- Sudesh, K., Abe, H., & Doi, Y. (2000). Synthesis, structure and properties of polyhydroxyalkanoates: biological polyesters. *Progress in Polymer Science*, 25(10), 1503–1555. [https://doi.org/10.1016/S0079-6700\(00\)00035-6](https://doi.org/10.1016/S0079-6700(00)00035-6)
- Tanaka, K., Shimakawa, G., Tabata, H., Kusama, S., Miyake, C., & Nakanishi, S. (2021). Quantification of NAD(P)H in cyanobacterial cells by a phenol extraction method. *Photosynthesis Research*, 148(1-2), 57–66. <https://doi.org/10.1007/s11120-021-00835-1>
- Trampe, E., & Kuhl, M. (2016). Chlorophyll f distribution and dynamics in cyanobacterial beachrock biofilms. *Journal of Phycology*, 52(6), 990–996. <https://doi.org/10.1111/jpy.12450>
- Troschl, C., Meixner, K., Fritz, I., Leitner, K., Romero, A. P., Kovalcik, A., Sedláček, P., & Drosig, B. (2018). Pilot-scale production of poly-β-hydroxybutyrate with the cyanobacterium *Synechocystis* sp. CCALA192 in a non-sterile tubular photobioreactor. *Algal Research*, 34, 116–125. <https://doi.org/10.1016/j.algal.2018.07.011>
- Vadia, S., Tse, J. L., Lucena, R., Yang, Z., Kellogg, D. R., Wang, J. D., & Levin, P. A. (2017). Fatty Acid Availability Sets Cell Envelope Capacity and Dictates Microbial Cell Size. *Current Biology : CB*, 27(12), 1757–1767.e5. <https://doi.org/10.1016/j.cub.2017.05.076>
- van Cauwenberghe, L., Vanreusel, A., Mees, J., & Janssen, C. R. (2013). Microplastic pollution in deep-sea sediments. *Environmental Pollution (Barking, Essex : 1987)*, 182, 495–499. <https://doi.org/10.1016/j.envpol.2013.08.013>
- van de Meene, Hohmann-Marriott, M. F., Vermaas, W. F. J., & Roberson, R. W. (2006). The three-dimensional structure of the cyanobacterium *Synechocystis* sp. Pcc 6803 // The three-dimensional structure of the cyanobacterium *Synechocystis* sp. Pcc 6803. *Archives of Microbiology*, 184(5), 259–270. <https://doi.org/10.1007/s00203-005-0027-y>

- van Gernerden, H. (1968). On the ATP generation by Chromatium in darkness. *Archiv Fur Mikrobiologie*, 64(2), 118–124. <https://doi.org/10.1007/BF00406970>
- Verlinden, R. A. J., Hill, D. J., Kenward, M. A., Williams, C. D., & Radecka, I. (2007). Bacterial synthesis of biodegradable polyhydroxyalkanoates. *Journal of Applied Microbiology*, 102(6), 1437–1449. <https://doi.org/10.1111/j.1365-2672.2007.03335.x>
- Wan, N., DeLorenzo, D. M., He, L., Le You, Immethun, C. M., Wang, G., Baidoo, E. E. K., Hollinshead, W., Keasling, J. D., Moon, T. S., & Tang, Y. J. (2017). Cyanobacterial carbon metabolism: Fluxome plasticity and oxygen dependence. *Biotechnology and Bioengineering*, 114(7), 1593–1602. <https://doi.org/10.1002/bit.26287>
- Wang, S., Chen, W., Xiang, H., Yang, J., Zhou, Z., & Zhu, M. (2016). Modification and Potential Application of Short-Chain-Length Polyhydroxyalkanoate (SCL-PHA). *Polymers*, 8(8). <https://doi.org/10.3390/polym8080273>
- Wang-Erlandsson, L., Tobian, A., van der Ent, R. J., Fetzer, I., te Wierik, S., Porkka, M., Staal, A., Jaramillo, F., Dahlmann, H., Singh, C., Greve, P., Gerten, D., Keys, P. W., Gleeson, T., Cornell, S. E., Steffen, W., Bai, X., & Rockström, J. (2022). A planetary boundary for green water. *Nature Reviews Earth & Environment*. Advance online publication. <https://doi.org/10.1038/s43017-022-00287-8>
- Watzer, B., Spät, P., Neumann, N., Koch, M., Sobotka, R., Macek, B., Hennrich, O., & Forchhammer, K. (2019). The Signal Transduction Protein PII Controls Ammonium, Nitrate and Urea Uptake in Cyanobacteria. *Frontiers in Microbiology*, 10, 1428. <https://doi.org/10.3389/fmicb.2019.01428>
- Welkie, D. G., Rubin, B. E., Diamond, S., Hood, R. D., Savage, D. F., & Golden, S. S. (2019). A Hard Day's Night: Cyanobacteria in Diel Cycles. *Trends in Microbiology*, 27(3), 231–242. <https://doi.org/10.1016/j.tim.2018.11.002>
- Whitton, B. A. (2012). *Ecology of Cyanobacteria II*. Springer Netherlands. <https://doi.org/10.1007/978-94-007-3855-3>
- Whitton, B. A., & Potts, M. (Eds.). (2002). *The Ecology of Cyanobacteria: Their Diversity in Time and Space*. Springer Netherlands. <https://doi.org/Brian>
- Williams, D. F. (2008). On the mechanisms of biocompatibility. *Biomaterials*, 29(20), 2941–2953. <https://doi.org/10.1016/j.biomaterials.2008.04.023>
- Wu, G., Wu, Q., & Shen, Z. (2001). Accumulation of poly- β -hydroxybutyrate in cyanobacterium *Synechocystis* sp. PCC6803. *Bioresource Technology*, 76(2), 85–90. [https://doi.org/10.1016/S0960-8524\(00\)00099-7](https://doi.org/10.1016/S0960-8524(00)00099-7)
- Zerobin, A. J. (2021). *Influence of temperature and light on photoautotrophic growth and PHB production in the cyanobacterium Synechocystis sp* [Master]. University of Natural Resources and Life Sciences, Vienna.

- Zhang, Y.-M., White, S. W., & Rock, C. O. (2006). Inhibiting bacterial fatty acid synthesis. *The Journal of Biological Chemistry*, 281(26), 17541–17544. <https://doi.org/10.1074/jbc.r600004200>
- Zilliges, Y. (2014). Glycogen, a dynamic cellular sink and reservoir for carbon. *The Cell Biology of Cyanobacteria*, 189–210. www.scopus.com